Université catholique de Louvain
Faculté d'Ingénierie biologique, agronomique et environnementale
Institut des sciences de la vie
Unité de biochimie physiologique

The yeast proteolipid Pmp3p is a new component of the plasma membrane microdomains associated with the eisosomes

Thèse présentée par Jean-François Hochstenbach en vue de l'obtention du grade de Docteur en sciences agronomiques et ingénierie biologique

Membres du jury :
Président : Prof. Jacques Mahillon
Promoteur : Prof. Pierre Morsomme
Prof. Anabelle Decottignies
Prof. André Goffeau
Prof. Patrice Soumillion
Prof. Hana Sychrova

Merci à tous ceux qui ont rendu cette aventure possible, enrichissante et agréable. Merci tout particulièrement à Pierre de m'avoir fait confiance dans les bons et les moins bons moments, merci de m'avoir donné l'opportunité de découvrir un monde passionnant.

Merci aux membres de mon jury pour l'attention qu'ils ont porté à ce manuscrit.

Merci aux membres de l'unité FYSA et plus particulièrement aux membres du groupe de Pierre pour l'excellente ambiance de travail durant ces 5 années.

Et, enfin, merci à ma famille, à mes parents, à mes amis et bien sur à Odile pour leur présence durant ces années et pour beaucoup d'autres choses aussi…

Table of contents

INTRODUCTION **17**

1. Ion homeostasis in *Saccharomyces cerevisiae* **19**
1.1. Proton transport 21
The plasma membrane H^+-ATPase (Pma1p) 21
1.2. Alkali metal cations transport 24
1.2.1 Potassium transport 25
TRK system 25
TOK1 27
NSC1 29
1.2.2. Sodium transport 31
PMR2/ENA1 31
NHA1 32
1.2.3. Compartmentalization of alkali metal cations 33
1.3. Illustration of a nutrient transport 36
1.3.1 Polyamines transport 36

2. *PMP3* related genes family **40**
Pmp3p/Sna1p 45

3. Plasma membrane compartmentalization **49**
3.1. Sterol-rich membrane domains (SRD) 55
3.2. Plasma membrane microdomains in the yeast *S. cerevisiae* 56
3.2.1. Membrane compartment of Can1p (MCC) and eisosomes 59
Overview of some proteins detected in MCC/eisosomes 62
3.2.2. Mesh-shaped membrane compartment of Pma1p (MCP) 70
3.2.3. TORC2 plasma membrane localization (MCT) 73
3.2.4. Homogeneous distribution of the plasma membrane: Hxt1, Gap1 74
3.2.5. Biogenesis and function of microdomains in yeast 74

OBJECTIVES **79**

RESULTS AND DISCUSSION.....83

1. Study of the putative partners of Pmp3p via a biochemical approach.....85
1.1. Construction of a functional tagged version of Pmp3p.....85
1.2. Phenotypic characterization of the strains expressing a tagged version of Pmp3p.....87
1.3. Solubilization of HA-Pmp3p.....92
1.4. Immunoprecipitation of HA-Pmp3p.....94
1.5. Physical interaction between Pmp3p and Pil1p.....97
1.6. Pmp3p and Pil1p colocalize in situ.....99
1.7. An endocytic regulatory role for Pmp3p.....102
1.8. Phenotypic characterization of the knockout genes corresponding to the putative partners.....106
1.9. Oligomerization of Pmp3p.....111

2. Study of the relation existing between the structure, the function and the trafficking of Pmp3p.....115
2.1. Study of the function of Pmp3p.....116
2.2. Study of the trafficking of Pmp3p towards plasma membrane.....120

3. The plasma membrane proteome of *Saccharomyces cerevisiae* and its response to the *PMP3* deletion.....131

CONCLUSIONS AND PERSPECTIVES.....149

MATERIALS AND METHODS.....157

1. Strains and media.....159
1.1. *Escherichia coli*.....159
1.2. *Saccharomyces cerevisiae*.....159

2. DNA constructs.....160

2.1. Strains 160
2.2. Plasmids 161

3. Drug tests 166

4. Fluorescence microscopy 166

5. Proteins 167
5.1. Plasma membrane preparation 167
5.1.1. Differential centrifugation 167
5.1.2. Acid precipitation 168
5.2. Protein quantification 168
5.3. Membrane solubilization 168
5.4. Protein separation and detection 169
5.4.1. SDS polyacrylamide gel electrophoresis (PAGE) 169
5.4.2. SDS polyacrylamide gel electrophoresis (Tris-Tricine) 169
5.4.3. Western blot analysis 170
5.5. Immunoprecipitation 171

6. Immunofluorescence 172

7. Endocytosis assays 173

8. iTRAQ analysis 174
8.1. iTRAQ labeling 174
8.2. Reverse phase chromatography 175
8.3. Mass spectrometry analysis and protein identification 175
8.4. Quantification of relative change 176

REFERENCES 177

ANNEXES 205

Abbreviations

ABC: ATP binding cassette
ACN: Acetonitrile
ATP: Adenosine-triphosphate
ATPase: ATP phosphatase
bp: base pair
BLM: Bleomycin
BSA: Bovine serum albumin
diS-C3(3): 3,3′-dipropylthiodicarbocyanine
DNA: Deoxyribose nucleic acid
DRM: Detergent resistant membrane
DTT: Dithiothreitol
ER: Endoplasmic reticulum
GFP: Green fluorescent protein
IP: Immunoprecipitation
kDa: kilo Dalton
LB: Luria-Bertani
MCC: Membrane containing Can1p
MCP: Membrane containing Pma1p
MCT: Membrane containing TORC2
MVB: Multi vesicular bodies
NMR: Nuclear magnetic resonance
OD: Optical density
ORF: Open reading frame
PCR: Polymerase chain reaction
PM: Plasma membrane
PMSF: Phenylmethylsulfonyl fluoride
PVDF: Polyvinylidine difluoride
rpm: revolutions per minute
RT: Room temperature
SDS: Sodium dodecyl sulphate

SDS-PAGE: Sodium dodecyl sulfate-polyacrylamide gel electrophoresis
SRD : Sterol-rich domain
TBS: Tris buffer saline
TFA: trifluoroacetic acid
TMA: tetramethylammonium
TMD: Transmembrane domain
Tris : Tris(hydroxymethyl)aminomethane
YD: Yeast extract dextrose
w/v: weight/volume
WB: Western blot
WT: Wild type

Abstract

Many prokaryotic and eukaryotic organisms possess small molecular weight hydrophobic proteins that respond differently to stresses, such as cold temperature, salt and dehydration. Yeast plasma membranes contain a small 55 amino acid hydrophobic polypeptide, Pmp3p/Sna1p, which belongs to the SNA (*S*ensitive to *Na*) proteins family and has three close homologues, called Sna2p, Sna3p and Sna4p. Previous work showed that the *PMP3* deletion increases the plasma membrane potential and confers sensitivity to cytotoxic cations.

In this study we present a further characterization of the molecular function of Pmp3p. We observed that Pmp3p physically interacts with Pil1p, a component of the eisosomes which are structures associated with some plasma membrane microdomains. We confirmed the localization of Pmp3p in these microdomains via indirect immunofluorescence. Using different techniques in molecular biology, biochemistry, cell biology and proteomics, we showed that Pmp3p could protect some transporters against endocytosis and link this process to cation homeostasis. Finally, a site-directed mutagenesis approach revealed that at least 9 conserved residues (F14, P17, G25, D29, L36, L39, P43, A48, Y50) are important for the function of Pmp3p.

INTRODUCTION

1. Ion homeostasis in *Saccharomyces cerevisiae*

Ion homeostasis is a fundamental property of living cells. Ion transporters and their accurate regulatory systems are essential to set the intracellular concentrations of the major monovalent cations (H^+, K^+, and Na^+) within the optimal range for cellular systems. A neutral pH is important for protein stability as well as a high potassium/sodium ratio. Indeed, a high concentration of sodium is toxic for yeast cell while intracellular potassium is essential in various physiological functions (maintenance of osmotic pressure, protein synthesis,…). Cations are also important for the generation of electrochemical gradients which in mammalian cells are maintained by the ion pump, Na^+/K^+ ATPase, and in non-animal cells by the proton pump (Serrano, 1996). It is interesting to note that fungi and plants have a similar mechanism for basic ion transport. The conservation of this basic transport mechanism makes the yeast, *Saccharomyces cerevisiae*, a model system of considerable value for understanding the ionic balance in plants.

The major transport systems for monovalent ions in *Saccharomyces cerevisiae* are shown in Figure 1. In yeasts, the major determinants of the plasma membrane potential are the H^+-ATPase (Pma1p) (Dufour and Goffeau, 1978), a generator of the membrane potential, and the Trk1,2p constituting the major high-affinity K^+ uptake system (Gaber et al., 1988; Ko et al., 1990), a consumer of the membrane potential. Pma1p pumps

protons out of the cell and thus plays an essential role in maintaining intracellular pH as well as in establishing a large electrochemical gradient, which is the driving force required for the transport of many nutrients into the cell (Vallejo and Serrano, 1989). The Trk1,2p transporters use the H^+ generated membrane potential to transport K^+ into the cell, creating an opposite gradient thus relieving membrane polarization. It is assumed that the relative activity of these two systems sets the steady-state value of the electrochemical membrane potential which in turn regulates the activity of secondary transport systems, such as those involved in the uptake of nutrients and various cations (Madrid et al., 1998).

In the following section we will discuss the main systems which co-operate to mediate intracellular cation homeostasis, including the plasma membrane H^+-ATPase, the Pmr2p/Ena1p sodium exporting ATPase, the Nha1p and the Nhx1p Na^+/H^+ antiporters, the Trk1/2p K^+ transporters, and various ion channels. Moreover, the transport of polyamines will be discussed in order to illustrate the transport of a nutrient for the yeast cell.

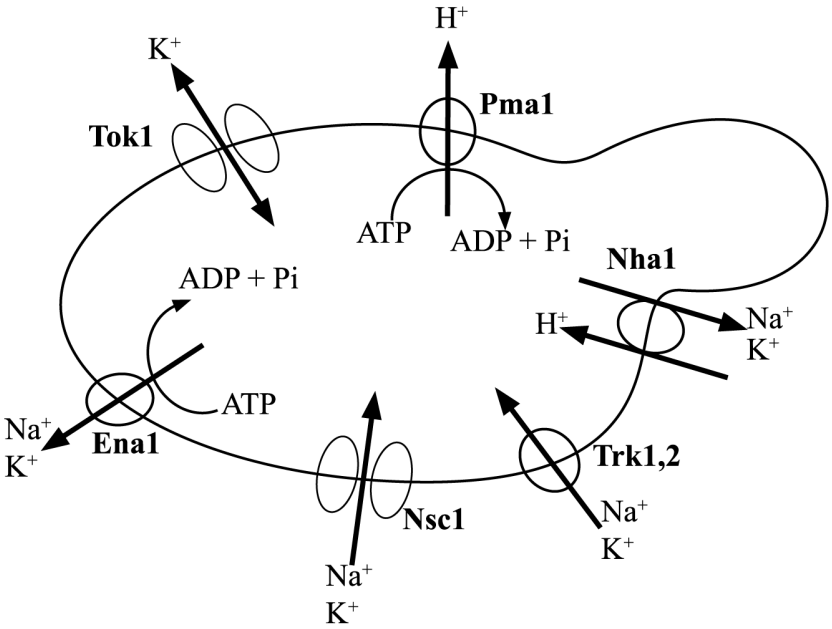

Figure 1. Transport systems involved in the uptake and efflux of potassium and sodium in the plasma membrane of *S. cerevisiae*. Pma1, H^+-ATPase; Trk, potassium uptake system; Nsc1, non-specific cation channel; Tok1, potassium channel; Ena1, Na^+-ATPase; Nha1, Na^+/H^+ antiporter.

1.1. Proton transport

The plasma membrane H^+-ATPase (Pma1p)

The proton pumping H^+-ATPase, Pma1p, belongs to the P-type ATPases, which couple ATP hydrolysis to the transport of cations across cell membranes. The existence of this electrogenic H^+ pump in yeast has been

demonstrated by physiological studies (Pena et al., 1972; Pena et al., 1969) followed by purified preparations (Dufour and Goffeau, 1978). A characteristic feature of P-type ATPases is that a strictly conserved aspartate residue is phosphorylated during the catalytic cycle (Pedersen and Carafoli, 1987). The family of P-type ATPase may be divided into five subfamilies according to the cation transported (Catty et al., 1997). Members of one group (P_1) transport heavy metals such as Cu^{2+}, Cd^{2+}, and Hg^{2+}, while members of the other group (P_2) transport a wide array of monovalent and divalent cations including H^+, Na^+, K^+, Mg^{2+}, and Ca^{2+}. The KdpB-ATPase from *Escherichia coli*, which accumulates K^+ under potassium starvation, shares structural features with both groups and has been classified as a P_3-ATPase (Lutsenko and Kaplan, 1995). The screening of the *Saccharomyces cerevisiae* genome has revealed a total of 16 P-type ATPases including two P_1-type ATPases, nine P_2-type ATPases (including two H^+- ATPases) and two new families of P-type ATPases called P_4 and P_5 (Axelsen and Palmgren, 1998; Catty et al., 1997; Morsomme et al., 2000).

The plasma membrane H^+-ATPase is encoded by the *PMA1* gene, which has been cloned and sequenced from *S. cerevisiae* (Serrano et al., 1986), *N. crassa* (Addison, 1986; Hager et al., 1986), *S. pombe* (Ghislain et al., 1987), and from a growing list of other fungal species.

Pma1p is a 100-kDa abundant protein of the cell surface (Goffeau and Dufour, 1988; Malpartida and Serrano, 1980), making up 10-20% of the total plasma membrane proteins. The Pma1 activity controls the intracellular pH and maintains the electrochemical gradient across the plasma membrane, two essential cellular functions. Glucose (Serrano, 1983) and acid pH (Eraso and Gancedo, 1987) are the two main factors controlling the activity of Pma1p. In agreement with its critical physiological function, the *PMA1* gene is essential for cell viability (Serrano et al., 1986).

An additional gene called *PMA2* encodes a nearly identical protein, but this homologue is only weakly expressed and it is not essential for viability and growth (Schlesser et al., 1988).

Evidence from electron crystallography (Auer et al., 1998) supports predictions from hydropathy analysis (Goffeau and de Meis, 1990; Serrano, 1988; Van Dyck et al., 1990) that P-type ATPases have 4 transmembrane segments in the amino terminus, followed by a large cytoplasmic domain and 6 transmembrane domains at the carboxy terminus (Figure 2). The cytoplasmic portion of the molecule is arranged into three distinct domains containing the ATP-binding site, a phosphorylation site, and the anchor domain. The catalytic activity of the fungal H^+-ATPases is activated by a large number of physiological stimuli. The model proposed to explain the mechanism of activation is

often similar: the activators overcome negative regulation by a regulatory domain located at the carboxy-terminus of the enzyme (Portillo et al., 1989).

Figure 2. Topological model of the fungal plasma membrane H^+-ATPase.

1.2. Alkali metal cations transport

Yeast cells use different mechanisms to maintain an optimum cytoplasmic concentration of potassium and a stable K^+/Na^+ ratio. Knowing that sodium is more abundant (~mM) than potassium (~μM) in the external environment, cells need a strict discrimination among alkali metal cations at the level of influx. The active transporter Trk1p, thanks to its high affinity for potassium, is the key factor responsible for potassium accumulation in the cell. Nevertheless potassium can also enter into the cell via another active transporter (Trk2p) and two channels (Tok1p and Nsc1p) (Figure 1). Unfortunately, when the external

concentration of sodium increases, sodium enters via these same proteins. Another mechanism to regulate the homeostasis of these cations is an efficient efflux system. Two different types of transport systems mediating active sodium efflux exist in yeast plasma membranes: Na^+,K^+-ATPase and Na^+,K^+/H^+ antiporter (Figure 1). Finally, yeast possesses an important system, including two Na^+,K^+/H^+ antiporters, involved in the compartmentalization of cations in yeast organelles (reviewed by Sychrova, 2004).

1.2.1 Potassium transport

TRK system

The primary K^+ uptake system in *S. cerevisiae* is encoded by the *TRK1* (Gaber et al., 1988) and the *TRK2* (Ko and Gaber, 1991) genes. *TRK1* encodes a 141 kDa protein containing eight membrane-spanning domains with a four-MPM (membrane-pore-membrane) structure (Figure 3), similar to that of KcsA K^+ channel from *Streptomyces lividans* (Durell and Guy, 1999; Gaber et al., 1988). Trk1p and Trk2p align with nearly 55% sequence identity, a major difference being the length of the large hydrophilic loop between transmembrane domain 3 and 4. Cells containing a *trk1* null allele are viable but they have lost their high affinity K^+ uptake abilities. Trk2p seems to play a role in high affinity K^+ uptake only under specific environmental conditions that remain to be

discovered (Michel et al., 2006). However, additional deletion of *TRK2* increases the potassium requirement by 5- to 10 fold. Normal growth of *trk1*Δ *trk2*Δ cells occurs only when the extracellular concentration of K^+ is approximately equal to the internal concentration (Ko and Gaber, 1991). The Trk1/2p system also permits influx of Na^+, however mutants defective in this system exhibit decreased NaCl tolerance due to the modification of the Na^+/K^+ balance within the cell (Garciadeblas et al., 1993; Gomez et al., 1996). Indeed, a notable characteristic of the Trk1/2p transport system is its ability to decrease K_m for potassium under conditions of Na^+ stress or K^+ starvation, thereby increasing K^+/Na^+ discrimination (Garciadeblas et al., 1993; Ramos et al., 1990). In the high affinity state, K_m for potassium might be as low as 15 μM and the discriminatory capacity between K^+ and Na^+ 1:700 (Rodriguez-Navarro, 2000).

Studies have investigated the molecular mechanism involved in the movement of alkali cations through Trk1p. The model that best explains the activity of this transporter is a cotransport of two K^+ or Rb^+, as both of them bind the two binding sites of Trk1p with very high affinities in K^+-starved cells. Na^+ can be transported in the same way but it exhibits a much lower affinity for the second binding site (Haro and Rodriguez-Navarro, 2002).

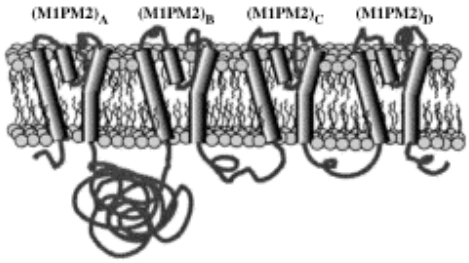

Figure 3. Schematic structural model of TRK transporters (from Haro and Rodriguez-Navarro, 2003). MPM: Structure composed of 4 X two transmembrane α-helices connected by the P segment.

TOK1

A part of the potassium that is taken up by growing *S. cerevisiae* is returned to the external medium (Rodriguez-Navarro and Ramos, 1984). Excess of potassium can be partially extruded by the proteins mediating sodium efflux (Nha1p and Ena1p). However, yeast also possesses a pathway for K^+ extrusion which is mediated by Tok1p/Duk1p/Ykc1p, an outward rectifying K^+ channel that is opening at positive (Ketchum et al., 1995; Reid et al., 1996; Zhou et al., 1995) and low negative membrane voltages (Bertl et al., 1993; Fairman et al., 1999).

Many different laboratories have participated in the characterization of this fungal channel (Bertl et al., 1998; Bertl et al., 2003; Lesage et al., 1996; Vergani and Blatt, 1999; Zhou et al., 1995) and have identified principal properties: Tok1p displays strong outward rectification, but

under certain conditions (at negative membrane voltages) it is able to mediate K^+ uptake as well (Bertl et al., 1993; Fairman et al., 1999).

Tok1 is a voltage-gated K^+ channel with two pore domains in series within a single polypeptide (Ketchum et al., 1995). Tandem pore-loop potassium channels differ from the majority of K^+ channels in that a single polypeptide chain carries two K^+-specific segments (P) each sandwiched between two transmembrane helices (M) to form an MP_1M-MP_2M series (Figure 4). Thus, the whole peptide comprises eight TM helices and two P motifs, the latter lying between TM helices 5 & 6 and 7 & 8 (Roller et al., 2008).

Moreover, it has been repeatedly observed that Tok1p-dependent currents, inward as well as outward, disappear at extracellular potassium concentrations below ~5 mM ; and then, even hyperexpression of *TOK1* does not complement the double *TRK* deletion strain. Such apparent "gating" effects of extracellular potassium have been shown- in high resolution crystal structures- to occur because the channel pore collapses within the selectivity filter, when extracellular potassium is depleted (Morais-Cabral et al., 2001; Zhou et al., 2001). In this respect, the two-pore K^+ channel of yeast is a typical potassium channel, whose critical structure is stabilized by the permeant ion itself (Roller et al., 2008).

Tok1p is also activated by plasma membrane depolarization (Bertl et al., 1993), and K^+ accumulated in the cells is probably released in order to

regenerate the membrane potential (Bertl et al., 1998). Some results based on electrophysiological measurements confirm that depolarization of the plasma membrane activates Tok1p. Indeed, when the potential decreases (for example via K^+ uptake), cells lacking the *TOK1* gene cannot react and therefore they stay depolarized, as shown by the lower diS-C3(3) staining level of *tok1*Δ mutant. These results support the hypothesis that one of the physiological roles of the Tok1 channel might be the regeneration of membrane potential when the cells are depolarized (Maresova et al., 2006).

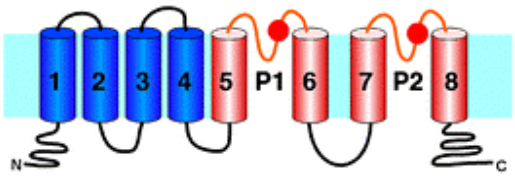

Figure 4. Schematic structural model of Tok1 channel (from Roller et al., 2008).

NSC1

In addition to Trk1, Trk2 and Tok1 proteins, it has been proved that yeast possesses other mechanisms that mediate either the import or the export of K^+. Whole-cell patch clamp experiments have provided evidence for the existence of a non-selective cation channel (Bihler et al., 1998).

Although the identity of the protein(s) responsible for this inwardly rectifying pathway is not known, it has been designated NSC1. A probable function is, as demonstrated by Bihler et al (2002), to control the primary low-affinity uptake route for potassium ions in yeast. NSC1 conducts strong currents at clamp potentials of –200 mV and it is blocked by divalent cations and at lower extracellular pH. In addition to potassium, this system is also able to facilitate the uptake of a wide range of cations including Na^+ and NH_4^+. This positive function requires that the activity of this transport system can be regulated under physiological conditions (Bertl et al., 2003).

The view that this current could be due to several transporters is supported by several evidences. First, Rb^+ uptake assays in *trk1*Δ *trk2*Δ cells suggested the existence of several pathways for the low affinity influx of the alkali metal cations (Madrid et al., 1998). Second, selection for spontaneous suppressors that restored growth of *trk1*Δ *trk2*Δ cells on K^+-limiting medium led to the isolation of cells with unusual gain-of-function mutations in the glucose transporter genes *HXT1* and *HXT3* and the glucose/galactose transporter gene *GAL2*. In addition to K^+, the mutant hexose transporters also conferred permeation of other cations, including Na^+. Moreover, the *HXT3* overexpression partially suppressed this defective growth at low K^+ (Madrid et al., 1998). In addition, amino acid (Wright et al., 1997) or drug/H^+ antiporter (Qdr2p) could also be

involved in this process. Qdr2p confers resistance to the yeast against the antiarrhythmic and antimalarial drug quinidine, the herbicide barban, and the antitumour agents bleomycin and cisplatin (Vargas et al., 2007).

1.2.2. Sodium transport

PMR2/ENA1

Na^+ efflux in *S. cerevisiae* is primarily mediated by the plasma membrane P_2-type Na^+-ATPase encoded by the *PMR2/ENA* locus. *S. cerevisiae* contains diverse copies of genes encoding identical or very similar Ena proteins. *ENA1* was initially identified as a putative calcium P-type ATPase gene on the basis of its sequence characteristics (Rudolph et al., 1989), and the locus was named *PMR2* (for *p*lasma *m*embrane ATPase *r*elated). Two years later, its capacity to extrude Na^+, Li^+, and probably K^+ was reported by Rodriguez-Navarro and coworkers, and its new name *ENA1* was born (Haro et al., 1991).

Localization at the cell membrane has been demonstrated for *S. cerevisiae* Pmr2a/Ena1 and Pmr2b/Ena2 proteins, although it has been reported that overexpression of *ENA1* also results in the presence of the protein in intracellular membrane structures (Benito et al., 1997). Deletion of *ENA1* leads to hypersensitivity to sodium stress while deletion of *ENA2* has no obvious effect (Wieland et al., 1995). Active research has revealed a

complex and sophisticated system of *ENA1* transcriptional regulation in response to specific environmental changes (reviewed by Ruiz and Arino, 2007). In contrast with the relatively abundant knowledge on its transcriptional control, the posttranscriptional mechanisms of the ATPase remain to be elucidated. *ENA1* is transcriptionally induced by salt (Garciadeblas et al., 1993), glucose (Alepuz et al., 1997), nitrogen (Crespo et al., 2001) starvation or by high extracellular pH (Garciadeblas et al., 1993).

NHA1

Prior et al. (Prior et al., 1996) have discovered the *NHA1* gene, which encodes an antiporter $H^+/Na^+,Li^+,K^+$ (985 amino acids long) in *Saccharomyces cerevisiae*. Nha1p is highly similar to antiporters responsible for sodium and lithium tolerance in *Schizosaccharomyces pombe* (*SOD2*) (Jia et al., 1992), in *Zygosaccharomyces rouxii* (*ZSOD2* and *ZSOD22*) (Iwaki et al., 1998; Watanabe et al., 1995) and in *Candida albicans* (*CNH1*) (Soong et al., 2000). The structure of these 5 antiporters consists of a very short hydrophilic N-terminus, probably 12 highly conserved hydrophobic transmembrane domains and a long hydrophilic tail domain. Unlike these 4 homologues, Nha1p also mediates the export of potassium in addition of sodium and lithium (Banuelos et al., 1998). The $H^+/Na^+,K^+$ exchange has been confirmed in reconstituted plasma

membrane vesicles (Sychrova et al., 1999) and by using secretory vesicles isolated from a temperature sensitive secretory mutant (Ohgaki et al., 2005).

In contrast to Ena1p which is active mainly at alkaline pH values, Nha1p is active in acidic pH conditions but plays a less decisive role in tolerance to sodium than the Ena1 protein. Indeed the *NHA1* transcription is constitutive and very low (Banuelos et al., 1998). Therefore, the antiporter must also play a role when the cytoplasmic pH increases. Researches have shown that Nha1p buffers the cytosolic pH thanks to its capacity to extrude K^+ (Banuelos et al., 1998; Kinclova et al., 2001).

1.2.3. Compartmentalization of alkali metal cations

The yeast vacuole is the major site of intracellular storage for numerous molecules and ions (Klionsky et al., 1990), mainly K^+ (Okorokov et al., 1980) and Ca^{2+} (Halachmi and Eilam, 1996). This organelle plays an important role in ionic homeostasis, pH and osmoregulation (Bryant and Stevens, 1998). The vacuole contains a proton translocating ATPase, the V-ATPase (Figure 5) (Powell et al., 2000; Uchida et al., 1988). Thanks to the proton electrochemical potential difference imposed through the vacuolar membrane by the V-ATPase, numerous ions and metabolites are

transported into the vacuole against their chemical gradient (Klionsky et al., 1990).

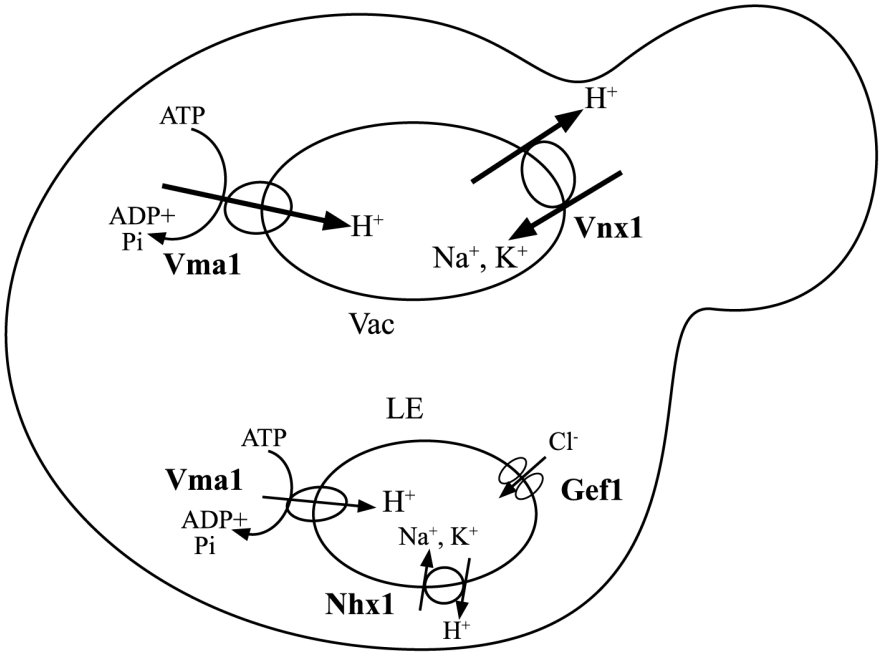

Figure 5. Transport systems involved in the compartmentalization of potassium and sodium in *S. cerevisiae*. Vma1, H^+-ATPase; Nhx1, K^+,Na^+/H^+ antiporter; Vnx1, K^+,Na^+/H^+ antiporter; Gef1, Cl^- channel. LE: Late Endosome; Vac: Vacuole.

Systematic sequencing of the yeast genome has revealed the presence of a gene on chromosome IV (*YDR456w*), which encodes a protein of 633 amino acids that Nass et al. (1997) appointed Nhx1 on the basis of

homology with the family of exchangers Na^+/H^+ (NHE1-9) found in mammals and other vertebrates (reviewed by Brett et al., 2005a). Nhx1p localizes itself to the endosomal/prevacuolar compartment (Nass and Rao, 1998) where it mediates intracellular transport of Na^+ by using the electrochemical proton gradient generated by the V-type H^+-ATPase. Efficient sequestration of Na^+ via Nhx1p requires additional presence of a chloride channel (Gef1p) in the prevacuolar membrane (Gaxiola et al., 1999) (Figure 5). The transport of chloride ions into the prevacuolar compartment via the Gef1p anion channel will neutralize the membrane potential, allowing further acidification of the compartment and increased activity of Nhx1p (Nass et al., 1997; Nass and Rao, 1998). More recently, it has been shown that Nhx1p transports K^+ in addition to Na^+ and that it is involved in the regulation of cellular pH and protein trafficking (Bowers et al., 2000; Brett et al., 2005b).

Another Nha1p homologue, Kha1p, has been identified in *S. cerevisiae*. Kha1p is a 97 kDa protein (873 amino acids) with 12 putative transmembrane domains and it has a very low level of expression. It was previously believed to extrude potassium from cells (Ramirez et al., 1998), but another study has shown that this protein does not carry out that function (Maresova and Sychrova, 2005). Indeed, it seems that the localization of Kha1p is in intracellular organelle (probably the Golgi apparatus) and its function is in relation with the regulation of ion

homeostasis and pH control. Kha1p has been described as a putative K^+/H^+ antiporter but its ability to mediate K^+/H^+ exchange has not been demonstrated yet.

Recently, Vnx1p has been identified and characterized as a new vacuolar monovalent cation/H^+ antiporter. Despite the homology of Vnx1p with other members of the CAX (calcium exchanger) family of transporters, Vnx1p is unable to mediate Ca^{2+} transport but it is a low affinity Na^+/H^+ and K^+/H^+ antiporter. *vnx1*Δ cells displayed growth inhibition when they are grown in the presence of hygromycin B or NaCl. Vnx1p activity was found in the vacuoles and proved to be dependent on the electrochemical proton gradient generated by the action of the V-type H^+-ATPase (Cagnac et al., 2007).

1.3. Illustration of a nutrient transport

1.3.1 Polyamines transport

The naturally occurring polyamines putrescine, spermidine and spermine have a low molecular weight, a simple chemical structure (aliphatic amines) and are highly charged cations at physiological conditions. Polyamines are essential for the maintenace of cell growth, survival and for macromolecular biosynthesis (Pegg and McCann, 1982). Therefore,

polyamines homeostasis is strongly regulated and depends on a balance between the rate of their biosynthesis, catabolism, excretion and uptake (reviewed by Porat et al., 2005). Their levels are tightly controlled, as low levels fail notably to support cell growth, while excesses are toxic because they stimulate abberant cellular proliferation. In yeast, polyamines uptake is energy dependent and it has recently been reported that Gap1p (Uemura et al., 2005) and Agp2p (Aouida et al., 2005) can catalize the uptake of polyamines together with amino acids in yeast and that Dur3p and Sam3p are polyamine transporters. Nevertheless, another polyamine uptake protein probably exists in yeast but it remains unidentified (Uemura et al., 2007). Concerning the excretion of polyamines, Uemura et al. (2005), have demonstrated that Tpo1p can excrete various substances including polyamines. The polyamine transport is illustrated in Figure 6.

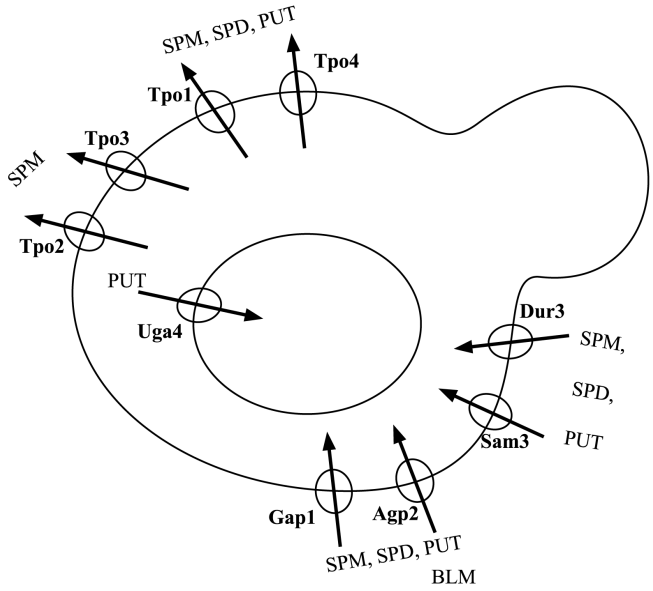

Figure 6. Polyamine transport in yeast (modified from Uemura et al., 2007)**.** Polyamine (SPM=spermine, SPD=spermidine, Put=putrescine) uptake is mainly catalyzed by Dur3 and Sam3. Putrescine uptake into vacuole is catalyzed by Uga4. Excretion of polyamines is catalyzed by Tpo1-4 located on the plasma membrane. Bleomycin (BLM) uptake is catalyzed by Agp2.

Interestingly, bleomycin contains a chemical structure similar to polyamines (annex 1). Bleomycin is a potent chemotherapeutic agent that can mediate cell death by attacking the DNA. It is used for treating various cancers including testicular carcinomas. Aouida et al. (2004a) revealed that the transport of bleomycin occurred in two phases, an early phase that may be time-independent and possibly due to passive

diffusion, and a late phase that is time dependent and may depend on a transporter. Using a genetic screen, they identified *PMP3* as a gene that cause sensitivity to bleomycin when deleted, and *AGP2* as a gene that cause resistance to bleomycin when deleted. Later, they showed that Agp2p is responsible for mediating the uptake of bleomycin into the cells (Aouida et al., 2004b) while the question about Pmp3p function is still not resolved.

2. *PMP3* related genes family

Many prokaryotic and eukaryotic organisms possess small molecular weight hydrophobic proteins that respond differently to stresses, such as cold temperature, salt and dehydration. For example, in plants, barley *BLT101.1* and *BLT101.2* genes were reported as low-temperature-inducible genes (Goddard et al., 1993). *Arabidopsis RCI2A* and wheatgrass *ESI3* play directly or indirectly a role in preventing accumulation of excess Na^+ and K^+ ions and contribute to salt tolerance (Mitsuya et al., 2005). *AcPMP3* in sheep grass has been proven to have a similar role (Inada et al., 2005). Moreover, in yeast, *PMP3* transcript is induced by salt stress (Yale and Bohnert, 2001) and the protein would be involved in controlling the plasma membrane potential, which, in turn, would control cations uptake in yeast cells (Navarre and Goffeau, 2000). All these proteins belong to the uncharacterized protein family (upf0057). These are small proteins from 52 to 140 amino-acid residues that contain two predicted transmembrane domains. Interestingly, they are not found in animals having complex organization such as vertebrates. Figure 7 shows the comparison among some representative examples of upf0057 related proteins from nematodes, fungi, prokaryotes and plants. Amino acids sequence similarity ranges from 41% to 78%, indicating that upf0057 proteins are conserved during evolution. Their hydropathy profiles (via the TMHMM program) predict two putative transmembrane

domains corresponding to hydrophobic regions. However, little is known about the function of upf0057 proteins. The high sequence similarity of upf0057 related proteins, their predicted common evolutionary origin and their conserved subcellular localization, suggest that upf0057 proteins may conserve a similar role (Medina et al., 2007). In this regard, complementation analysis have revealed that *AtRCI2A* from *Arabidopsis thaliana* (Navarre and Goffeau, 2000; Nylander et al., 2001), *WP16* from wheat (Koike et al., 2005), *AcPMP3* from sheep grass (Inada et al., 2005), *PutPMP3* from the alkali grass and *OsLti6a* from rice (Chang-Qing et al., 2008) restore the *pmp3Δ* strain growth in presence of high concentrations of hygromycin B and salt.

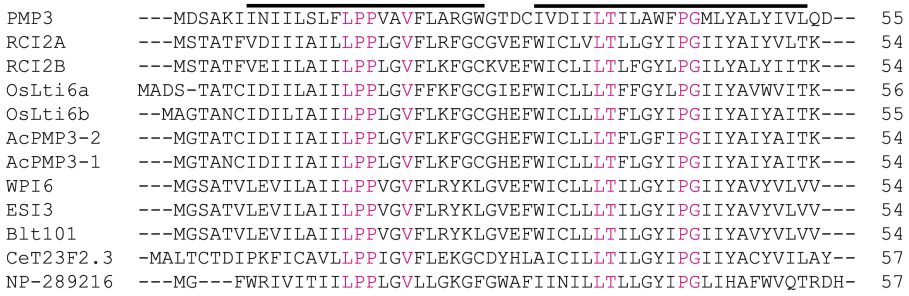

Figure 7. Sequence comparison of Pmp3p-related proteins. Alignement of amino acid sequences of Pmp3p/Sna1p and homologue proteins from different organisms, like *Arabidopsis thaliana* (RCI2A/B), *Oryza sativa* (OsLti6a/b), *Hordeum vulgare* (Blt101), *Aneurolepidium chinense* (AcPMP3-2/1), *Triticum aestivum* (WPI6), *Lophophyrum elongatum* (ESI3), *Caenorhabditis elegans* (CeT23F2.3), *Escherichia coli* (NP-289216). Bars over the sequences indicate the transmembrane domains (TMDs). The number of residues in each sequence is indicated on the right, conserved residues are in red. TMDs were predicted using the TMHMM software v. 2.0.

Upf0057 related genes often belong to gene families within the organisms. Medina et al. (2007) have identified six new *Arabidopsis* genes homologous to *AtRCI2A* and *AtRCI2B*. These 8 genes are distributed among four out of the five *Arabidopsis* chromosomes and only one corresponding protein is not localized to the plasma membrane. In rice and *C. elegans*, 12 and 13 different upf0057 related genes have been found respectively. At least, seven different upf0057 related genes were identified from wheat (*Triticum aestivum*), five from maize (*Zea mays*), and four from soybean (*Glycine max*). In yeast, Pmp3p has three homologues distributed on 2 chromosomes. Interestingly, it is also shown

that some *PMP3* related gene families from rice, sheep grass, alkali grass or *Arabidopsis* (Chang-Qing et al., 2008; Inada et al., 2005; Medina et al., 2001; Morsy et al., 2005) are differently regulated in response to abiotic stresses and their localizations in the cell. In addition to *AtRCI2A*, only *AtRCI2B*, *AtRCI2C*, and *AtRCI2H* genes are able to complement the *PMP3* deletion in yeast. These results suggest that all these proteins do not have exactly the same function. As already mentioned, Pmp3p/Sna1p has three homologues in yeast, called Sna2p, Sna3p and Sna4p which are localized in different subcellular compartments, multivesicular bodies (MVB) and vacuolar membrane (Pokrzywa et al., 2009; Reggiori and Pelham, 2001; Stawiecka-Mirota et al., 2007). These Sna proteins share high sequence identity through the two putative transmembrane domains (Figure 8).

```
                                 ___________________      ___________________
PMP3 ----------------MDSAKIINIILSLFLPPVAVFLARGW-GTDCIVDIILTILAWFPGMLYALYIVLQD--- 55
SNA2 ----------------MHARDWFLVFIAIFIPPLAVWLKRGFFTKDLLINFLLFLLGFFPGLIHALYVISCHPYE 56
SNA3 MDRDHINDHDHRMSYSINKDDLLLMVLAVFIPPVAVWKRKGMFNRDTLLNLLLFLLLFFPAIIHACYVVYETSSE 72
SNA4 ---------MCCYCVCCTVSDFILYIVAFFFPPAAVLLRSGPCSSDFLLNVLLTLLGFLPGMLHAFYYITITSPL 63

PMP3 ------------------------------------------------------------------------  55
SNA2 ENEARYSHLSSSDDNYGSLA--------------------------------------------------------  79
SNA3 RSYDLSRRHATAPAVDRDLEAHPAEESQAQPPAYDEDDEAGADVPLMDNKQQLSSGRT---------------- 105
SNA4 RNAEYVYYYQQGWVDSERNVPSNRPQNSQTPQNRPQQGSSARNVYPSVETPLLQGAAPHDNKQSLVESPPPYVP 123
```

Figure 8. Sna family sequences. Bars over the sequences indicate the transmembrane domains (TMDs). TMDs were predicted using the TMHMM software v. 2.0. Conserved residues are in red and known targeting motifs in bold. Alignement has been performed with ClustalW.

Strickingly, two well conserved prolines and a proline/glycine motif are predicted in the middle of the two TMDs. These PP and PG motifs could be important for the protein conformation and thus its function. Indeed, it has been reported that a proline residue in a peptide chain cannot form hydrogen bonds that stabilize an α-helix and it restricts the rotation of the backbone of the chain. Moreover, proline is the only naturally occurring amino acids for which both the cis and trans peptide bond conformations are thermodynamically feasible (reviewed Sansom and Weinstein, 2000). As a consequence, proline has a tendency to break α–helices and to form a hairpin-loop topology. In other words, it is possible that proline "switches" the protein topology from a membrane-associated hairpin form to a transmembrane form (Figure 9).

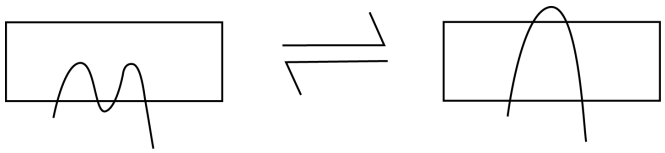

Figure 9. Scheme illustrating the hypothetical hairpin-loop and transmembrane topologies of Pmp3p.

Altough the TMDs are well conserved through the SNA family, very low similarity can be detected in the N- and C-terminal regions. It seems that the C-terminus is important for the localization of SNA proteins in the cell. Indeed, Sna2p possesses two important motifs (Y_{65}xxL and Y_{75}xxL)

responsible for its trafficking to the vacuolar membrane (Renard et al, 2010). Sna3p physically interacts with Rsp5p via its P_{78}PxY motif, and this interaction is essential for sorting of Sna3p to the endosomal pathway (Stawiecka-Mirota et al., 2007). And finally, Sna4p contains an acidic dileucine motif (E_{98}xxLL) which directs it to the vacuolar membrane. A second motif, P_{118}PxY, targets a part of Sna4p to the vacuole lumen thanks to its interaction with Rsp5p (Pokrzywa et al., 2009). Therefore we could postulate that different members from the Pmp3 protein family share a similar function but at a specific location in the cell and/or under specific conditions.

Pmp3p/Sna1p

In 1978, Dufour and Goffeau suggested the presence of proteolipidic material with the purified fungal H^+-ATPase (Dufour and Goffeau, 1978). But it is only in 1992 that Navarre and Goffeau (1994; 1992) purified a proteolipidic fraction extracted from yeast plasma membranes treated with chloroform-methanol. They microsequenced two small (38 residues) and highly hydrophobic isoproteins, named Pmp1p and Pmp2p. The deletion of both genes, *PMP1* and *PMP2*, significantly decreases the rate of ATP hydrolysis of Pma1p. A close examination of this chloroform-methanol extract revealed the presence of a third hydrophobic

polypeptide. Therefore, using the mutant strain containing a deletion of both *PMP1* and *PMP2* genes, they determined unambiguously the first 25 residues of Pmp3p. The open reading frame (ORF) was found to encode a highly hydrophobic 55 amino acid protein (Mr = 6109), which is predicted to contain two membrane-spanning segments. The *PMP3* gene is not essential under normal growth conditions (Navarre and Goffeau, 2000). However, its deletion increases Na^+ sensitivity in a strain deficient in the major plasma membrane Na^+ efflux system: the Ena1 Na^+-ATPase and Nha1 Na^+/H^+ antiporter. Loss of *PMP3* also partially suppresses the K^+ requirement of the *trk1Δtrk2Δ* mutant and reduces its hypersensitivity to low pH. They also showed that *pmp3Δ* strain is sensitive to toxic cations such as hygromycin B or tetramethylammonium (TMA) (Navarre and Goffeau, 2000). Moreover, a genome-wide screen using a *Saccharomyces cerevisiae* mutant collection identified *pmp3Δ* strain as a bleomycin hypersensitive mutant (Aouida et al., 2004b). Together, these results indicate that the absence of Pmp3p induces a hyperpolarization of the plasma membrane. However, unlike *PMP1* and *PMP2*, deletion of *PMP3* had no effect on Pma1p activity (Navarre and Goffeau, 2000). Hyperpolarization is a change in the membrane potential of the cell. Membrane potential is the voltage difference between the interior and the exterior of the cell. It depends on the action of ion channels, ion pumps and ion transporters embedded in the lipidic bilayer. Relatively static

membrane potential of cells is called resting membrane potential. It is expressed as a negative value because the interior of the cell is negative with respect to the exterior, as the negative charges inside the cell are in slight excess over positive charges (Maresova et al., 2009). Therefore, when the membrane is hyperpolarized, the membrane potential is more negative.

It is interesting to note that *PMP3* deletion mimics Nsc1p activation (described above): it increases the Na^+ sensitivity but reduces the K^+ dependance of the *trk1Δtrk2Δ* strain. Moreover, calcium reverses the phenotypes of *PMP3* deleted strain, which implies again a link between Pmp3p and Nsc1p (Bihler et al., 2002). These different phenotypes are summarized in the Table 1 below.

Table 1: Phenotypes of *PMP3* deleted strain.

	WT	***pmp3Δ***
Hygromycin (100 µg/ml)	Resistant	Sensitive
Hygromycin (100 µg/ml) + $CaCl_2$ (10 mM)	Resistant	Resistant
NaCl (1 M)	Resistant	Sensitive
NaCl (1 M) + $CaCl_2$ (10 mM)	Resistant	Resistant
Bleomycin (5 µg/ml)	Resistant	Sensitive

Surprisingly, a few years later, Erez and Kahana (2002) showed that the disruption of *PMP3* slightly improves growth in the presence of LiCl (0.2

M) and confers moderate spermine tolerance (0.2 mM) (Erez and Kahana, 2002). It is particularly noteworthy since it distinguishes the Pmp3 protein from many other yeast proteins involved in the regulation of the plasma membrane potential. Indeed, it is known that monovalent cations like hygromycin B (annex 1) (Mulet et al., 1999), Na^+, Li^+ (Goossens et al., 2000) and spermine (annex 1) (Erez and Kahana, 2001) enter cells in amounts proportional to their membrane potential. The LiCl resistance was also confirmed by another group (Nylander et al., 2001) and those two phenotypes (lithium and spermine resistance) therefore suggest, in addition to the hyperpolarization, a more specific role in lithium and spermine tolerance for the Pmp3 protein.

3. Plasma membrane compartmentalization

The understanding of membranes has long rested on the principle of Davson and Danielli (Danielli and Davson, 1935) which assumes that the bilayer contains only phospholipids, neutral lipids and glycolipids, with membrane proteins covering the two polar interfaces of the bilayer. The fluid-mosaic model, proposed by Singer and Nicholson in the early 1970s (Singer and Nicolson, 1972), was a major conceptual breakthrough not only because it recognized that amphiphilic proteins reside within the bilayer but also because it viewed the membrane as a dynamic structure. In fact, it became clear that the membrane components 'travel' laterally within the two-dimensional fluid membrane (Frye and Edidin, 1970) and, in addition, that the thickness of the membrane at any given point varies with time (Borochov and Shinitzky, 1976). Further extensive research of biological and model membranes have led to major modifications of the Singer–Nicholson model. For example, more and more clues would indicate that the plasma membrane is compartmentalized. Indeed it was observed that membrane lipids and proteins do not distribute randomly over the membrane (Lisanti and Rodriguez-Boulan, 1990; van Meer and Simons, 1982). Some classes of membrane associated proteins are sequestered within small compartments of the membrane, thus enhancing protein–protein interactions and speeding up signal transduction and enzymatic reactions (Casey, 1995; Sargiacomo et al., 1993). Another

factor in favor of the membrane compartmentalization is the observation of the coexistence of two liquid lipid phases in bilayers containing high fractions of cholesterol – a phenomenon not observed in phospholipid mixtures in the absence of sterols. According to Ipsen et al. (1987), it is caused by the existence of two distinct types of liquid phases: a liquid-ordered (lo) phase and a liquid-disordered (ld) phase. A few years later, in addition of sterols and phospholipids without unsaturated side chains, it has been shown that sphingolipids favored the clustering of these liquid-ordered domains (Mouritsen and Jorgensen, 1997). The underlying basis for this is that sterols are composed of a four-ring structure and an aliphatic tail that can pack together in a favorable manner with both sphingolipids, which are comprised of sphingosine and long saturated acyl chain, and with the saturated side chains of the phospholipids (Megha et al., 2006) (Figure 10). The lipid acyl chains pack tightly with the rigid sterols to create a compacted zone of condensed bilayer that has been termed as liquid-ordered state. Individual lipid molecules have a high degree of lateral diffusion in this bilayer (Brown and London, 1998; Munro, 2003). Glycerophospholipids with unsaturated side chains do not pack in this manner and are excluded from those domains. In model membrane, lo-phase domains can coexist with liquid-disordered (ld)-phase domains, in which lipids are much less condensed, and with gel-phase domains, in which lipids are highly condensed and essentially

immobile (Heberle et al., 2005). The raft hypothesis proposes that lo-phase domains also form in sterol-rich cell membranes, especially the plasma membrane, where they coexist with disordered membrane domains (Hancock, 2006; Lagerholm et al., 2005; Pike, 2003).

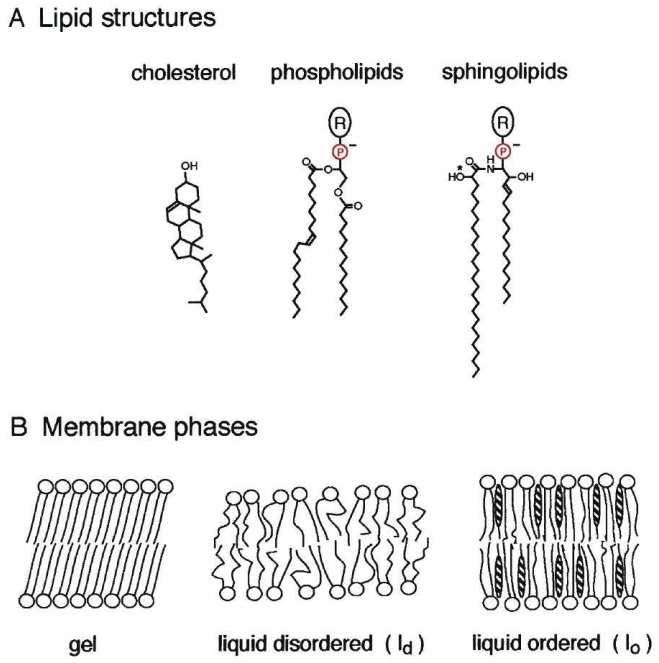

Figure 10. The lipids of the plasma membrane (Munro, 2003) (A) Structures of the major lipid classes of eukaryotic cells. (B) Structures of lipid bilayers with the sterol which pack the lipid acyl chains in the liquid ordered phase.

The first concept of plasma membrane compartmentation comes from mammalian cells and more precisely from the epithelial cells which are polarized into apical and basolateral domains with different protein and lipid compositions in each of these domains (Simons and Ikonen, 1997; Simons and van Meer, 1988). Then, a first method to biochemically define these microdomains is created and is based on the resistance to extraction by Triton X-100 at 4°C (Brown and Rose, 1992). Indeed, because of their unique lipid composition, the liquid-ordered domains are more resistant to extraction by nonionic detergents also explaining why these domains are sometimes referred to as detergent resistant membranes (DRMs). However, much like many other techniques, DRMs extraction characterizes the properties of a molecule in terms of its differential affinity to various (artificial) environments. This is undoubtedly interesting, but the discovery of DRMs does not seem to justify the conclusion that microdomains are present in the native membrane, and finding a molecule in DRMs does not prove its localization in microdomains (and vice versa) (Korzeniowski et al., 2003). Despite the limitations of detergent-dependent methods and the caution that must be exercised when interpreting the resulting data, the isolation of DRMs remains a useful tool for investigating protein–lipid interactions and membrane domains (Brown and London, 1998; Shogomori and Brown, 2003).

A complementary approach consists in visualizing microdomain components directly in the plasma membrane of living cells. Membrane microdomains in living cells have been visualized by microscopy in the budding yeast *S. cerevisiae* (Malinska et al., 2003; Young et al., 2002), in plants (Homann et al., 2007; Sutter et al., 2006) and even in bacteria (Johnson et al., 2004; Matsumoto et al., 2006). New high resolution techniques of light microscopy can be used to visualize even very small microdomains in mammalian cells (Tian et al., 2007).

Therefore, it is interesting to note that plasma membranes from most organisms seem to be compartimentalized. Plasma membranes differ from most subcellular membranes because they contain a high fraction of sterols and sphingolipids in addition to the glycerophospholipids. Although the pioneering studies on microdomains and their biological roles have been primarily carried out in mammalian cells, the general properties of plasma membrane organization and lipid raft function appear to be similar in fungi. Indeed, in mammalian cells, cholesterol, sphingomyelin, and glycosphingolipids are the basic constituents of rafts (Rietveld and Simons, 1998), whereas in yeast these are ergosterol, inositolphosphoceramide, and its mannosylated derivatives (Bagnat et al., 2000; Kubler et al., 1996). The primary sterol found in fungi is ergosterol, which is a better raft component than cholesterol (Xu et al., 2001). The

next part will now focus on the study of plasma membrane organization in *S. cerevisiae*.

Different studies (Grossmann et al., 2007; Malinska et al., 2003; Malinska et al., 2004) show that the plasma membrane proteins in *S. cerevisiae* are distributed in different modes: they are concentrated in discrete patches (called MCC for *m*embrane *c*ompartment occupied by *C*an1p), each patch being ~300 nm in diameter, or they occupy a mesh-shaped compartment, which spreads between the patches, or they are homogeneously dispersed throughout these two areas. Walther and coworkers have recently discovered large immobile structures called eisosomes (from the Greek “eis” meaning “into” or “portal” and “some” meaning “body”), which are closely related to the MCC patches, and mark sites of endocytosis (Moreira et al., 2009; Walther et al., 2006). Moreover, a fourth mode of plasma membrane distribution has just been discovered by Berchtold and Walther (2009). It consists in a patchy distribution different from the others. Finally, recent studies based on filipin staining have identified sterol-rich domains in fungi that are much greater in size than the microdomains mentioned above and which have not been seen in mammalian cells (reviewed by Alvarez et al., 2007).

3.1. Sterol-rich membrane domains (SRD)

The sterol-rich membrane domains have been identified by the fluorescent dye filipin (Severs, 1997) which binds to the sterols of the plasma membrane (see annex 1). Several fungal species, including the budding yeast *Saccharomyces cerevisiae*, the fission yeast *Schizosaccharomyces pombe* as well as the pathogens *Cryptococcus neoformans* and *Candida albicans*, show sterols enriched areas (Bagnat and Simons, 2002; Martin and Konopka, 2004; Nichols et al., 2004; Wachtler et al., 2003). These large SRDs are located at sites of active morphogenesis and are regulated in a developmental or cell cycle-dependent manner. For example, SRDs were detected at the tips of mating projections in *Saccharomyces cerevisiae* and hyphae in *Candida albicans*, but not in budding cells. In the fission yeast *Schizosaccharomyces pombe*, a SRD is formed in a cell-cycle regulated manner in the medial zone of the rod shaped cells at the future site of cell division. Examples of filipin staining are shown in Figure 11. Although the size of microdomains is still debated, it is safe to assume that microdomains are much smaller than the filipin-stained domains which might represent clusters of microdomains. A filipin staining indicates the relative distribution of sterols in the membrane; whether a sterol enrichment is related to functional lipid rafts should be the object of further investigation.

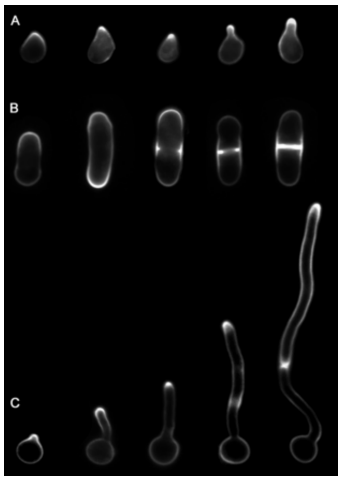

Figure 11. Examples of filipin staining (Alvarez et al., 2007). (A) *S. cerevisiae* cells induced with α-factor. (B) *S. pombe* cells grown to log phase. (C) *C. albicans* induced to form hyphae with serum. The cells were stained with filipin and then viewed by fluorescence microscopy.

3.2. Plasma membrane microdomains in the yeast *S. cerevisiae*

Until now, four different kind of microdomains have been observed in the yeast plasma membrane. Tanner and collaborators (2003) have shown that two proteins, the Pma1 H^+-ATPase and the arginine permease Can1, are located in mutually exclusive discrete domains in the plasma membrane of cells (Figure 12) (Malinska et al., 2003). The compartment defined by the presence of Pma1p is called the *m*embrane *c*ompartment occupied by *P*ma1p (MCP), whereas the *m*embrane *c*ompartment occupied by *C*an1p (MCC) contains several other proteins, namely the

uracil permease Fur4 (Malinska et al., 2004), the Sur7 protein (Malinska et al., 2004), the tryptophan permease Tat2 (Grossmann et al., 2007), and the heterologously expressed hexose transporter Hup1 of *Chlorella kessleri* (Grossmann et al., 2006). At the same time, Walther and coworkers observed a similar patchy distribution for Pil1 and Lsp1 proteins and called these plasma membrane structures eisosomes. It will be shown subsequently that the components of eisosomes colocalize with those of MCC (Walther et al., 2006). Whether MCC and eisosomes define the same structure is still not known although they are closely connected at the plasma membrane. Both MCC/eisosomes and MCP compartments are stable over time (Malinska et al., 2003), and they are independent of the actin or microtubule cytoskeleton and of the cell wall (Malinska et al., 2004). Recently, Walther's team has described the TORC2 localization in a previously unrecognized plasma membrane domain (Figure 12) (Berchtold and Walther, 2009). They called it membrane compartment containing TORC2 (MCT). These three sub-compartments will be discussed more precisely in the following paragraphs. A fourth mode of distribution exists, containing Gap1p and Hxt1p that are distributed homogeneously to the plasma membrane (Lauwers et al., 2007; Malinska et al., 2003).

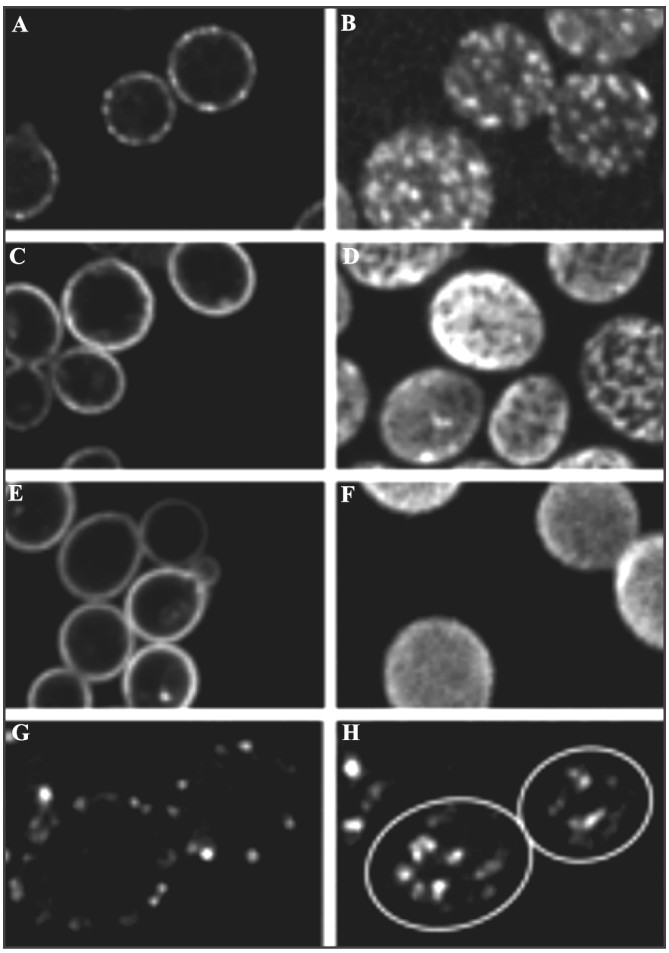

Figure 12. Localization of different proteins within the plasma membrane (Berchtold and Walther, 2009; Malinska et al., 2003). Fluorescence patterns of Can1p-GFP (A and B), Pma1p-GFP (C and D), Hxt1p-GFP (E and F), and subunit of TORC2 tagged with GFP (G and H) in living *S. cerevisiae* cells are shown. An individual transverse optical section (A, C, E, and G) and superposition of four consecutive surface optical sections (B, D, F, and H) are presented for each protein.

3.2.1. Membrane compartment of Can1p (MCC) and eisosomes

Independent works based on the examination of a library of yeast proteins tagged with GFP have highlighted a similar patchy distribution in the plasma membrane for 21 proteins. These proteins are presented in Table 2. Surprisingly, 9 of these proteins are membrane proteins because they possess at least 4 TMD but 12 proteins are soluble. For clarity, we will identify the membrane components to the MCC (Grossmann et al., 2008) and the soluble components to the eisosomes (Walther et al., 2006). It has been postulated that eisosomes lie underneath each MCC, forming a punctate pattern in the cell periphery. The MCC contains, in addition to the arginine transporter Can1, two other proton symporters, Fur4 and Tat2, a family of four tetraspan proteins of unknown function (Sur7, Fmp45, Ylr414c and Ynl194c), one protein (Nce102) which probably acts as a sensor of sphingolipids and finally one protein of unknown function (Ygr131w). Pil1 and Lsp1 proteins are the most studied cytosolic proteins associated with eisosomes. This list makes no claim to be complete, but it already presents a considerable number of proteins, which either reside within the membrane or are situated intracellularly. We will look in more details on these various proteins in the following text.

Yeast mother cells possess ~50 MCC/eisosomes that can be visualized as discrete foci in the plasma membrane (Deng et al., 2009; Frohlich et al., 2009). It was also reported that the MCC contain a distinct lipid

composition enriched in ergosterol, as visualized by staining with filipin (Grossmann et al., 2007; Malinska et al., 2003). However, they are distinct from the SRDs that are only observed at sites of active morphogenesis and are much bigger. As already mentioned, the number and the positions of the MCC/eisosomes were shown to be stable (Malinska et al., 2003) and independent from the main cytoskeletal components (Malinska et al., 2004). However, the expression of proteins like Can1p, Fur4p or Tat2p, and consequently their appearance in the plasma membrane, is substrate-regulated (Kodama et al., 2002; Seron et al., 1999). Therefore, these proteins appear in the patches in different amounts and at different times. Thus, the composition of the MCC patches changes in time and depends on the cell physiology.

Interestingly, a recent paper has showed that MCC patches and eisosomes correspond to furrow-like invaginations of the plasma membrane (Stradalova et al., 2009). These are highly conserved plasma membrane structures reported in early freeze-fracture studies (Moor and Muhlethaler, 1963).

Table 2. Members of MCC/eisosome (Grossmann et al., 2008). TMD, transmembrane domain. Putative transmembrane domains are given as predicted by transmembrane hidden Markov model (TMHMM).

Name	Molecular function	TMDs
Integral MCC components		
Can1	Arginine transporter	12
Fur4	Uracil transporter	12
Tat2	Tryptophan and tyrosine transporter	12
Nce102	Unknown	4
Fmp45	Unknown	4
Sur7	Unknown	4
Ygr131w	Unknown	4
Ylr414c	Unknown	4
Ynl194c	Unknown	4
MCC-associated cytosolic proteins		
Lsp1	Component of eisosome	0
Pil1	Component of eisosome	0
Mdg1	Unknown	0
Pkh1	Ser/Thr protein kinase	0
Pkh2	Ser/Thr protein kinase	0
Pst2	Unknown	0
Rfs1	Unknown	0

Slm1	Phosphoinositide binding	0
Slm2	Phosphoinositide binding	0
Ycp4	Unknown	0
Ygr130c	Unknown	0
Ymr031c	Unknown	0
Ymr086w	Unknown	0

Overview of some proteins detected in MCC/eisosomes

Pil1p and Lsp1p

Pil1 and Lsp1 are the major cytosolic proteins associated with eisosomes. Each eisosome contains ~2000–5000 copies of Pil1 and Lsp1 (Deng et al., 2009). It has been shown that Pil1p controls eisosome biogenesis (Moreira et al., 2009). Deletion of *PIL1* is reported to lead to clustering of the eisosomes to a few spots (called eisosomes remnants) that are associated with aberrant plasma membrane invagination (Walther et al., 2006). Moreover, in *pil1*Δ strain, a significant fraction of MCC transmembrane proteins, such as Sur7, Can1 and Fur4, localizes uniformly in the plasma membrane and at eisosome remnants. Similarly, the ergosterol marker filipin looses its normal punctate eisosome localization in *pil1*Δ cells and distributes more homogeneously over the plasma membrane surface (Grossmann et al., 2007).

Pkh kinases and Nce102 protein

It has been shown that Pkh kinases localize at eisosomes and that Pil1 and Lsp1 proteins are Pkh kinase substrates (Luo et al., 2008; Walther et al., 2007; Zhang et al., 2004). In addition of eisosome assembly, Pkh kinases regulate physiology and plasma membrane functions such as actin patch organization and endocytosis (Daquinag et al., 2007; deHart et al., 2002; Friant et al., 2001; Grosshans et al., 2006; Inagaki et al., 1999; Liu et al., 2005; Luo et al., 2008; Sun et al., 2000; Walther et al., 2007). The Pkh kinases are homologues of mammalian phosphoinositide-dependent kinases, which influence a variety of processes including endocytosis, cell wall integrity, actin localization, and response to heat stress (Dickson, 2008). Pkh kinases are regulated by sphingoid long chain bases such as phytosphingosine (PHS) and dihydrosphingosine, which are precursors in sphingolipid synthesis (Zhang et al., 2004). In a new study, Frölich and coworkers have identified Nce102p in a genome-wide screen for genes involved in eisosome organization and Pkh kinase signaling. Nce102p possesses 4 putative TMD and it is an excellent example of MCC proteins functionally associated with cytosolic proteins of eisosomes. The relative abundance of Nce102p in these domains compared to the surface of the plasma membrane is dynamically regulated by sphingolipids. Furthermore, Nce102p inhibits Pkh kinase signaling and is required for

plasma membrane organization (Figure 13). Moreover, Pil1p hyperphosphorylation caused by decreased sphingolipid synthesis causes eisosome disassembly (Walther et al., 2007). Therefore, Nce102p might act as a sensor of sphingolipids that regulates plasma membrane function.

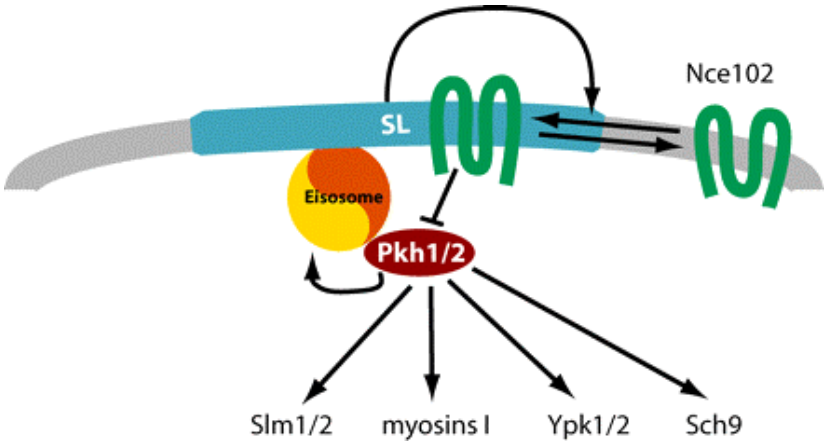

Figure 13. Model for Nce102p function in sphingolipid sensing (Frohlich et al., 2009). SL: Sphingolipids.

Can1p, Fur4p and Tat2p

Until now, Can1p, Fur4p and Tat2p are the only three yeast transporters located in the MCC. They transport respectively arginine, uracil and tryptophane/tyrosine. Interestingly, they are all H^+-symporters, but other studies have still to confirm whether all yeast symporters are localized in the MCC or whether their functionalities require that location. Moreover,

these H^+ symporters are distinct from the other MCC components in that they are present in the MCC in a manner that depends on the membrane potential (Grossmann et al., 2007). Indeed, partial depolarization of the plasma membrane caused by an uncoupler, by mitochondrial mutations, or by applying an external electric field, results in a massive redistribution of these H^+-symporters. Yeast H^+-symporters move out of the patches under depolarizing conditions (Grossmann et al., 2007).

Independent researches have revealed that the MCC localization of Can1, Tat2 and Fur4 proteins is affected in mutants presenting a decreased content of sphingolipids or sterols (Dupre and Haguenauer-Tsapis, 2003; Malinska et al., 2003; Umebayashi and Nakano, 2003). Indeed, most of the Can1p-GFP in *erg24* cells and in *erg6* cells (Figure 14) (Daum et al., 1998) remained in perinuclear or peripheral endoplasmic reticulum and did not reach the plasma membrane.

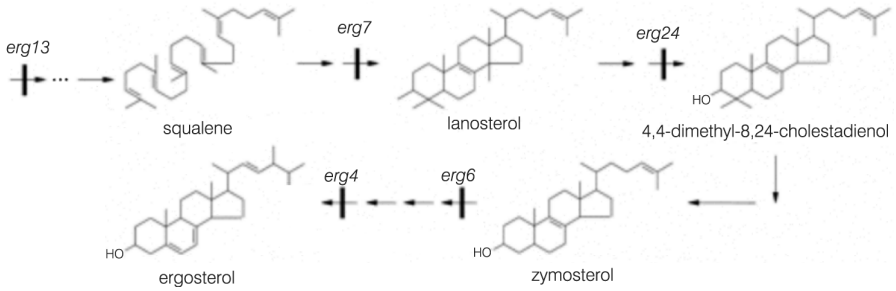

Figure 14. Pathway of ergosterol biosynthesis in *S. cerevisiae* (Grossmann et al., 2006). Only the *erg7* mutation, blocking the conversion of squalene epoxide via ring closures to lanosterol, is lethal.

Moreover, vacuolar degradation of a significant amount of Can1-GFP is observed in sphingolipid-deficient *lcb1-100* cells. The *lcb1-100* mutation (Zanolari et al., 2000) is a temperature-sensitive mutation in a subunit of serine palmitoyltransferase that blocks the first step of the sphingolipid biosynthetic pathway (Figure 15) (Malinska et al., 2003).

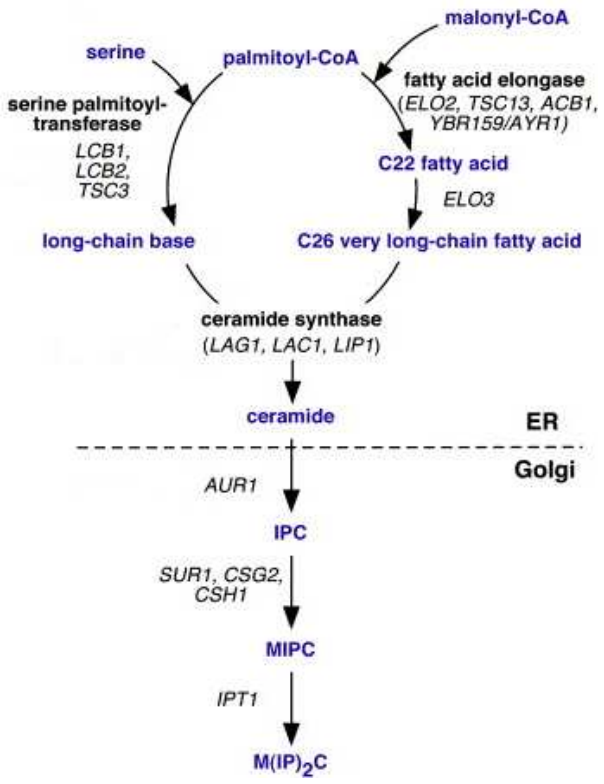

Figure 15. Outline of the sphingolipid biosynthetic pathway in *S. cerevisiae* (Toulmay and Schneiter, 2007). IPC is for inositol-phosphoceramide, MIPC for mannose-inositol-phosphoceramide and $M(IP)_2C$ for mannose-(inositol-$P)_2$-ceramide.

Similarly, the tryptophan permease Tat2 requires ergosterol for the plasma membrane targeting (as demonstrated in *erg13* cells, Figure 14) and experiments with the *sec14* mutants grown in low tryptophan conditions have indicated that Tat2p becomes associated with detergent-resistant membranes in the Golgi (Figure 16) (Umebayashi and Nakano, 2003).

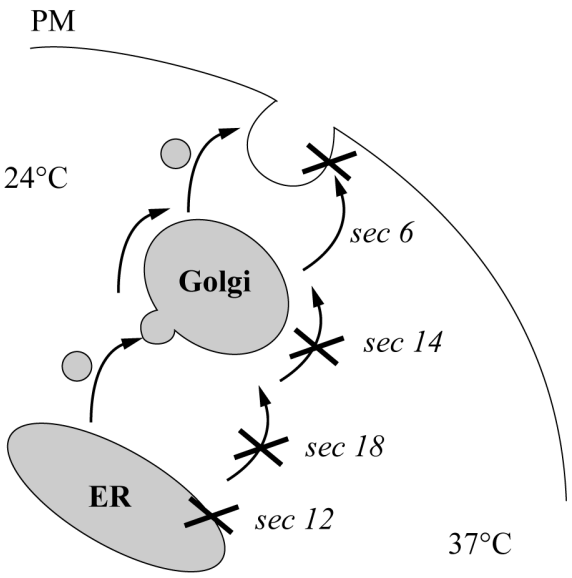

Figure 16. Schematic illustration of the trafficking of a membrane protein from the ER to the plasma membrane through the secretory pathway. The protein biogenesis is blocked by temperature-sensitive mutations in genes that govern successive steps of the pathway: *SEC12* (ER to COPII vesicles), *SEC18* (ER to Golgi complex), *SEC14* (Golgi complex to secretory vesicles) and *SEC6* (secretory vesicles to plasma membrane).

Dupre and coworkers (2003) observed, using the *lcb1-100* mutant, a delay in Fur4p plasma membrane targeting. Fur4p seems to be associated with DRMs early in the secretory pathway because newly synthesized Fur4p is TX100-insoluble in a *sec18* mutant at restrictive temperature (Figure 16) (Dupre and Haguenauer-Tsapis, 2003; Hearn et al., 2003).

Interestingly, a heterologously expressed glucose/H^+-symporter (Hup1p) of *Chlorella kessleri* (Sauer et al., 1990) is also localized in yeast MCC (Grossmann et al., 2006). Moreover, as reported, the targeting of this protein to the plasma membrane in the *erg6* mutant is almost homogeneously distributed and not concentrated in the typical 300-nm patches. Similar pictures were obtained with the *erg24* mutant and the *lcb1-100* mutant (Grossmann et al., 2006). In addition, the sterol enrichment found in MCC is confirmed by a lipid analysis of Hup1p purified to homogeneity from yeast membranes that have revealed that the protein is specifically associated with ergosterol (Robl et al., 2000).

Sur7p , Fmp45p, Ylr414c, Ynl194c

Saccharomyces cerevisiae contains a family of integral proteins (4 putative TMDs) localized in the MCC/eisosomes, including Sur7p, Fmp45p, Ynl194p and Ylr414p (Sivadon et al., 1997; Young et al., 2002).

Their function is not known but these four paralogs contain a cysteine motif in the middle of the first extracellular loop which is very similar to the conserved motif found in the claudin family of tetraspanning proteins (Alvarez et al., 2008). The claudin proteins associate to form tight junctions in animal cells (Furuse and Tsukita, 2006), suggesting a common role for the yeast membrane proteins in specialized membrane domains. An interesting feature is that Sur7p, like Nce102p, are transmembrane protein continuously localized to MCC, even in the absence of membrane potential (Grossmann et al., 2007).

Unknown proteins

The remaining 10 proteins suffer from a lack of information; however, some indications can help to better understand these new structures that are the MCC/eisosomes. Indeed, the promoter of Ygr131w contains a sterol regulatory element motif (Agarwal et al., 2003), which could make sense knowing that the amount of sterol is abundant in the MCC. Slm1 and Slm2 are proteins implicated in the organization of the actin cytoskeleton. Pst2, Rfs1 and Ycp4 are proteins with similarities to members of a family of flavodoxin-like proteins (Grandori and Carey, 1994) and Pst2p is induced by oxidative stress (Lee et al., 1999). And finally, the team of Krutchinsky has recently discovered that Ygr130c,

Ymr031c and Ymr086w physically interact and colocalize with Lsp1p and thus are integral components of eisosomes (Deng et al., 2009).

3.2.2. Mesh-shaped membrane compartment of Pma1p (MCP)

Pma1p is excluded from the MCC compartment and apparently occupies other space of the cell surface, called the MCP (Grossmann et al., 2006; Malinska et al., 2003; Malinska et al., 2004). The fact that Pma1p mediates proton efflux unlike Can1p, Fur4p and Tat2p may explain the segregation in a different compartment of the plasma membrane for these proteins. Furthermore, unlike proteins localized to the MCC, only the content in sphingolipids seems required for proper localization of Pma1p to the MCP. Indeed, research carried out by the Schekman and Chang laboratories have established that the biogenesis of Pma1p only depends on ongoing sphingolipid synthesis and not on ongoing ergosterol synthesis. Using the *lcb1-100* mutant, these groups showed that an ongoing long-chain base synthesis is required for oligomerization of Pma1p in the ER membrane and for its association with detergent-resistant membranes. In the absence of long-chain base synthesis, monomeric, non-DRM associated Pma1p is still exported from the ER but it is mistargeted to the vacuole and degraded (Bagnat et al., 2001; Lee et al., 2002).

Schneiter laboratory confirmed the role of lipids in surface trafficking of Pma1p because they observed that Pma1p was rapidly degraded in cells that fail to elongate the ceramide-bound C22 fatty acid to the mature C26 very long-chain fatty acid, as it is the case in cells lacking Elo3p, a component of the ER localized acyl chain elongase (Figure 15). Interestingly, this rapid turnover of Pma1p in the *elo3*Δ mutant correlates with a lack of the newly synthesized protein to acquire detergent resistance. Turnover of Pma1p in *elo3*Δ is dependent on ongoing endocytosis, indicating that the protein reaches the plasma membrane first, but that it fails to become stabilized there and instead is endocytosed and delivered to the vacuole for degradation (Eisenkolb et al., 2002; Oh et al., 1997).

Surprisingly, other mutations that affect the structure of the sphingolipid head group or its hydroxylation pattern did not affect DRM association or turnover of Pma1p (Gaigg et al., 2005). These results thus suggested that the synthesis of C26-containing lipids rather than ceramide or sphingolipids per se is important for stable delivery of newly synthesized Pma1p to the cell surface and for its DRM association.

Pulse chase analysis revealed that Pma1p was stable in all the viable mutants that affect ergosterol biosynthesis. Even a total block of the ergosterol synthesis induced by terbinafine, an inhibitor of squalene

epoxidase, did not affect the stability of newly made Pma1p in the MCP (Gaigg et al., 2005).

The association of Pma1p with DRMs takes place in the ER apparatus (Bagnat et al., 2000; Wang and Chang, 2002), suggesting that the association of plasma membrane proteins with DRMs occurs at early steps (ER or Golgi) in the secretory pathway.

Pma1p is the most abundant protein in the yeast plasma membrane, does this gives it the privilege of occupying alone the MCP? Until now, no protein has been shown colocalized with Pma1p. However, several indications lead us to believe that Nha1p could be located in the MCP with Pma1p. First, Mitsui and collaborators observed a regular punctate distribution pattern of Nha1p-GFP throughout the cell membrane. Second, the fact that unlike sphingolipids, ergosterol is not essential for the proper localization of Nha1p-GFP to the plasma membrane drives us to classify this protein in the MCP compartment, knowing that the colocalization with Pma1p has neither been demonstrated nor disproved (Mitsui et al., 2009).

Surprisingly, these same authors have shown that the association of Nha1p with DRMs occurs predominantly at the plasma membrane, the last stage of the secretory pathway, rather than in the ER or Golgi (Mitsui et al., 2009).

3.2.3. TORC2 plasma membrane localization (MCT)

A third domain exists in the yeast plasma membrane; it has recently been termed as *m*embrane *c*ompartment containing *T*ORC2 (MCT) (Berchtold and Walther, 2009). According to these authors, this domain does not correspond to MCC or MCP. It is known that the conserved target of rapamycin (TOR) kinases (Heitman et al., 1991) regulate many aspects of cellular physiology. They exist in two distinct complexes, termed as TOR complex 1 (TORC1) and as TOR complex 2 (TORC2), which posses both overlapping and distinct components. TORC1 and TORC2 respond differently to the drug rapamycin and have different cellular functions: whereas the rapamycin-sensitive TORC1 controls many aspects of cell growth and has been characterized in great detail (reviewed bySoulard et al.), the TOR complex 2 is less understood and regulates actin polymerization, efficient endocytosis, cell polarity, and sphingolipid metabolism (Aronova et al., 2008; deHart et al., 2003; Jacinto et al., 2004; Kunz et al., 1993). TORC1 and TORC2 have different localizations in *Saccharomyces cerevisiae*. Indeed, TORC1 is localized exclusively to the vacuolar membrane, whereas TORC2 is localized in a previously unrecognized plasma membrane domain (Berchtold and Walther, 2009).

3.2.4. Homogeneous distribution of the plasma membrane: Hxt1, Gap1

Surprisingly, two proteins are not localized in one of the three subcompartments of the yeast plasma membrane. Indeed, Hxt1-GFP and Gap1-GFP display a rather homogeneous signal at the plasma membrane, and do not colocalize with MCC or MCP components (Lauwers et al., 2007; Malinska et al., 2003).

On the other side, de novo sphingolipids but not the ergosterol biosynthesis are crucial for the general amino acids permease to be functional and stable at the plasma membrane. Indeed, the permease synthesized in the *lcb1-100* mutant at the restrictive temperature of 37°C is delivered to the cell surface, but it is rapidly down-regulated in a ubiquitin-dependent manner. However, the fate of Gap1 protein in the *erg6*Δ mutant is not modified (Lauwers and Andre, 2006).

Moreover, experiments with thermosensitive *sec* mutants suggest that newly synthesized Gap1 acquires detergent insolubility at the level of the Golgi complex (Lauwers and Andre, 2006).

3.2.5. Biogenesis and function of microdomains in yeast

We note that for many of these proteins localized in different microdomains, the ergosterol and/or sphingolipids content plays an important role in their correct localization. Moreover, two independent

screens identifying mutants affecting the MCC formation confirm the importance of these two compounds in the structure of these membrane domains. Indeed, two categories of genes are overrepresented: mutants involved in vesicular transport and those involved in lipid metabolism (Frohlich et al., 2009; Grossmann et al., 2008). In fact, these two categories are functionally interconnected. The membrane proteins are trafficked with lipids within the vesicle membrane. One possibility is that during its biogenesis, the protein is associated with neosynthesized ergosterols and/or sphingolipids. What it would be incorporated into the plasma membrane in areas enriched in ergosterol and/or sphingolipids. These intrinsic plasma membrane proteins tightly associated with lipids are at the heart of the “lipid shell” model proposed by Anderson and Jacobson (2002). This model suggests that some transmembrane proteins have an affinity for sterols and/or sphingolipids and that they become surrounded by a shell of these lipids during their synthesis. Because of the molecular compatibility between lipids of the shell and those present in rafts, these proteins would be inclined to associate with pre-existing rafts. This might explain why lipid rafts selectively include (or exclude) some proteins, which acquire then some specific functional properties (Anderson and Jacobson, 2002). This assumption is supported by the fact that in many cases the protein is already associated with DRM at the level

of ER or Golgi. Even if this experiment based on the triton insolubility must be approached with caution.

However, for the first time, Mitsui and coworkers have recently demonstrated that a plasma membrane protein associates itself with DRMs in the plasma membrane rather than the ER or Golgi. So, why not imagine that Nha1p specifically recognize microdomains without any "lipid shell". An interesting model suggests that sterols and sphingolipids interact specifically and functionally in biological membranes. Indeed, a recent study provided evidence that cells adjust their membrane composition in response to mutant sterol structures preferentially by changing their sphingolipid composition. Moreover, it is shown that sterols and sphingolipids function together to carry out a wide variety of cellular functions (Guan et al., 2009). However, it remains to prove that the increased order produced by sterol-sphingolipid interactions is important for function and that the segregation of the proteins in different microdomains is really due to the content in sterol-sphingolipid and even phospholipids.

In mammalian cells, microdomains enriched in sphingolipids and cholesterol are involved in numerous cellular functions, from membrane traffic and cell morphogenesis to cell signaling (reviewed by Munro,

2003). The precise molecular function of the yeast microdomains is still unclear.

An interesting link between plasma membrane compartmentation and protein turnover has been proposed by Grossmann *et al.* (2008). Indeed, they showed that the MCC localization protects symporters proteins against endocytosis and thus allows to regulate their activity. This has been shown via three approaches. They first showed that components of endocytosis does not colocalized with those of MCC. They also observed a faster Can1p internalization when MCC are destabilized in both *pil1*Δ and *nce102*Δ mutants. And finally, they observed a gradual release of Can1-GFP from its compartment when endocytosis was induced by an excess of arginine. Collectively, the separation of the endocytosis machinery from MCC and the delayed rate of endocytosis in wild type cells support the idea of MCC as a protective area providing Can1p with higher stability. As soon as the transporter is released from the protective surrounding, it is exposed to internalization by classical mechanisms. The same features have been observed for the Fur4 transport protein.

On the other side, Walther and coworkers suggested that MCC/eisosomes regulate sites of endocytosis based on their colocalization with endocytic

intermediates visualized by the lipophilic dye FM4-64 and a hexose transporter fused to GFP (Walther et al., 2006).

Endocytosis is a complex and efficient process that cells utilize to control the protein and lipid composition of the plasma membrane, to control the cell surface area, to take up nutrients and pathogens, and to regulate signaling pathways. This process involves coordination of effector proteins at the membrane where they induce membrane invagination and vesicle scission. Moreover, it is known that actin plays an essential role in the uptake step (Engqvist-Goldstein and Drubin, 2003; Girao et al., 2008; Toret and Drubin, 2006). In function of the cargo, several distinct endocytic pathways cargo may exist, like in mammalian cells, and may be localized to discrete domains of the cell surface. It is intriguing to find proteins (Pkh1,2 and Slm1,2) implicated in the organization of the actin cytoskeleton in yeast microdomain (MCC) and to find a possible link between these microdomains and endocytosis (MCC and TORC2). Whether yeast microdomains are sites of distinct endocytic pathways or protect cargo from degradation is still debated.

OBJECTIVES

Research in our laboratory focuses on the study of the SNA (**S**ensitive to **Na**$^+$) proteins which form a membrane proteins family in yeast *Saccharomyces cerevisiae* composed of four members: Pmp3p/Sna1p, Sna2p, Sna3p and Sna4p. Previous work by C. Navarre and A. Goffeau (2000) showed that the *PMP3* deletion increases the plasma membrane potential and confers sensitivity to cytotoxic cations. The observed phenotypes for a *pmp3*Δ strain (sodium and hygromycin sensitivity; suppression of the potassium dependency of a strain lacking the K^+ transporters; reversion of these phenotypes by addition of calcium to the medium) can be explained if Pmp3p inhibits the sodium and potassium uptake via the uncharacterized channel Nsc1p. In this model, calcium could also inhibit Nsc1p but probably via another mechanism. So, our working hypothesis was that Pmp3p interacts with Nsc1p and regulates cations transport through the plasma membrane. This is illustrated in the Figure 17.

The aim of our thesis was to elucidate the molecular function of Pmp3p using three different approaches. The first chapter will develop the co-immunoprecipitation experiment to identify some biochemical partners of Pmp3p. Then, the second chapter will explore the relation existing between the structure, the function and the trafficking of Pmp3p. For this, we have modified by site-directed mutagenesis the residues which are

highly conserved among Pmp3p homologues and we have analyzed the impact of these mutations on the function and the localization of the protein. Finally, the last chapter will present the results of the quantification of yeast plasma membrane proteins in response to the *PMP3* deletion via a mass spectrometry-based approach.

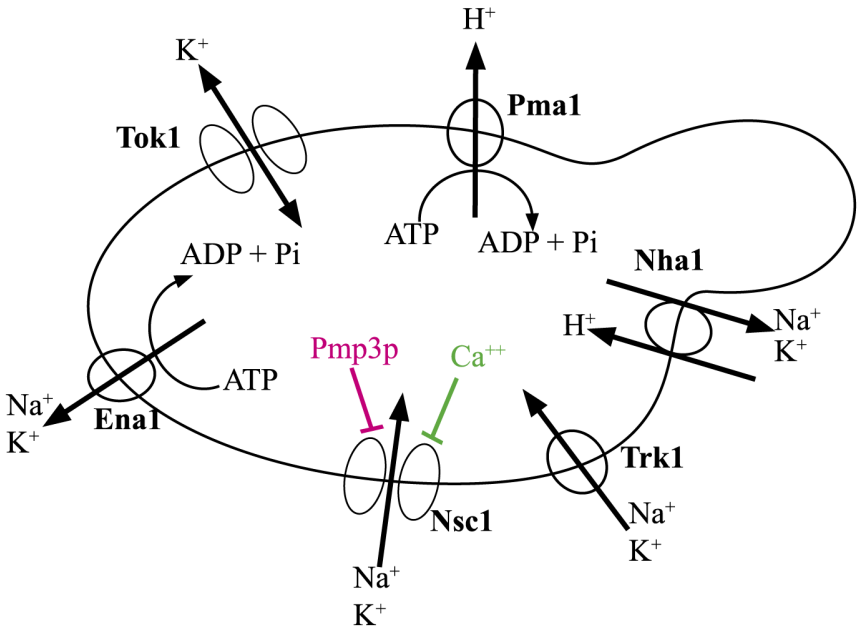

Figure 17. Hypothetical model explaining the Pmp3p function.

RESULTS AND DISCUSSION

1. Study of the putative partners of Pmp3p via a biochemical approach

1.1. Construction of a functional tagged version of Pmp3p

Our first aim was to construct a functional tagged version of Pmp3p which complements the growth defect of the *pmp3*Δ strain in presence of toxic cations (Navarre and Goffeau, 2000). We first constructed yeast strains in which the endogenous chromosomal *PMP3* gene was fused in frame with sequences coding for HA, Myc or His tags (annex 1). We chose to position each of the tags either at the N terminus or the C terminus of Pmp3p. This strategy ensured that only endogenous levels of Pmp3p would be produced. The wild type protein has been localized to the plasma membrane (Navarre and Goffeau, 2000). Therefore, purified plasma membranes extracts prepared from parental, *pmp3*Δ and the six Pmp3p-tagged strains were analysed by silver-stained SDS-polyacrylamide gel to check the presence of the fusion proteins in the plasma membranes. A band of 6.2 kDa corresponding to Pmp3p was detected in wild type strain but not in *pmp3*Δ strain (Figure 18A). Moreover, we have detected a band corresponding to the size of Pmp3p for the strains expressing Pmp3p-HA, HA-Pmp3p and Pmp3p-myc but not in the case of the three other strains.

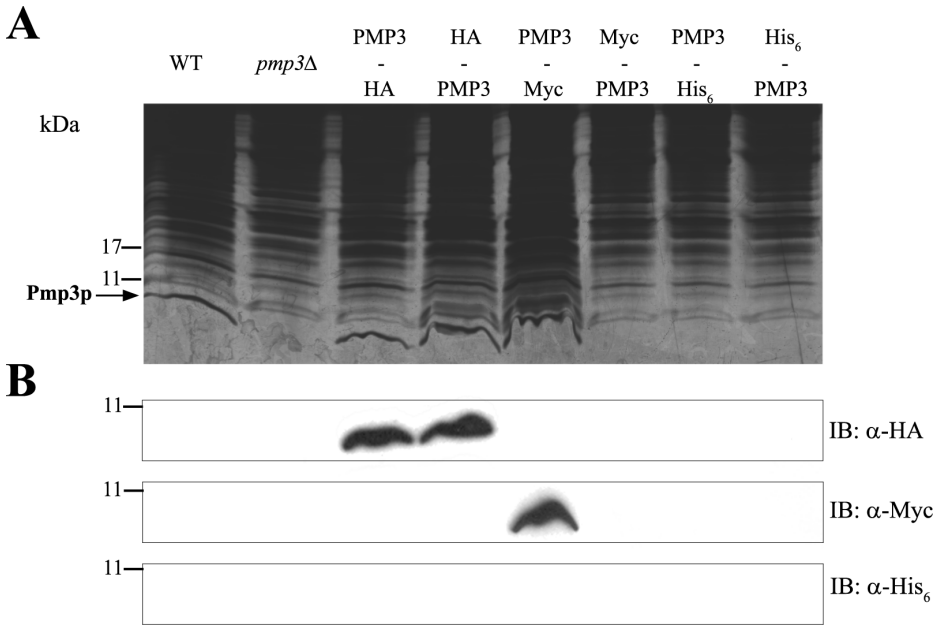

Figure 18. Pmp3p is present in the yeast plasma membrane. (**A**) Silver-stained Tricine-SDS-polyacrylamide gels of purified plasma membrane preparations (30 µg/gel lane). Lane 1, WT : wild type strain W303-1B; lane 2, *pmp3*Δ mutant strain; lane 3, *PMP3*Δ*::PMP3-HA*; lane 4, *PMP3*Δ*::HA-PMP3*; lane 5, *PMP3*Δ*::PMP3-Myc*; lane 6, *PMP3*Δ*::Myc-PMP3*; lane 7, *PMP3*Δ*:: PMP3-His*$_6$; lane 8, *PMP3*Δ*::His*$_6$*-PMP3*. (**B**) Immunodetection of tagged Pmp3p in *S. cerevisiae*. Purified plasma membrane preparations (30 µg/gel lane) were subjected to Tricine-SDS-polyacrylamide gels and immunodetection using anti-HA, anti-Myc and anti-His antibodies.

In order to confirm the presence of the tagged Pmp3p in the strains PMP3-HA, HA-PMP3 and PMP3-Myc, we have performed an immunodetection by Western blotting using both anti-HA, anti-Myc and

anti-His antibodies (Figure 18B). A band of ~6.5 kDa corresponding to the expected size corresponding to the tagged proteins was observed in the purified plasma membrane extracts from PMP3-HA, HA-PMP3 and PMP3-Myc but not from Myc-PMP3, PMP3-His_6 and His_6-PMP3. Unfortunately, it is impossible to detect Pmp3p in the crude membranes probably due to the amount of expressed protein. These results show that addition of a tag to Pmp3p is not neutral and can affect its localization or its stability to the plasma membrane. Indeed, Pmp3p is very hydrophobic and contains only 55 residues. So when we fuse a tag, we increase the size of the protein by nearly 15 % and we change its hydrophobicity.

1.2. Phenotypic characterization of the strains expressing a tagged version of Pmp3p

Functional expression of the tagged proteins can be evaluated by testing their capacity to grow in presence of various drugs. As mentioned in the introduction, deletion of *PMP3* confers sensitivity to toxic cations such as hygromycin B and Na^+. We reproduced the hygromycin B and sodium (not shown) phenotype sensitivity. Indeed, *pmp3*Δ cells failed to grow on media containing 100 µg/ml hygromycin B, whereas the growth of the WT cells was not modified under the same condition (Figure 19). HA tagged Pmp3p restored partially wild type growth while the cells expressing Myc- or His_6-tagged Pmp3p were unable to grow in presence of 100 µg/ml of hygromycin B. The presence of Pmp3p-Myc in the

plasma membranes (Figure 18), prompted us to investigate the growth on a medium containing 25 µg/ml of hygromycin B (Figure 19). In these conditions, we noticed that the strain PMP3-Myc grows better than the *pmp3*Δ, Myc-PMP3, PMP3-His_6 and His_6-PMP3 strains but more slowly than the WT, PMP3-HA and HA-PMP3 strains. These data show that the addition of a tag to Pmp3p can alter its presence in the plasma membrane (Myc-PMP3, PMP3-His_6 and His_6-PMP3) or modify its function (PMP3-Myc).

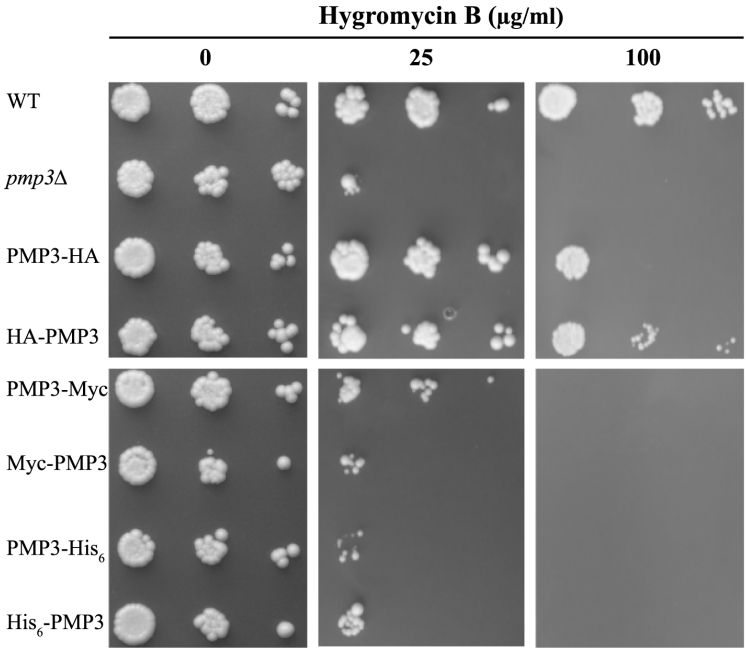

Figure 19. HA tagged *PMP3* restores *pmp3*Δ growth defect in presence of hygromycin B. Serial 10-fold dilutions of overnight cultures of W303-1B, *pmp3*Δ mutant strain, *PMP3*Δ*::PMP3-HA*, *PMP3*Δ*::HA-PMP3*, *PMP3*Δ*::PMP3-Myc*, *PMP3*Δ*::Myc-PMP3*, *PMP3*Δ*::PMP3-His*$_6$, *PMP3*Δ*::His*$_6$*-PMP3* in YD medium were spotted onto YD plates supplemented with the indicated concentrations of hygromycin B. The plates were photographed after 2 days of incubation at 30°C.

As mentioned in the introduction, three reports have indicated that a strain deleted for *PMP3* is also sensitive to the anti-cancer DNA damaging agent bleomycin (Aouida et al., 2004b) and confers spermine (0.2 mM) (Erez and Kahana, 2002) and lithium (200 and 700 mM) tolerance (Erez

and Kahana, 2002; Nylander et al., 2001). In our laboratory, we found that cells lacking *PMP3* gene are more resistant to rhodamine 6G (Figure 20). However, we were unable to observe any difference between the WT and the *pmp3*Δ strains in the presence of lithium and spermine (data not shown).

Rhodamine 6G is a cationic lipophilic dye (annex 1) which binds to the mitochondria of the living cells. It was also shown that yeast can protect itself against rhodamine 6G by the extrusion of this toxic compound via Pdr5p, an ABC plasma membrane transporter (Kolaczkowski et al., 1996). However, Johanna Dodzian found that the resistance to rhodamine 6G for *pmp3*Δ strain is not linked to Pdr5p (data not shown) and moreover that this resistance is due to a decrease of the rhodamine 6G uptake in comparaison with the WT strain (data not shown). As illustrated in figure 20, the WT and the HA-PMP3 strains are more sensitive than the *pmp3*Δ strain and the other tagged strains. This confirms that HA-Pmp3p complements almost completely the absence of the WT gene. Therefore, we decided to use this version of tagged-Pmp3p for further experiments.

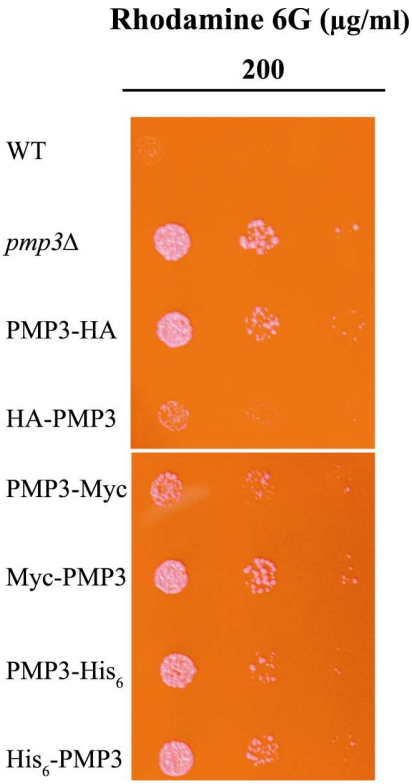

Figure 20. Growth test of *pmp3*Δ mutant strains in presence of rhodamine 6G. Sensitivity of yeast cultures was assayed by spotting serial dilution of cell cultures onto plates containing 200 µg/ml rhodamine 6G. The plates were observed after 2 days of incubation at 30°C.

The presence of divalent cations (Ca^{2+}, Mg^{2+}) in the external medium restores the growth of the *pmp3*Δ strain in presence of hygromycin B (Navarre and Goffeau, 2000). Consistently, we found that the growth defect observed for some tagged Pmp3p was restored in the presence of 10 mM $CaCl_2$ (Figure 21).

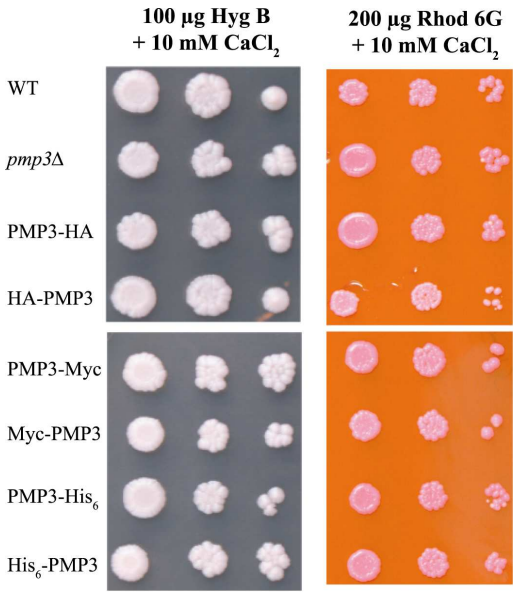

Figure 21. Effect of Ca^{2+} on the growth defect caused by the *PMP3* deletion. Serial 10-fold dilutions of cultures of W303-1B, *pmp3*Δ strain, *PMP3*Δ*::PMP3-HA*, *PMP3*Δ*::HA-PMP3*, *PMP3*Δ*::PMP3-Myc*, *PMP3*Δ*::Myc-PMP3*, *PMP3*Δ*::PMP3-*His_6, *PMP3*Δ*::*His_6-PMP3* in YD medium were spotted onto YD plates supplemented with the indicated concentrations of hygromycin B or rhodamine 6G and 10 mM $CaCl_2$. The plates were observed after 2 days of incubation at 30°C.

1.3. Solubilization of HA-Pmp3p

In order to purify the protein of interest, we had to solubilize HA-Pmp3p with detergents. We decided to avoid the mixture of chloroform-methanol to solubilize HA-Pmp3p because we were concerned about losing potential partner(s) of Pmp3p. Although a large number of molecules

have been designed with detergent properties, selection of the proper solubilizing agent is largely a matter of trial that depends on the protein of interest (Schimerlik, 2001). In a solubilization test, we tested and compared different non-ionic and zwitterionic detergents. A fraction corresponding to the purified plasma membranes was solubilized with detergents at a 1/10 protein/detergent ratio. The different fractions corresponding to the pellet (P) or the supernatant (S) after centrifugation were subjected to SDS-PAGE followed by immunodetection with anti-HA antibodies (Figure 22). Among the non-ionic detergents, only the Triton X-100 and the thioglucopyranoside seem to solubilize HA-Pmp3p but their solubilization yield is not better than this from the zwittergent 3-14. It is not surprising to note that Triton X-100 does not really solubilize Ha-Pmp3p because Pmp3p is associated with DRM (data not shown). The denaturating detergent sodium dodecyl sulfate (SDS) was used as a control. Although the global yield of solubilization is rather poor in all cases, we choose the zwittergent 3-14 at a 1/10 protein/detergent ratio for further experiments. Varying protein/detergent ratio did not improve HA-Pmp3p solubilization (data not shown).

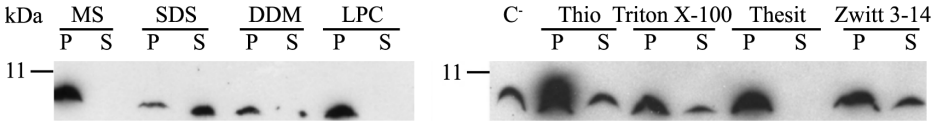

Figure 22. Solubilization of HA-Pmp3p with different detergents. Purified plasma membranes (30 µg) from HA-PMP3 strain were solubilized with the following detergents during 30 min at 4°C : $MgCl_2$ 1 mM and imidazole 10 mM (MS), Sodium dodecyl sulphate (SDS), n-dodecyl β-D-maltoside (DDM), Lysophosphatidylcholine (LPC), Thioglucopyranoside (Thio), Triton X-100, Thesit and Zwittergent 3-14 (Zwitt 3-14). MS buffer was used as negative control for solubilization. Pellets (P) and supernatants (S) obtained after centrifugation were subjected to SDS-PAGE and immunodetection using anti-HA antibodies.

1.4. Immunoprecipitation of HA-Pmp3p

In order to identify proteins that physically associate with Pmp3p, we used co-immunoprecipitation. Briefly, this method uses monoclonal antibodies raised against the HA epitope to isolate proteins from extract where one of the proteins is tagged with HA. To determine whether HA-Pmp3p can be immunoprecipitated, we used the solubilized plasma membranes from the WT strain (used as negative control) and from the HA-PMP3 strain. The immunoprecipitates were analyzed by SDS-PAGE and immunoblotting. We observed a signal around 6.5 kDa for the HA-PMP3 strain but not in the case of the negative control (Figure 23). We also noticed that this signal is more intense when we perform an immunoprecipitation from a strain overexpressing HA-Pmp3p (Figure

23). Moreover a specific signal appeared around 15 kDa wich could correspond to a dimer or a trimer of HA-Pmp3p.

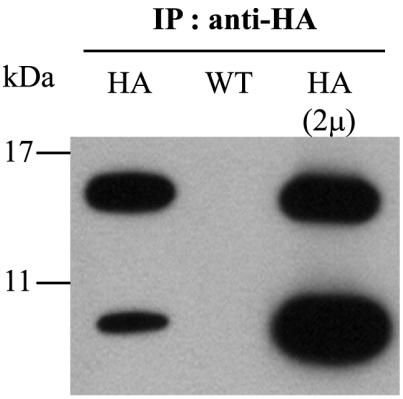

Figure 23. Detection of HA-Pmp3p after immunoprecipitation. 400 µg of purified plasma membranes from HA-PMP3 (HA) and WT strains and the strain overexpressing HA-Pmp3p (2µ) were solubilized, immunoprecipitated with anti-HA antibodies, and analyzed by western blotting using anti-HA antibodies. Molecular size markers are indicated on the left.

When the immunoprecipitates were analyzed by colloidal blue stained SDS-PAGE, several distinct proteins species were detected that co-immunoprecipitated with HA-Pmp3p. We repeated this immunoprecipitation at least 10 times, two examples are illustrated in Figure 24. These proteins were specifically associated with HA-Pmp3p because they were not present when control purified plasma membranes, prepared from the parental untagged strain, were used for immunoprecipitation and because they were observed in most immunoprecipitations. To identify the proteins that copurified with HA-Pmp3p, we have cut out from the gel the six interesting bands, digested

with trypsin and subjected to mass spectrometry analysis. For comparison, the untagged control bands were also analyzed. The identification of the proteins is presented in Table 3.

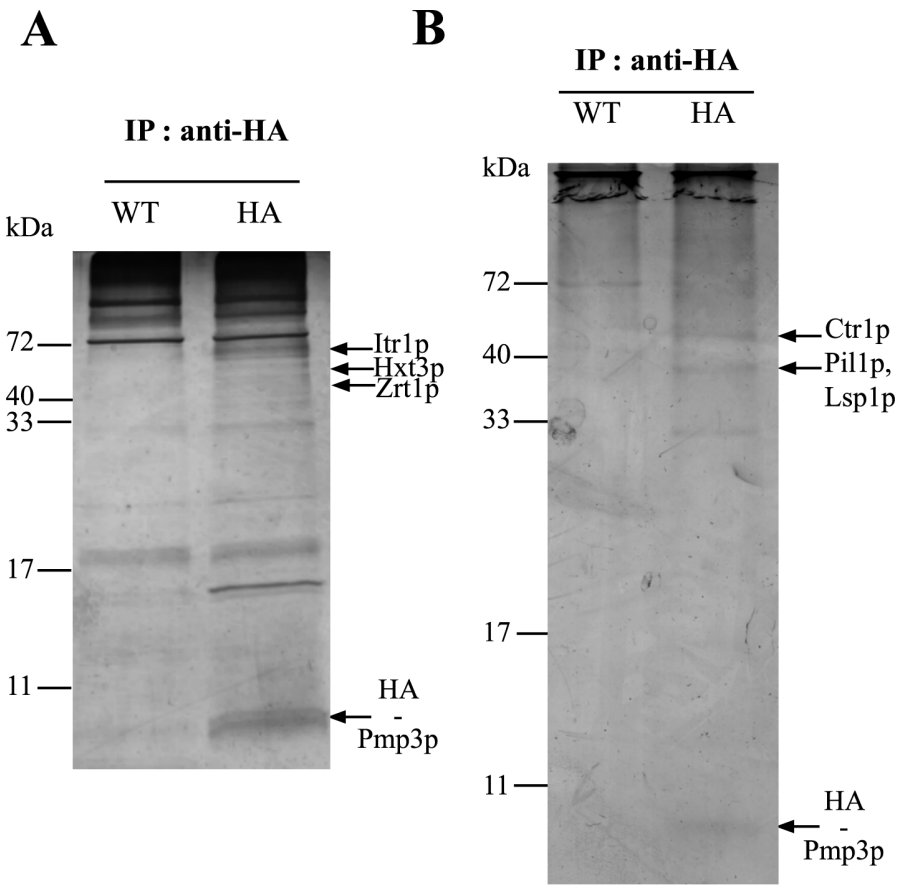

Figure 24. Co-immunoprecipitation of HA-Pmp3. The immunoprecipitates from W303-1B strain, used as control (WT), and from HA-Pmp3p strain (HA) were loaded onto a Tris-tricine gel for SDS-PAGE. The gel were stained with colloidal blue. Positions of molecular size markers (kDa) are indicated on the left. Two independent experiments are shown (A and B).

Table 3. Proteins co-immunoprecipitated with HA-Pmp3p. Peptide shows the number of identified peptides. Score is calculated by the Mascot algorithm. The mascot score is given as S=-10 log P where P is the probability that the observed match is a random event. Mascot scores greater than 53 are significant.

Standard name	Systematic name	Predicted mass (kDa)	Score (Mascot)	Peptide	Description summary
Pil1p	YGR086C	38	663	12	Component of eisosomes
Lsp1p	YPL004C	38	151	5	Component of eisosomes
Zrt1p	YGL255W	41	69	4	High affinity zinc transporter
Hxt3p	YDR345C	62	362	11	Glucose transporter
Ctr1p	YPR124W	44	110	7	Copper transporter
Itr1p	YDR497C	63	249	6	Myo-inositol transporter

1.5. Physical interaction between Pmp3p and Pil1p

Eisosomes have recently been described as fungal structures that play a role in the organization of the plasma membrane and endocytosis. These structures are composed primarily of two cytoplasmic proteins, Pil1p and Lsp1p (Walther et al., 2006). We therefore decided to explore the

relationship between Pmp3p and Pil1p in greater detail given that the mascot score of this protein makes its identification unambigous. We first wanted to verify whether these two proteins interact physically, as suggested by the first experience of immunoprecipitation. We reasoned that we should be able to perform the reciprocal experiment and co-immunoprecipitate Pmp3p by using an antibody specific for Pil1p. Accordingly, we introduced into the HA-PMP3 strain a plasmid bearing the *PIL1* gene tagged with green fluorescent protein (GFP-PIL1). We prepared plasma membrane extracts and used anti-GFP antibodies to precipitate GFP-Pil1p, followed by western blot analysis with anti-HA antibodies to detect HA-Pmp3p. The results showed a weak signal for HA-Pmp3p suggesting that HA-Pmp3p associated with GFP-Pil1p in the plasma membranes (Figure 25). The interaction was specific because no HA-Pmp3p was detected in the control. We performed again the co-immunoprecipitation experiment with anti-HA antibodies to precipitate HA-Pmp3p. We first checked that HA-Pmp3p immunoprecipitated efficiently and that no signal appeared in the control. Then, we reprobed the membrane with anti-GFP antibodies and a signal corresponding to GFP-Pil1p was detected in samples from cells expressing both HA-Pmp3p and GFP-Pil1p but not in the sample in which HA-Pmp3p was absent (Figure 25). This experiment shows that Pmp3p and Pil1p are likely to be in close physical contact in plasma membranes.

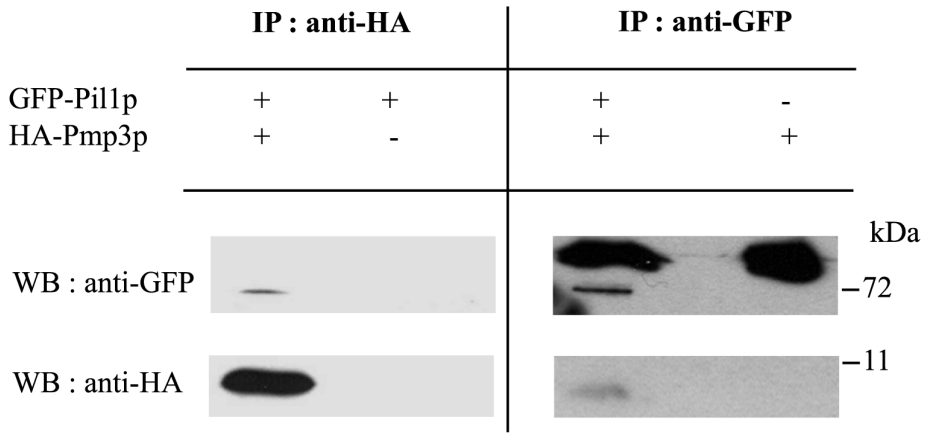

Figure 25. Pmp3p interacts with Pil1p. Immunoprecipitation was performed with 800 µg of plasma membrane extracts from cells producing HA-tagged Pmp3p under the control of its own promoter and transformed by a plasmid encoding GFP-tagged Pil1p under the control of *SNA2* promoter. Tagged proteins were immunoprecipitated with anti-HA or anti-GFP antibodies. Cells producing untagged Pmp3p or Pil1p were used as controls for immunoprecipitations. Immunoprecipitated proteins were detected by immunoblotting with anti-HA and anti-GFP antibodies.

1.6. Pmp3p and Pil1p colocalize in situ

Examination of Pmp3p and Pil1p tagged with green fluorescent protein (GFP) revealed that those proteins localize respectively to the plasma membrane and in some dots at the cell periphery underneath the plasma membrane (Figure 26).

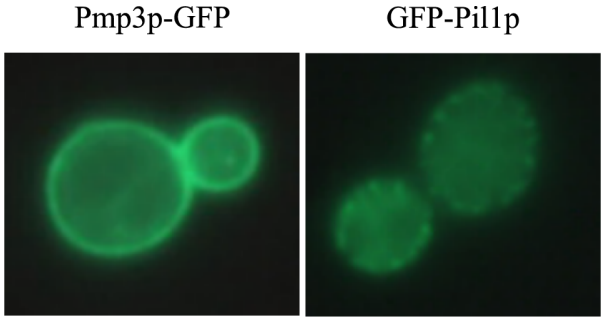

Figure 26. Cellular localization of Pmp3p-GFP and GFP-Pil1p. Fluorescence microscopy-based images of WT cells expressing Pmp3p-GFP or GFP-Pil1p under the control of *TPI1* and *SNA2* promoters, respectively.

The fact that GFP-Pmp3p is not functional (Catherine Navarre, personnal communication) supports the hypothesis that GFP fusion could interfere with the correct localization of the protein. Therefore, we decided to further investigate the localization of the functional tagged HA-Pmp3p by indirect immunofluorescence microscopy. Incubation of cells expressing both HA-Pmp3p and GFP-Pil1p with anti-HA antibodies produced a punctuated pattern that was absent in cells expressing the wild type version of Pmp3p and the GFP tagged version of Pil1p (Figure 27). The signal obtained by indirect fluorescence is different from that obtained by direct fluorescence microscopy, which means that the Pmp3p localization is disturbed by the GFP tag. Recently, a list of proteins fused to GFP which cluster or associate with the MCC patches has been published (Grossmann et al., 2008), but Pmp3p was not found in this list. The

difference of distribution observed between the GFP fluorescence and the immunofluorescence experiments explains why Pmp3p has not been found previously as a component of the Can1p-containing compartments. A similar pattern was observed when cells were stained with anti-GFP antibodies and we observed a partial colocalization between HA and GFP-positive dots, indicating that the two proteins occupy the same structures (Figure 27). Nevertheless, there are also green and red spots, indicating that the proteins do not colocalize everywhere in the cell. The minority of the green spots could be explained by the fact that HA-Pmp3p is not completely functional (cfr phenotypic test) or that Pmp3p is not always localized to the eisosomes.

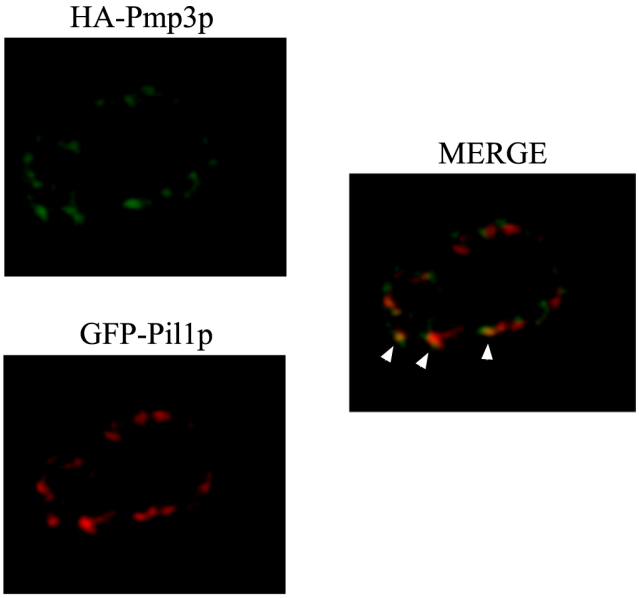

Figure 27. Pmp3p colocalizes partially with Pil1p. HA-Pmp3p and GFP-Pil1p were visualized by indirect fluorescence. Cells producing HA-Pmp3p and GFP-Pil1p were fixed and processed for immunofluorescence with monoclonal anti-HA and polyclonal anti-GFP antibodies followed by FITC-labeled goat anti-rat IgG and $Alexa_{633}$-labeled goat anti-mouse IgG as described in Materials and Methods. The immunostained cells were examined with a confocal microscope.

1.7. An endocytic regulatory role for Pmp3p

Two independent works have shown that MCC/eisosomes might have a role in endocytosis. Indeed, the team of Walter, by monitoring the time course of FM4-64 internalization in WT and in strain bearing the *pil1*Δ mutation, has shown that the deletion of *PIL1* decreased the rate of

endocytosis compared with wild type cells (Walther et al., 2006). We reproduced this uptake of the fluorescent dye FM4-64, a lipid marker for endocytosis, in WT (BY4741), *pil1*Δ and *pmp3*Δ strains. We labeled cells with FM4-64 and blocked endocytosis shortly after labeling by poisoning the cells with azide and fluoride on ice as described in Materials and Methods. Observation of FM4-64 uptake in living cells highlighted a delay of the internalization of the dye in the *pmp3Δ* strain compared to the WT (Figure 28A and B). Indeed, we can notice that, although the signal intensity of the vacuolar membrane is similar in both cases, we can still see dots (likely endosomes) in the case of *pmp3*Δ strain 50 min after FM4-64 pulse. As expected, in the absence of Pil1p, one big dot per cells is observed (Figure 28A).

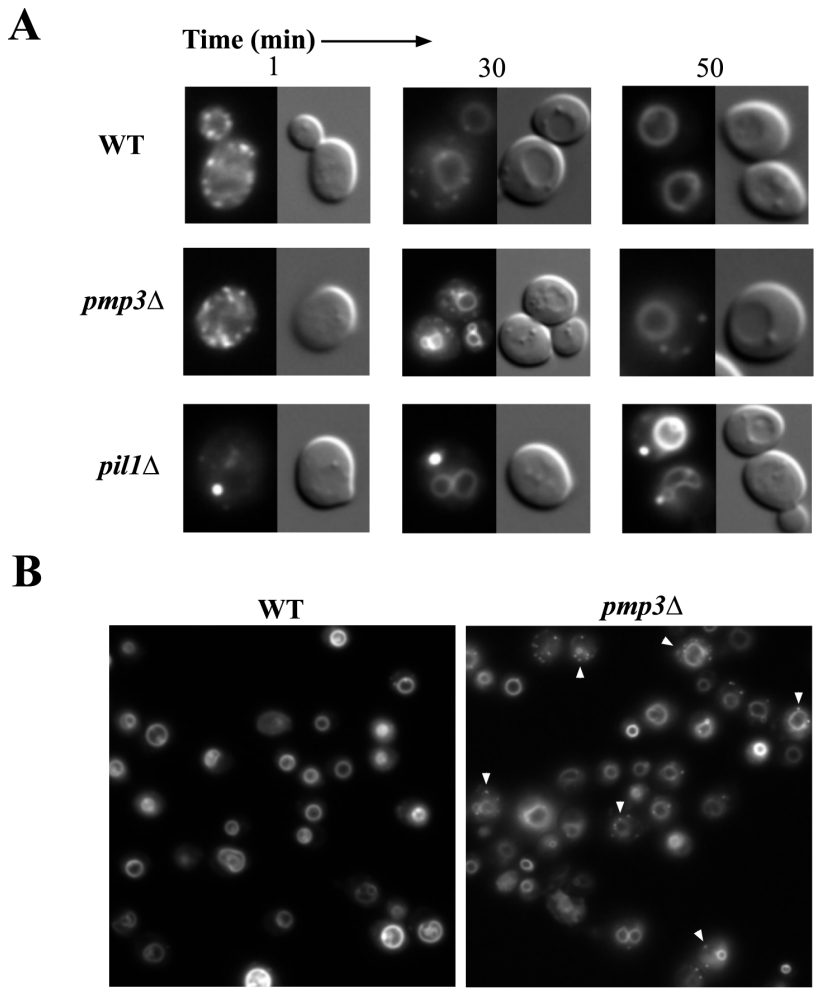

Figure 28. FM4-64 uptake in WT (BY4741), *pmp3*Δ and *pil1*Δ strains. Cells were labeled with FM4-64 on ice, washed with ice-cold YD and subsequently resuspended in YD at 30°C. Endocytosis was stopped by transfer to ice and addition of 10 mM NaN_3 and 10 mM NaF after 1, 30 and 50 min. **(A)** Cells imaged at the indicated times. **(B)** Larger sample of WT and *pmp3*Δ cells imaged after 50 min.

In another study, Grossmann and colleagues have shown that the turnover of Can1p is faster in mutants that are unable to build up the MCC/eisosomes (Grossmann et al., 2008). So, we observed the localization of Can1-GFP in WT and *pmp3*Δ strains by epifluorescence and confocal microscopy. The localization of Can1-GFP in MCC has been confirmed in WT and *pmp3Δ* strains. However, we observed by confocal microscopy labeled internal structures in the *pmp3Δ* strain that were not present in the WT strain (Figure 29). These structures could represent endosomes but this has still to be confirmed. Whether MCC/eisosomes are sites of endocytosis or protect transporter from degradation is still debated, however Pmp3p seems to make the link between endocytosis and MCC/eisosomes.

The FM4-64 internalization delay does not necessarily contradict the fact that endocytosis of Can1p occurs faster in *pmp3*Δ strain. Indeed, proteins submitted to the endocytosis could be occasional competitors of the FM4-64 in endocytosis. Taken together, these results confirm the role of the MCC/eisosomes in endocytosis.

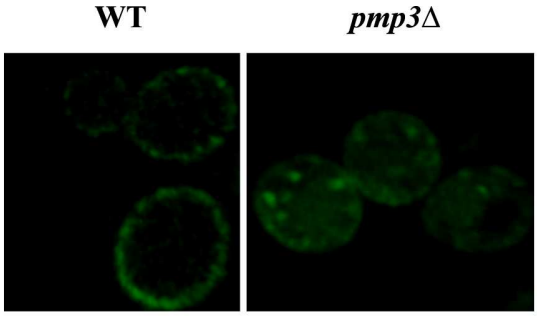

Figure 29. Internalization of Can1-GFP is accelerated in *pmp3*Δ strain. Can1-GFP was localized in the wild type (WT) and the *pmp3*Δ cells. Note the presence of labeled internal structures in the *pmp3*Δ strain.

1.8. Phenotypic characterization of the knockout genes corresponding to the putative partners

Our results show that Pmp3p interacts and colocalizes with Pil1p. Pmp3p is thus a new component associated to the MCC/eisosomes, and one of its functions is to regulate the Can1p internalization. In addition, Pmp3p plays a role in ion homeostasis and cation transport. For instance Pmp3p could regulate directly or indirectly some transporters localized in the MCC/eisosomes and therefore modulate their internalization rate. If these transporters control plasma membrane potential, we could postulate that disruption of Pmp3p modify their internalization rate and consequently modify the plasma membrane potential. These transporters have still to be

identified but the co-immunoprecipitation experiment has shown that four transporters (Hxt3p, Zrt1p, Itr1p and Ctr1p) would be interesting.

We first checked cell growth in presence of hygromycin B (Figure 30). We can see that only the *ctr1*Δ strain is sensitive in presence of 100 µg/ml hygromycin B as the *pmp3*Δ strain. At 200 µg/ml hygromycin B, we noticed that the six strains are unable to grow while the WT (BY4741) strain can still grow. Addition of calcium to this medium restores the growth of those strains.

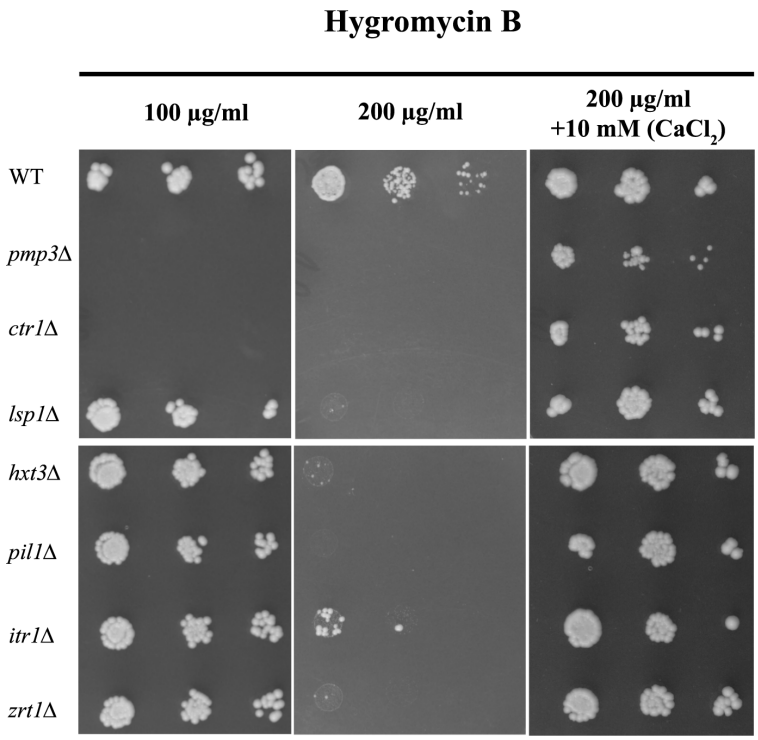

Figure 30. Hygromycine phenotype of the knockout genes corresponding to the putative partners. Serial 10-fold dilutions of saturated cultures of BY4741, *pmp3*Δ, *ctr1*Δ, *lsp1*Δ, *hxt3*Δ, *pil1*Δ, *itr1*Δ and *zrt1*Δ mutant strains in YD medium were spotted onto YD plates supplemented with the indicated concentrations of hygromycin B and $CaCl_2$. The plates were observed after 2 days of incubation at 30°C.

A growth test has been performed with 200 µg/ml rhodamine 6G (Figure 31). No growth defect is observed for *pmp3*Δ. We observed an intermediate phenotype for the *hxt3*Δ, *pil1*Δ, *itr1*Δ and *zrt1*Δ strains. Indeed those four strains can grow better than the WT in presence of this

dye but not as well as the *pmp3*Δ strain. The opposite is observed for the *ctr1*Δ and *lsp1*Δ which cannot grow on this medium. All those strains grow normally when we add 10 mM calcium.

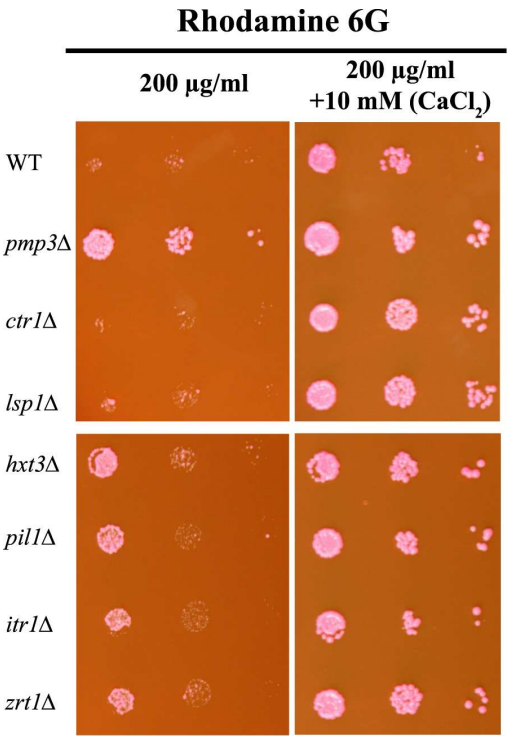

Figure 31. Rhodamine 6G phenotype of the knockout genes corresponding to the putative partners. Serial 10-fold dilutions of saturated cultures of BY4741, *pmp3*Δ, *ctr1*Δ, *lsp1*Δ, *hxt3*Δ, *pil1*Δ, *itr1*Δ and *zrt1*Δ mutant strains were spotted onto YD plates supplemented with the indicated concentrations of rhodamine 6G and 10 mM $CaCl_2$. The plates were observed after 2 days of incubation at 30°C.

The most surprising is that the *PMP3* deletion causes sensitivity in presence of one cationic compound and resistance in presence of another one. One way to explain this is that Pmp3p controls the internalization

rate of some transporters responsible for the plasma membrane potential and also more specifically responsible for the rhodamine 6G uptake.

This phenotypic test teaches us that Hxt3p, Zrt1p and Itr1p could be transporters of rhodamine 6G in addition to influence plasma membrane potential. And, on the other side, Ctr1p seems to control the membrane potential, without being implicated in the transport of rhodamine 6G. The *PIL1* deletion disturbs the MCC/eisosomes formation and causes the apparition of 1 eisosome remnant where the MCC transporters are confined probably with Pmp3p. The control of the endocytosis still seems to be partially functional because we observed a partial hyperpolarization and a partial uptake of rhodamine 6G in this mutant. The precise function of Lsp1p is not yet completely known but it has been shown that it is not responsible for the stability of MCC and that its endocytic function is different from that of Pil1p (Walther et al., 2006).

Interestingly several clues strengthen the fact that Hxt3p, Zrt1p and Itr1p could be component of NSC1. First, some studies have shown that this activity could be due to some transporters involved in glucose and inositol uptake (Madrid et al., 1998; Mulet et al., 1999) and the co-immunoprecipitation experiment identified Hxt3 and Itr1 proteins. Second, the *PMP3* deletion mimics NSC1 activation, this suggests that NSC1 is probably regulated by Pmp3p. And finally, the growth of these

three mutants (*zrt1*Δ, *hxt3*Δ and *itr1*Δ*)* in presence of hygromycin B and rhodamine 6G supplemented or not with calcium, is similar.

1.9. Oligomerization of Pmp3p

Immunoprecipitation of HA-Pmp3p revealed a specific band around 15 kDa wich could correspond to a dimer of Pmp3p (Figure 23). To determine whether Pmp3p molecules oligomerize in physiological conditions, we performed a co-precipitation experiment with cell lysates that co-expressed a chromosomal version of HA-Pmp3p and Pmp3p-Myc from a high-copy vector. We chose to use this tagged version of Pmp3p with Myc in C terminus because it is localized to the plasma membrane, unlike Myc-Pmp3p. Plasma membranes were first solubilized with zwittergent 3-14 and the solubilized extracts were immunoprecipitated with either anti-HA or anti-Myc antibodies. The precipitates were then resolved by SDS-PAGE and analyzed by immunoblotting using anti-HA and anti-Myc antibodies. When HA-Pmp3p and Pmp3p-Myc were co-expressed, HA-Pmp3p was detected in the fraction immunoprecipitated with anti-Myc antibodies. In contrast, HA-Pmp3p was not found in the anti-Myc immunoprecipitates of cells expressing only HA-Pmp3p (Figure 32). We also found that Pmp3p-Myc was co-immunoprecipitated with the anti-HA antibodies when it was co-expressed with HA-Pmp3p (Figure

32). These results confirm that Pmp3p-Myc specifically interacts with HA-Pmp3p, and suggest that Pmp3p exists in the membrane as an oligomeric form.

It has been reported that transmembrane domain (TMD) interactions play a crucial role in the folding of integral membrane proteins and their association to oligomeric complexes. Moreover these helix-helix interfaces frequently depend on specific amino acid patterns. For example small-xxx-small motifs which are not satisfied by intrachain contact may promote oligomeric structure. The small-xxx-small motif colocalizes Ala, Gly and Ser residues to a single helical surface that promotes close helix-helix contacts (Rath and Deber, 2008). Interestingly, we noticed 2 small-xxx-small motifs, A_{40}-xxx-G_{44}-xxx-A_{48}, in the second putative span of Pmp3p which could be implicated in its oligomerization.

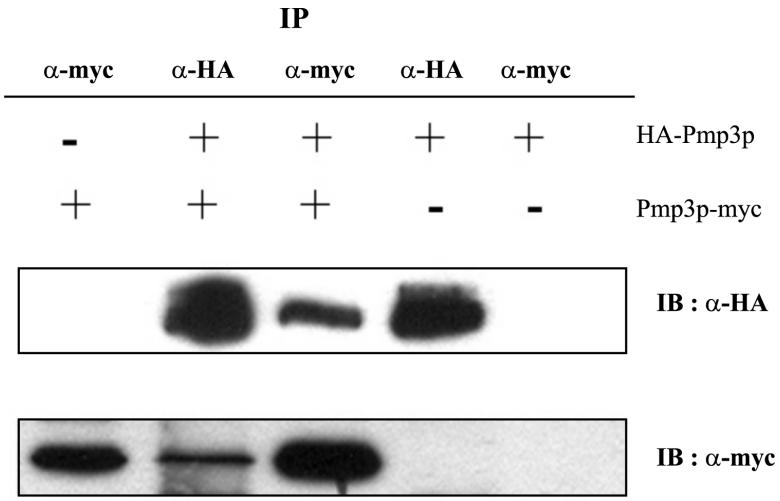

Figure 32. Detection of Pmp3p oligomerization by co-precipitation analyses. 800 µg of purified plasma membranes from strains expressing HA-Pmp3p, Pmp3p-Myc or both were solubilized, incubated with agarose beads coupled to the G protein and either anti-HA antibodies or anti-Myc antibodies. The specific precipitates were then subjected to immunoblotting analysis after separation by SDS-PAGE. The antibodies used were the anti-HA and the anti-Myc antibodies.

In this chapter, we found that Pmp3p is localized in plasma membrane microdomains associated with the eisosomes. Moreover, Pmp3p is implicated in the plasma membrane stabilization of Can1p which is a marker of these microdomains (Figure 33).

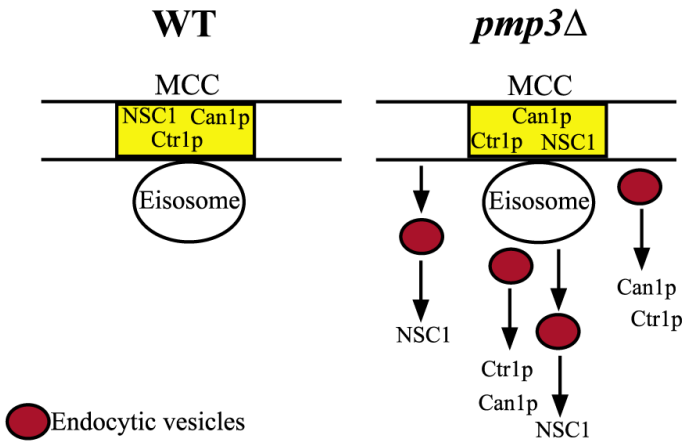

Figure 33. Model for Pmp3p function in proteins turnover implication. MCC are represented in yellow.

Whether Pmp3p stabilizes all the transporters of the MCC has still to be proved. Nevertheless, several observations (Co-IP experiments, phenotypic test…) support the idea that Pmp3p could also stabilize other transporters (Hxt3p, Itr1p, Zrt1p, Ctr1p) some of them being possibly members of NSC1. Whether MCC/eisosomes are sites of endocytosis or protect transporters from degradation is still debated. However Pmp3p seems to make the link between endocytosis and MCC/eisosomes.

2. Study of the relation existing between the structure, the function and the trafficking of Pmp3p

Pmp3p/Sna1p belongs to Sna (Sensitive to Na) proteins family and has three close homologues, called Sna2p, Sna3p and Sna4p. The alignment of the four sequences (Figure 34) shows twelve conserved residues almost all located in the transmembrane domains. Site-directed mutagenesis has been used to replace these amino acids in order to analyze their importance on the localization and the function of Pmp3p. All the conserved residues have been replaced individually by the hydrophobic leucine or by an alanine when the conserved residue is a leucine.

```
PMP3 ----------------MDSAKIINIILSLFLPPVAVFLARGW-GTDCIVDIILTILAWFPGMLYALYIVLQD--- 55
SNA2 ----------------MHARDWFLVFIAIFIPPLAVWLKRGFFTKDLLINFLLFLLGFFPGLIHALYVISCHPYE 56
SNA3 MDRDHINDHDHRMSYSINKDDLLLMVLAVFIPPVAVWKRKGMFNRDTLLNLLLFLLLFFPAIIHACYVVYETSSE 72
SNA4 ---------MCCYCVCCTVSDFILYIVAFFFPPAAVLLRSGPCSSDFLLNVLLTLLGFLPGMLHAFYYITITSPL 63

PMP3 ------------------------------------------------------------------------  55
SNA2 ENEARYSHLSSSDDNYGSLA--------------------------------------------------------  79
SNA3 RSYDLSRRHATAPAVDRDLEAHPAEESQAQPPAYDEDDEAGADVPLMDNKQQLSSGRT---------------- 105
SNA4 RNAEYVYYYQQGWVDSERNVPSNRPQNSQTPQNRPQQGSSARNVYPSVETPLLQGAAPHDNKQSLVESPPPYVP 123
```

Figure 34. Sna family sequences. Bars over the sequences indicate the transmembrane domains (TMDs). TMDs were predicted using the TMHMM software v. 2.0. Conserved residues are in red and known targeting motifs in bold. Alignement has been performed with ClustalW.

2.1. Study of the function of Pmp3p

In order to analyze the impact of these mutations on the function of the protein, we compared the growth, in presence of hygromycin B and rhodamine 6G, of the 12 points mutants obtained. These 12 points mutants have been inserted in an expression plasmid pRS316 under the control of the *PMP3* promoter. In presence of 400 µg/ml hygromycin B, we observed that only V20L, A19L and P16L mutants can grow as well as the WT strain (Figure 35). But when we decreased the drug concentration, we noticed that A48L, L39A, D29L and P17L mutants can grow better than *pmp3*Δ but less than WT strain. Moreover, in presence of 100 µg/ml of hygromycin, the Y50L and the P43L mutants are still more sensitive than the *pmp3*Δ strain while the L36A, the G25L and the F14L mutants are as defective as *pmp3*Δ strain.

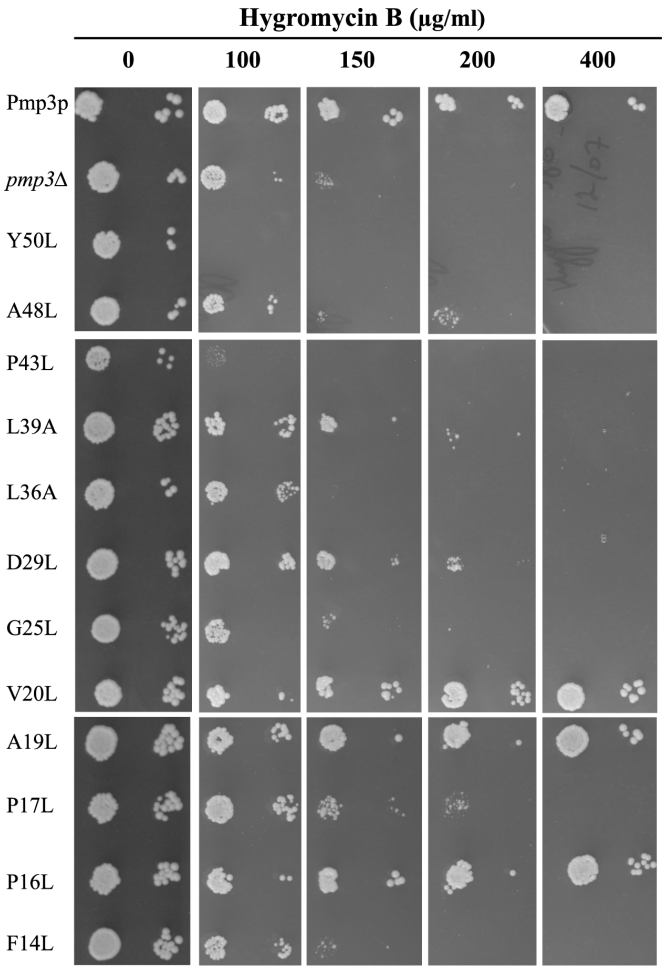

Figure 35. Hygromycin phenotype of *pmp3*Δ cells transformed with *PMP3* mutant constructs bearing single amino-acid substitutions. *pmp3*Δ cells transformed with wild type (WT), vector alone (*pmp3*Δ) or mutant pRS316-*PMP3* constructs were grown to the logarithmic phase, diluted serially, and spotted onto minimal medium plates, pH 5.5, supplemented with hygromycin B as indicated. The plates were incubated at 30 °C for 4 days.

When we compared the growth in presence of rhodamine 6G (Figure 36) with the growth in presence of hygromycin B, we noticed generally the same profile for the different mutants (for example the V20L, the A19L and the P16L mutants are sensitive in presence of rhodamine 6G but resistant in presence of hygromycin B). The D29L mutant, however, seems more resistant in presence of rhodamine 6G than the *pmp3*Δ strain but is also more resistant in presence of hygromycin B. Finally, the addition of calcium restores the growth defect for each mutant (data not shown).

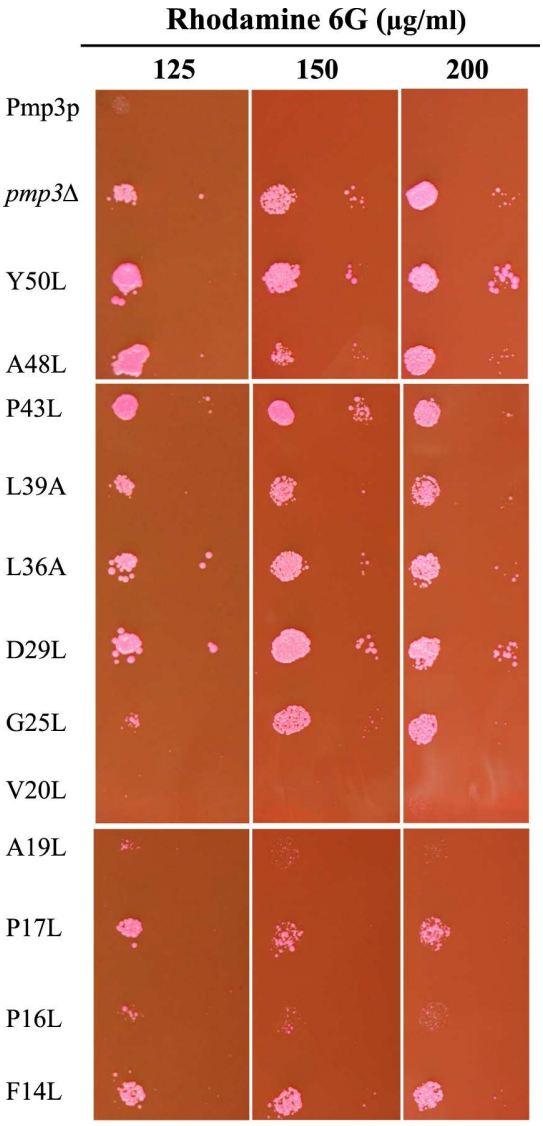

Figure 36. Rhodamine 6G phenotype of *pmp3*Δ cells transformed with *PMP3* mutant constructs bearing single amino-acid substitutions. *pmp3*Δ cells transformed with wild-type (WT), vector alone (*pmp3*Δ) or mutant pRS316-*PMP3* constructs were grown to the logarithmic phase, diluted serially, and spotted onto minimal medium plates, pH 5.5, supplemented with rhodamine 6G as indicated. The plates were incubated at 30 °C for 4 days.

2.2. Study of the trafficking of Pmp3p towards plasma membrane

In order to establish a correlation between the structure and the impact of these mutations on the traffic and on the function of the protein, we fused the twelve point mutants to GFP in the centromeric yeast plasmid pRS416, under the control of the strong triose-phosphate isomerase (TPI) constitutive promoter. The fusion protein was then visualized by fluorescence microscopy (Figure 37), bearing in mind that the GFP fusion may affect localization (cfr immunofluorescence experiment). As expected, Pmp3p WT localized to the plasma membrane. The mutants Pmp3p-F14L, Pmp3p-D29L, Pmp3p-L36A, Pmp3p-L39A and Pmp3p-Y50L show a fluorescence pattern similar to that of WT cells. It is not the case for the others mutations. Indeed, the mutants Pmp3p-P16L, Pmp3p-P17L, Pmp3p-A19L, Pmp3p-V20L, Pmp3p-G25L and Pmp3p-A48L show fluorescence in internal membranes surrounding the nucleus and a signal close to the plasma membrane, which are indications of ER localization. We detected for the Pmp3p-P43L mutant a signal localized in internal structures.

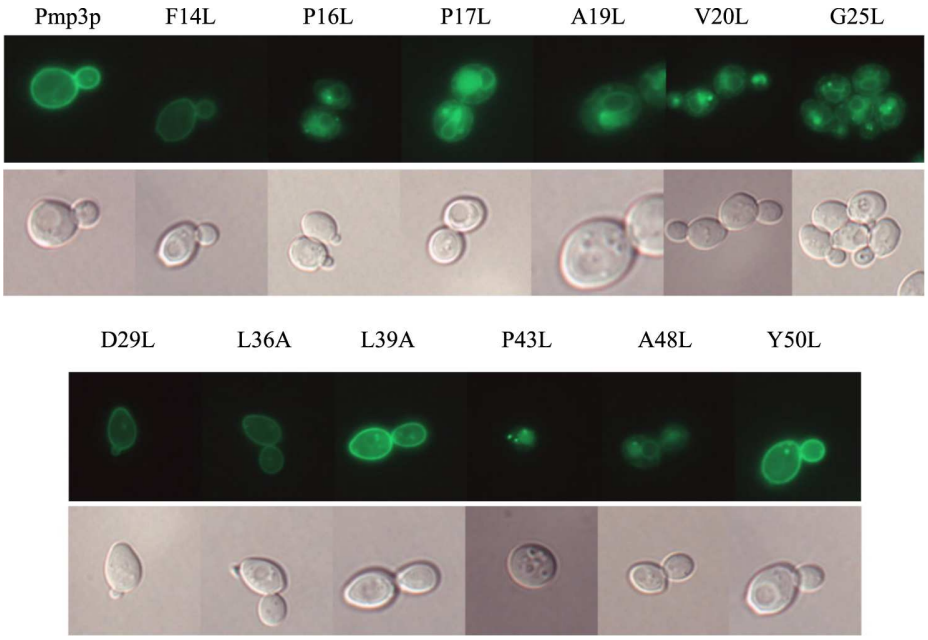

Figure 37. Targeting of Pmp3p-GFP to the plasma membrane is abolished in the Pmp3p-P16L, Pmp3p-P17L, Pmp3p-A19L, Pmp3p-V20L, Pmp3p-G25L, Pmp3p-P43L and Pmp3p-A48L mutants. Microscopic images of Pmp3p-GFP in living cells. Cells transformed by a Pmp3p-GFP plasmid under the control of the TPI1 promoter were examined for fluorescence and with Nomarski optics.

At this point, it is quite difficult to find a good correlation between the localization and the function of the protein. Indeed, how could we explain the fact that the three mutants (P16L, A19L and V20L) are functional but are not localized to the plasma membrane? To answer this question, we

decided to check again the localization of these 12 mutated proteins via another technique than the GFP fusion. We purified the plasma membranes from the strains expressing the untagged versions of the 12 mutants. The figure 38 shows a silver stained tricine-SDS-polyacrylamide gel of purified plasma membrane preparations. We detected a band around 6.2 kDa for the WT, P16L, A19L and V20L strains but not for the other mutants. These data are contradictory with the GFP fusion observations (Figure 37) but correlates perfectly with the phenotypic analysis. Therefore we can conclude that the GFP fusion also interferes with the localization of the mutated Pmp3p.

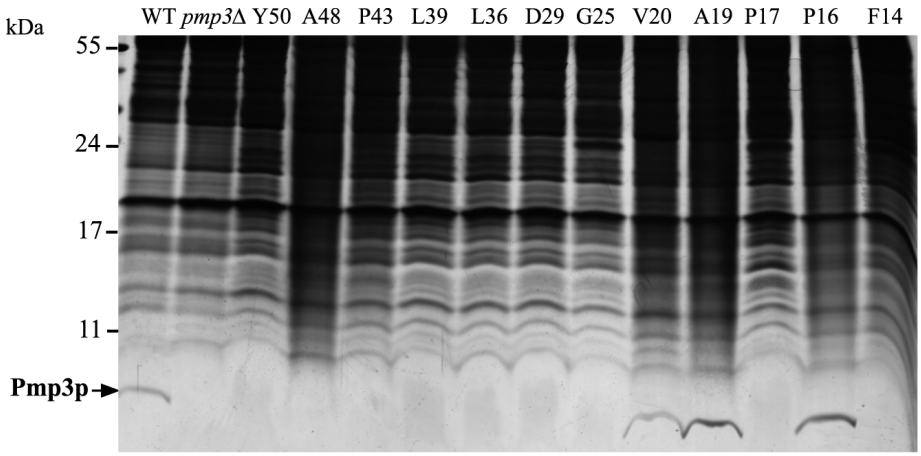

Figure 38. Only P16L, A19L and V20L mutants are well located to the plasma membrane. Silver stained gel of purified plasma membranes from cells expressing different mutated version of the Pmp3p. Molecular weight marker (kDa) is indicated on the left.

Altogether, these results indicate that at least nine residues (F14, P17, G25, D29, L36, L39, P43, A48, Y50) seem important for the function of Pmp3p. This confirms that the well conserved residues seem to play an important role for the protein. Whether they are important for plasma membrane localization has still to be proved. However, we obtained mutants which present a phenotype more severe than the *PMP3* deletion as well in the presence of hygromycin B as in the presence of rhodamine 6G although no band of 6.5 kDa was detected in the enriched plasma membrane (Figure 39).

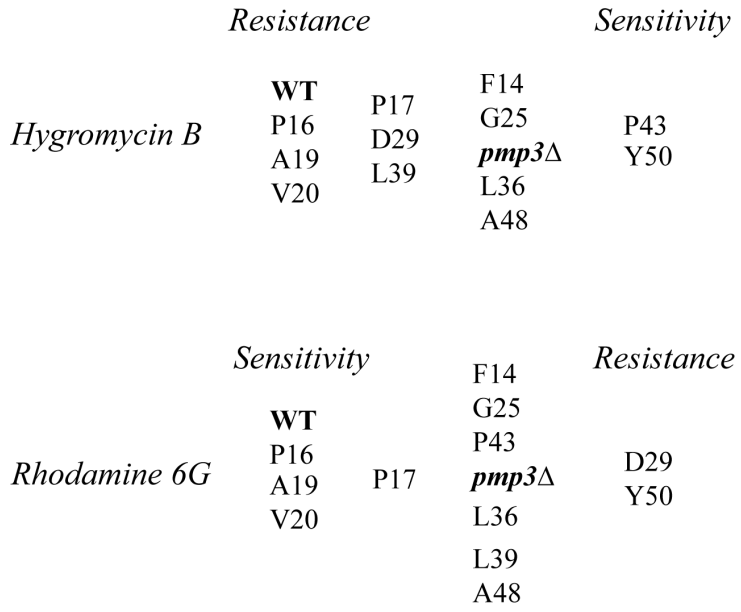

Figure 39. **Scheme illustrating the growth in presence of hygromycin and rhodamine 6G of the 12 points mutant obtained.**

One possibility is that these mutants are present in the plasma membane but are unstable and therefore, the 6.5 kDa band is not visible on the gel (Figure 38). The fusion of a HA tag to these different mutated versions could provide answers. The D29 mutation has a stronger effect on the rhodamine 6G phenotype than on hygromycin B. This suggests that these drugs are transported by different mechanisms and that this mutation could discriminate between these mechanisms. The role of oligomerization could also be tested with this mutant as describe above. The effect of the Y50 mutation is also striking because the hygromycin B sensitivity and rhodamine 6G resistance are stronger than the *pmp3*Δ strain. This suggests that the mutation has a dominant effect affecting both mechanisms implicated in hygromycin B and rhodamine 6G phenotypes.

On the other hand, it is quite surprising that P16, A19 and V20 residues are less important because they are localized in a region containing proline residues. As discussed in the introduction, a proline residue could form a kink in the α-helix and be a key element in the conformation of the protein. For instance, it has been shown that a single conserved proline residue of Stomatin which is an integral membrane protein of human erythrocytes is responsible for the unique hairpin-loop topology (Kadurin et al., 2009). However, it is also known that 44 % of

hydrophobic helices possess a kink, these kinks are not always due to prolines (35 %) but could be formed by others residues (serines, glycines,…). Other information shows that only 20 % of all prolines located in helical regions cause a significance kink (Hall et al., 2009). In the sequence of Pmp3p, we found 2 prolines in the first hydrophobic domain (P16 and P17) and a proline followed by a glycine in the second hydrophobic domain (P43 and G44). These residues could be very important for the topology of the protein. One could imagine that the polypeptide chain does not span entirely the membrane but turns inside the bilayer (Figure 40). This conformation could be affected by the mutations and could affect for the function of Pmp3p.

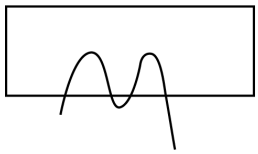

Figure 40. Scheme illustrating the possible hairpin-loop topology of Pmp3p.

If the oligomerization of Pmp3p is needed for its function, hetero-dimers composed of one mutated and one WT monomer could be defective. We transformed WT cells containing the endogenous *PMP3* gene with the plasmids containing the mutated versions of *PMP3*. We observed that in the presence of rhodamine 6G, only the *pmp3*Δ strain can grow while in

the presence of hygromycin B only the *pmp3*Δ strain is sensitive (Figure 41 and 42). The association of WT and mutated Pmp3p does not affect yeast growth in presence of hygromycin B or rhodamine 6G. This suggests that the mutation is not dominant but it does not mean that oligomerization is not necessary for the function. Another possibility is that the majority of the oligomers is formed by the association of wild type monomers. In order to ensure that most of the wild type versions of Pmp3p oligomerize with the mutated version, we should have expressed the mutated version of Pmp3p from a high-copy plasmid under the control of a strong promoter. Curiously, we observed a delay in the growth of each mutant except for the P16L and P17L mutants. This effect is not linked to the presence of the drug, because it is also observed without drugs. This observation should be repeated before further analysis.

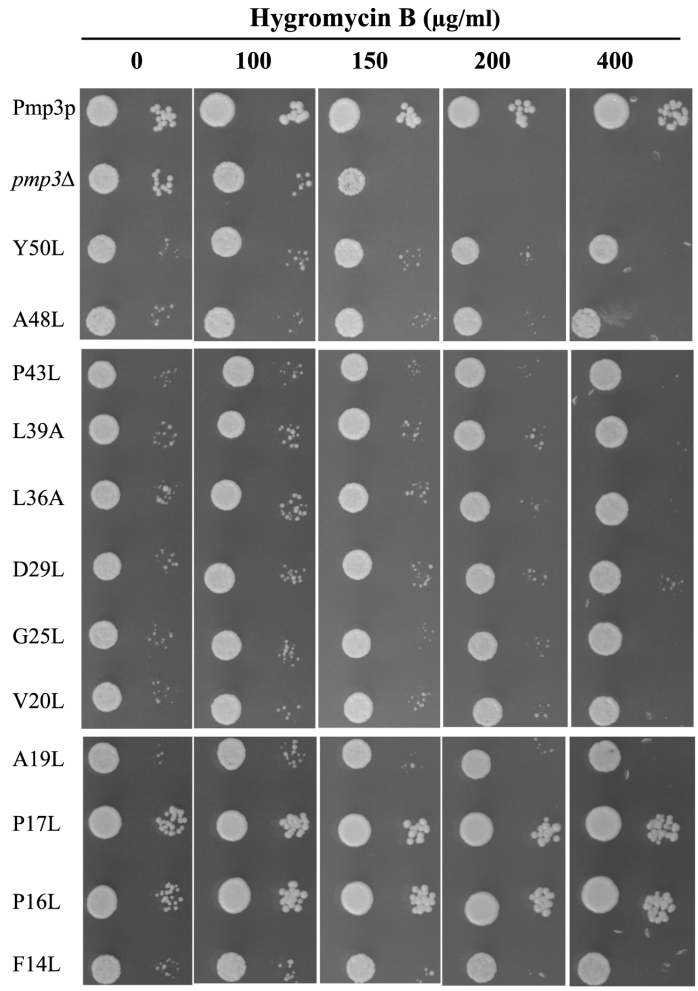

Figure 41. Phenotypic analysis of WT transformed with single-point *PMP3* mutants. WT cells transformed with wild type (WT) or mutant pRS316-*PMP3* constructs and *pmp3*Δ cells transformed with vector alone (*pmp3*Δ) were grown to the logarithmic phase, diluted serially, and spotted onto minimal medium plates, pH 5.5, supplemented with hygromycin B as indicated. The plates were incubated at 30 °C for 4 days.

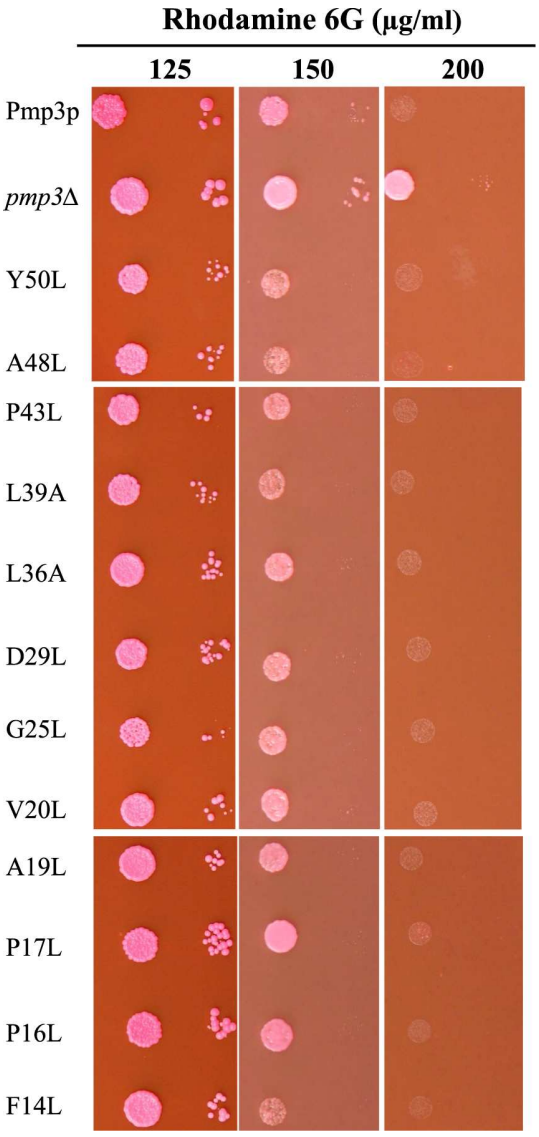

Figure 42. Rhodamine 6G phenotype of WT cells transformed with *PMP3* mutant constructs bearing single amino-acid substitutions. WT cells transformed with wild type (WT) or mutant pRS316-*PMP3* constructs and *pmp3*Δ cells transformed with vector alone (*pmp3*Δ) were grown to the logarithmic phase, diluted serially, and spotted onto minimal medium plates, pH 5.5, supplemented with rhodamine 6G as indicated. The plates were incubated at 30 °C for 4 days.

This second part revealed that 9 conserved residues are important for the function of Pmp3p. Among these 9 residues, the D29 is specifically important for the plasma membrane stabilization of the transporters (Hxt3p, Zrt1p, Itr1p,…) responsible for the rhodamine 6G phenotype and not for the one responsible of the hygromycin phenotype (Ctr1p,…). While the Y50 is a residue particularly important for the plasma membrane stabilization for all of these transporters.

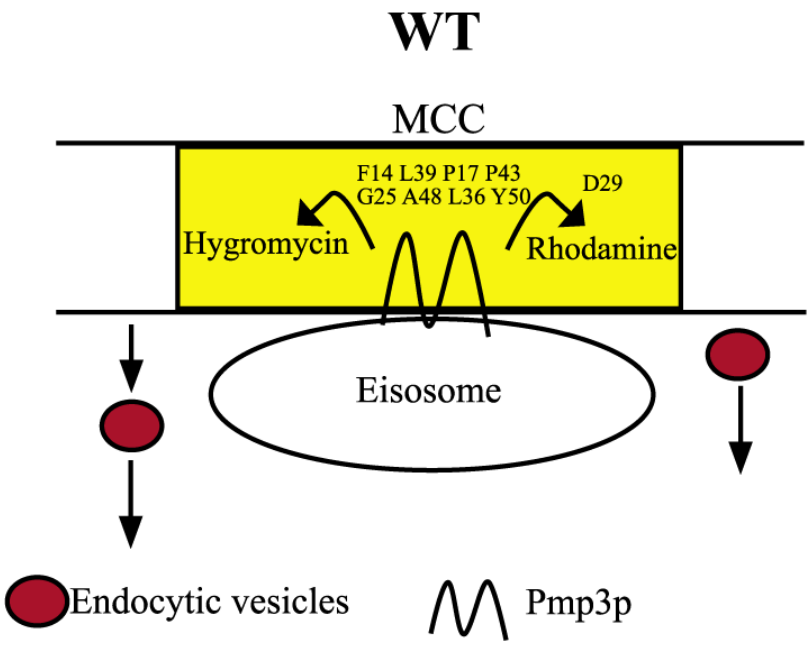

Figure 43. Scheme illustrating the importance of these 9 residues for the function of Pmp3p.

3. The plasma membrane proteome of *Saccharomyces cerevisiae* and its response to the *PMP3* deletion

This part presents the use of proteomic approach for the quantitative profiling of protein expression of the plasma membrane of yeast cells in response to the *PMP3* deletion. We applied a non-gel based quantitative proteomic approach called iTRAQ (Isobaric Tags for Relative and Absolute Quantitation) (Applied Biosystems). This approach has allowed us to avoid facing all the limitations of traditional gel-based techniques. The iTRAQ method uses four amine specific isobaric reagents to label the primary amines of tryptic peptides from four different biological states (Figure 44).

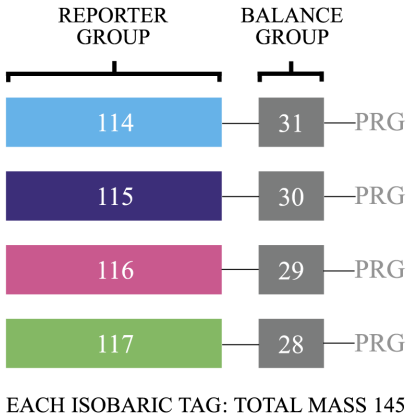

Figure 44. The four amine specific isobaric reagents (structure in annex 1) was designed as an isobaric tag consisting of a charged reporter group, a peptide reactive group (PRG) and a neutral balance portion to maintain an overall mass of 145.

The labeled peptides from each sample are mixed, separated using reversed phase chromatography and analyzed using mass spectrometry (MS) and tandem mass spectrometry (MS/MS) (Figure 45). Because of the isobaric nature of these reagents, the same peptide from each sample appears as a single peak in the MS spectrum, but upon collision induced dissociation during MS/MS the iTRAQ-tagged peptides fragment to release reporter ions (at 114.1, 115.1, 116.1 and 117.1 m/z). The peak area of the reporter ions are used to asses relative abundance of peptides and consequently the proteins (Aggarwal et al., 2006; Ross et al., 2004). In our study, the protein abundance of the yeast plasma membrane from the WT and from the *pmp3*Δ strains were compared using iTRAQ method. Reproducibility of the overall procedure was tested by performing three runs on independent protein preparations.

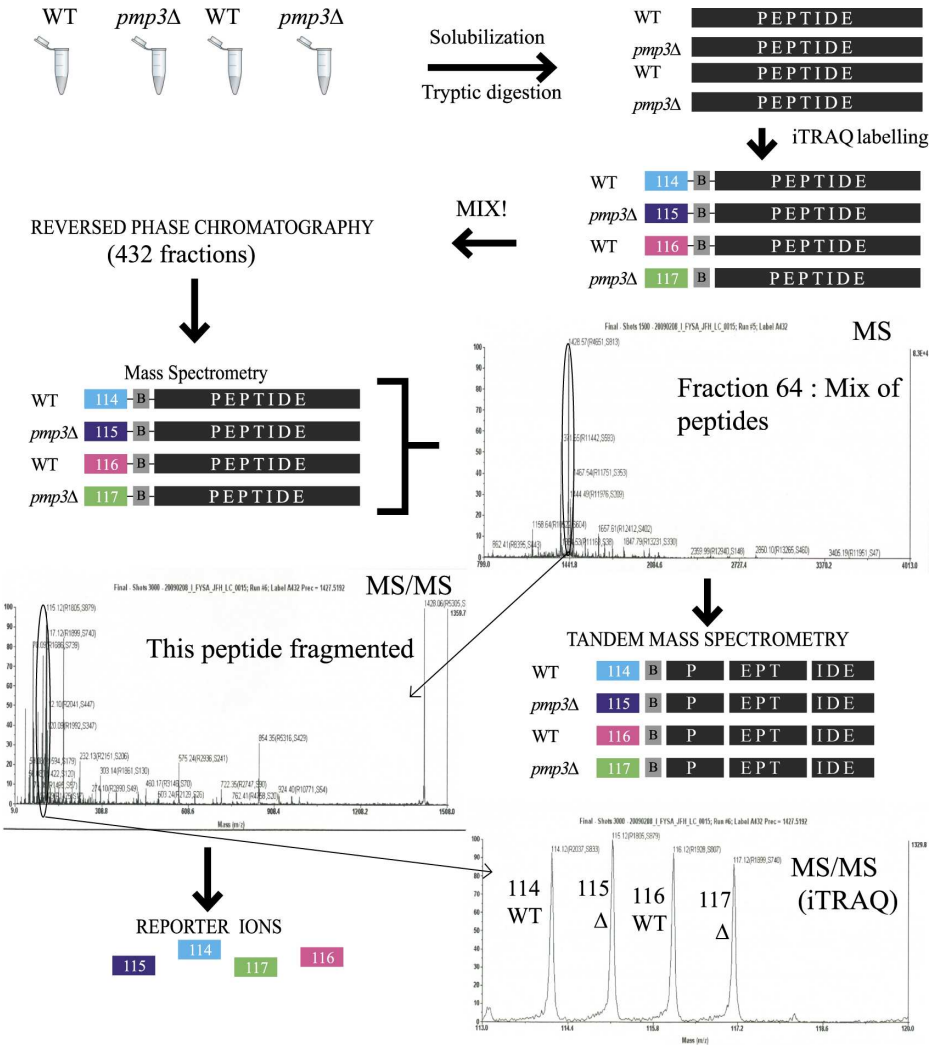

Figure 45. General scheme of a multiplex reaction of four different samples.

This experiment has started with the isolation of plasma membrane (PM) from parental and *pmp3*Δ strain. Mitochondria, the major component of the initial membrane pellet (C15/40), were eliminated by subjecting membranes to acidic precipitation. The intensity of the band corresponding to Pma1p (a PM marker) increased in the supernatant containing unprecipitated membranes (PM fraction) (Figure 46). As expected SDS-PAGE patterns of C15/40 and PM fractions differed strongly.

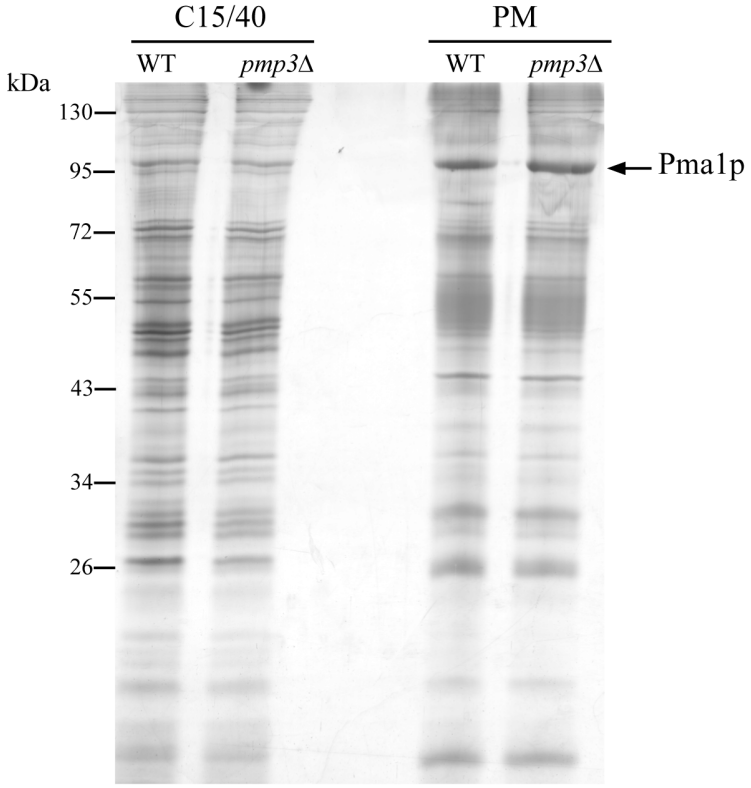

Figure 46. SDS-PAGE of membrane fractions along the course of purification of yeast PM. The successive membrane fractions were prepared as described in Material and Methods. C15/40 : crude membranes (10 µg/lane**)**; PM : purified plasma membranes (10 µg/lane**)**. Gel was silver stained.

Samples containing 100 µg of protein were used for further study. To solubilize intrinsic PM proteins, a mass spectrometry compatible detergent (rapigest) was used. We verified that proteins like Gas1p (a glycosylphosphatidylinositol GPI-anchored protein), Hsp30p (seven

TMDs) or Pma1p (ten TMDs) were identified in the fractions obtained from solubilized proteins. This finding validates the efficiency of the solubilization procedure since these proteins have been shown to localize in plasma membrane (Nuoffer et al., 1991; Panaretou and Piper, 1992; Serrano et al., 1986).

The solubilized plasma membrane fractions corresponding to WT and *pmp3*Δ strains were digested with trypsin and the digests were tagged with iTRAQ tags separately and mixed together. Peptides were separated by reverse phase chromatography (432 fractions) (Figure 47) and analyzed with mass spectrometry. MS analysis was performed on the 432 fractions and 6804 peptides were selected and further analyzed by MS/MS (Figure 45).

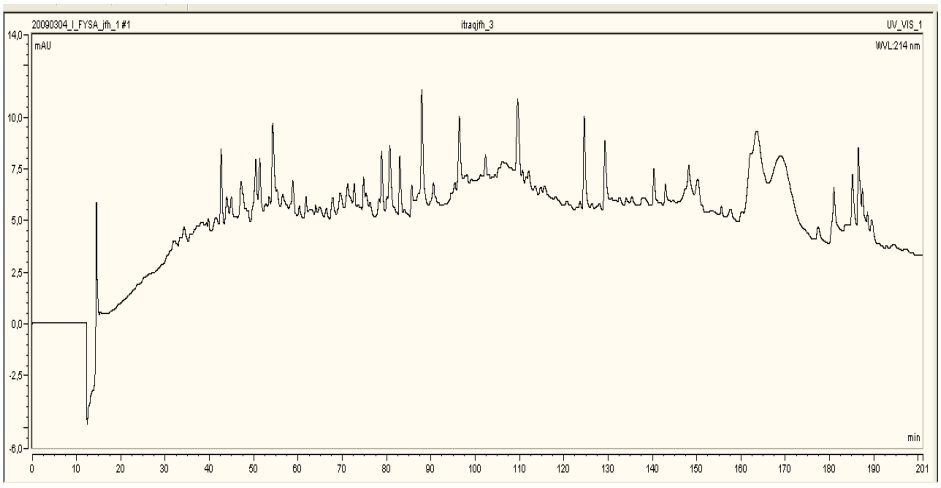

Figure 47. Chromatogram for a yeast sample labeled with iTRAQ tags.

From 196 to 224 proteins were identified, from three repetitions of the experiment. 23% to 27,7% of the proteins were predicted to be localized at the plasma membrane as refered in the *Saccharomyces* Genome database (SGD, http://www.yeastgenome.org), supporting the conclusion that the fraction analyzed is enriched in plasma membrane. A representative list of the identified proteins (shown here from one of the three independent repetitions) is detailed in the annex 2. Nevertheless, it is important to know that a same peptide coming from two isoforms is assigned to both isoforms. It explains why Pma2p is identified with a mascot score of 772 while its expression level is very weak. The majority of the peptides assigned to Pma2p are indeed shared peptides with Pma1p (an abundant plasma membrane protein).

The most abundant contaminants were ribosomal proteins (Figure 48). Similar set of contaminants was observed during all independent repetitions. The 62 plasma membrane proteins identified in this experiment are listed in Table 4. The 34 proteins predicted to display at least 8 TMDs are well known as PM proteins. The presence of soluble proteins could result from PM contamination, as illustrated with the presence of cytosolic translation initiation factors or ribosomal proteins. However, some cytosolic proteins, like Eno2 (involved in glycolysis), Pil1p, Lsp1p have been shown to colocalized with a PM marker (Grossmann et al., 2008; Lopez-Villar et al., 2006). Moreover, Ras2p is a

GTP-binding protein localized to PM when palmitoylated, as well as the casein kinases Yck1 and Yck2. Rsp5p, involved in ubiquitin-mediated degradation, is functionally localized in PM and other compartments. These data suggest that these proteins may interact transiently with the PM.

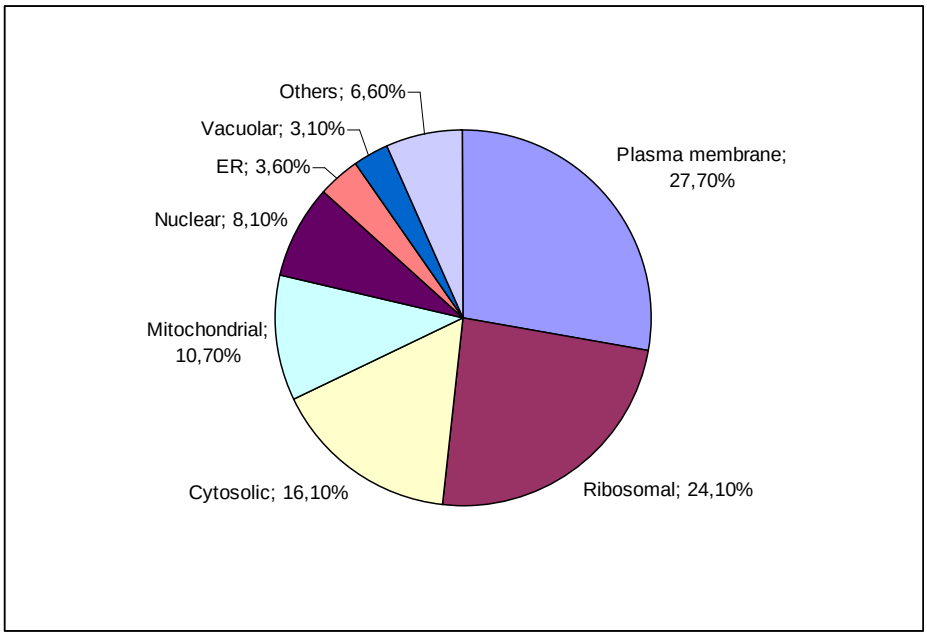

Figure 48. Annotated protein localizations of identified proteins from one of the three independent repetitions. Isolated plasma membrane proteins cover 27,7 % of all identified proteins.

Table 4. Plasma membrane proteins identified in the yeast PM fraction. Proteins are grouped according to functional similarities. TMD shows number of TMD, Peptide shows the number of identified peptides, Plasma membrane location is from SGD and the score is calculated by the Mascot algorithm. The mascot score is given as S=-10 log P where P is the probability that the observed match is a random event. Mascot scores greater than 22 are significant.

Standard Name	Systematic Name	Description summary	TMD	Score	Peptide	Sequence coverage (%)	Location
Transport							
PMA1	YGL008C	Proton transporter	10	1159	26	29	PM
PMA2	YPL036W	Proton transporter	10	772	18	22	PM
HXT7	YDR342C	Glucose transporter	11	595	6	16	PM
HXT6	YDR343C	Glucose transporter	11	489	6	16	PM
THI7	YLR237W	Thiamine transporter	12	205	8	11	PM
NRT1	YOR071C	Nicotinamide riboside transporter	10	190	7	11	PM
MEP2	YNL142W	Ammonium transporter	11	153	2	9	PM
ADY2	YCR010C	Acetate transporter	5	139	3	19	PM
JEN1	YKL217W	Lactate transporter	12	112	3	13	PM
HXT3	YDR345C	Glucose transporter	11	86	5	12	PM
YOR1	YGR281W	Multidrug transporter	11	81	13	14	PM
HXT4	YHR092C	Glucose transporter	11	76	5	9	PM
HXT2	YMR011W	Glucose transporter	12	72	7	12	PM
GAL2	YLR081W	Galactose transporter	12	71	3	8	PM
PNS1	YOR161C	Similar to a choline transporter (*T.californica*)	10	59	2	6	PM

Standard Name	Systematic Name	Description summary	TMD	Score	Peptide	Sequence coverage (%)	Location
HXT15	YDL245C	Protein of unknown function with similarity to hexose transporter	12	56	3	7	PM
HXT13	YEL069C	Hexose transporter	12	56	2	5	PM
MEP3	YPR138C	Ammonium transporter	11	56	2	7	PM
SNQ2	YDR011W	Multidrug transporter	12	50	11	10	PM
MEP1	YGR121C	Ammonium transporter	11	49	2	7	PM
HXT5	YHR096C	Hexose transporter	11	49	4	10	PM
PTR2	YKR093W	Di- and tri-peptides transporter	11	48	6	15	PM
HXT1	YHR094C	Glucose transporter	11	45	4	9	PM
HXT9	YJL219W	Putative hexose transporter	11	45	2	4	PM
HXT10	YFL011W	Putative hexose transporter	11	45	3	8	PM
HXT8	YJL214W	Protein of unknown function with similarity to hexose transporter	10	45	2	5	PM
FPS1	YLL043W	Glycerol transporter	5	39	3	5	PM
ENA1	YDR040C	Sodium transporter	10	38	6	8	PM
THI73	YLR004C	Putative carboxylic acid transporter	12	36	2	6	PM
PDR5	YOR153W	Multidrug transporter	14	33	12	12	PM
TPO3	YPR156C	Polyamine transporter	12	30	2	6	PM
PDR15	YDR406W	Multidrug transporter	12	29	6	8	PM

Standard Name	Systematic Name	Description summary	TMD	Score	Peptide	Sequence coverage (%)	Location
PDR12	YPL058C	Multidrug transporter	11	25	4	7	PM
THI72	YOR192C	Thiamine transporter	10	24	3	6	PM
TPO4	YOR273C	Polyamine transporter	11	24	3	6	PM
Signaling							
PIL1	YGR086C	Primary component of eisosomes	0	463	9	13	Cyt, PM
YCK2	YNL154C	Casein kinase	0	143	8	21	PM
LSP1	YPL004C	Primary component of eisosomes	0	119	3	13	Cyt, PM
RAS2	YNL098C	GTP-binding protein	0	61	3	15	PM
MID2	YLR332W	Protein that acts as a sensor for cell wall	1	58	1	3	PM
BCY1	YIL033C	Component of a signaling pathway	0	56	6	23	PM, Cyt, Nuc
SUR7	YML052 W	Component of eisosomes	4	42	6	17	PM
YCK1	YHR135C	Casein kinase	0	37	5	15	PM
Cell wall							
GAS1	YMR307 W	Beta-1,3-glucanosyltransfer ase	0	214	7	17	PM
FMP45	YDL222C	Required for viability in stationary phase	4	172	4	21	Mit, PM
FKS1	YLR342W	Involved in cell wall synthesis	13	58	15	10	PM
ECM33	YBR078W	GPI-anchored protein involved in apical budding	2	54	3	6	PM

Standard Name	Systematic Name	Description summary	TMD	Score	Peptide	Sequence coverage (%)	Location
GAS5	YOL030W	Beta-1,3-glucanosyltransferase	0	43	3	5	PM, Wall
DCW1	YKL046C	GPI-anchored protein	1	30	2	6	PM
Stress							
MRH1	YDR033W	Protein related to Hsp30p	7	126	3	12	PM
HSP30	YCR021C	Protein negatively regulates Pma1p	7	123	5	27	PM
PST2	YDR032C	Protein induced by oxidative stress	0	25	2	30	PM, Mt
Targeting/ Vesicular transport							
SSO2	YMR183C	Plasma membrane t-SNARE	1	93	4	18	PM
Biosynthesis/degradation							
RSP5	YER125W	Ligase involved in ubiquitin-mediated protein degradation	0	43	9	15	Various

Standard Name	Systematic Name	Description summary	TMD	Score	Peptide	Sequence coverage (%)	Location
Metabolism							
FET3	YMR058W	Membrane multicopper oxidase	1	70	2	7	PM
ENO2	YHR174W	Enolase II	0	59	3	10	Cyt
CHS1	YNL192W	Chitin synthase	7	40	4	4	PM
MSS4	YDR208W	Phosphatidylinositol-4-phosphate 5-kinase	0	25	6	11	PM
Cellular organisation							
YNL194C	YNL194C	Required for sporulation and plasma membrane sphingolipid content	4	33	4	29	PM
Unknown function							
YJR1	YJL171C	GPI-anchored cell wall protein of unknown function	0	66	4	15	Wall, PM
YCP4	YCR004C	Protein of unknown function	0	32	3	26	PM
	YGR266W	Protein of unknown function	1	29	4	11	PM, Mt

The reporter peaks of the iTRAQ reagents in the MS/MS spectra were used for quantitation. The experiment was repeated three times and the results are analyzed from the three independent experiments (Table 5). Only iTRAQ ratios for which $p<0.05$ calculated by Protein Pilot Software were considered as significant.

Table 5. Membrane proteins for which significant (p< 0,05) changes of abundance were observed. Changes are presented as ratio of *pmp*3Δ to WT sample. Score is calculated by the Pro Group algorithm. A score higher than 4 is significant.

Protein name	Score	Quantification				
		*pmp3*Δ/WT	*pmp3*Δ/WT	*pmp3*Δ/WT	WT/WT	*pmp3*Δ/*pmp3*Δ
Pdr15p	20.17	0.7843	0.7815	0.7683	1.0466	1.0118
Eno2p	23.83	0.4658	0.4641	0.4418	1.0312	1.0066
Scw4	4.89	0.5873	0.5429	0.5838	1.0456	1.0179

We observed 3 proteins with a significant change in protein level in response to the deletion of *PMP3*, the 3 were down-regulated: the plasma membrane ATP binding cassette (ABC) transporter (Pdr15p), the Enolase II which is implicated in glycolysis (Eno2p) and a cell wall protein (Scw4p).

Eno2 is a protein that catalyzes the conversion of 2-phosphoglycerate to phosphoenolpyruvate during glycolysis. Therefore, it is quite difficult to imagine a link with Pmp3p although the difference observed is important and reproducible. For Scw4p, it is interesting to note that a possible role in cell wall synthesis has been postulated for the MCC/eisosomes. Indeed, a *C. albicans sur7*Δ mutant displayed obvious defects in cell wall synthesis (Alvarez et al., 2008). Moreover, in another study, Walther and coworkers have found that two cell wall proteins (Gas1 and Fks1) are important for the eisosomes stabilization (Frohlich et al., 2009). Therefore, it would be interesting to deepen the possible link between Pmp3p and the cell wall. Concerning Pdr15p, it is an ABC transporter which is the closest homologue of the multidrug efflux transporter Pdr5p. However, Pdr15p becomes most abundant when cells exit the exponential growth phase, whereas its closest homologue, Pdr5p, disappears after exponential growth. A study revealed that Pdr15p displays limited drug transport capacity, mediating chloramphenicol and detergent tolerance. Nevertheless, Pdr15p is strongly induced even at exponential growth by various stress conditions including heat shock, low pH, weak acids, or salt (Wolfger et al., 2004). The observation that Pdr15p is down-regulated in response to the deletion of *PMP3* should be verified using western blot analysis but it has a sense according to the model in which Pmp3p is implicated in the protection against endocytosis of some MCC

transporters. Unfortunately, some plasma membrane proteins like Zrt1p, Itr1p and Ctr1p have not been identified and quantified by the proteomic approach. In addition, some of the observed changes were not significant because the number of available peptides was probably not sufficient (Hxt3p). It would be interesting to repeat this quantitative proteomic approach after the introduction of another step of purification-fractionation with sucrose gradient in order to remove more contaminants from the sample and increase the signal coming from the plasma membrane proteins.

This analysis based on a mass-spectrometric approach highlighted 3 proteins (Pdr15p, Scw4p and Eno2p) down-regulated in response to the deletion of *PMP3*. Pdr15p is the only one plasma membrane transporter and this result has a sense according to the model in which Pmp3p is implicated in the protection against endocytosis of some MCC transporters (Figure 49). The interaction with Pmp3p for the two others proteins has still to be confirmed.

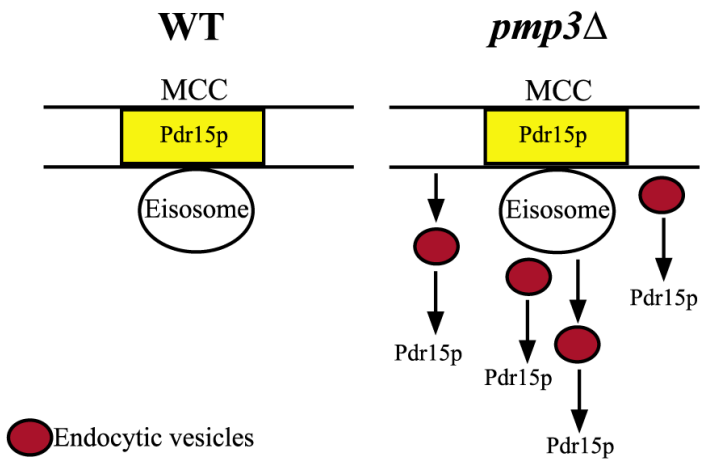

Figure 49. The absence of Pmp3p promotes Pdr15p internalization.

CONCLUSIONS AND PERSPECTIVES

In various eukaryotes, cellular membranes contain distinct microdomains which have been proposed to play important roles in cell signaling, endocytosis, polarity and sorting but their precise functions remain unknown.

The budding yeast has four SNA (Pmp3p/Sna1p, Sna2p, Sna3p and Sna4p) proteins that have different localizations in the cell. Pmp3p/Sna1p is a small plasma membrane hydrophobic polypeptide involved in cation homeostasis. However the *PMP3* gene is not essential under normal growth conditions. Pmp3p shows high sequences similarity with a family of plant proteins that are overexpressed under conditions of high salt concentration or low temperature (Navarre and Goffeau, 2000).

In this study we showed by indirect immunofluorescence that Pmp3p is localized in dots at the plasma membrane and not homogenously as suggested earlier. Moreover, we found by co-immunoprecipitation experiments that Pmp3p interacts with known components of the eisosomes. This suggests that the Pmp3p-containing dots correspond to the recently discovered eisosomes-associated microdomains called MCC. In addition, we observed that a MCC transporter (Can1p) is more prone to internalization in *pmp3*Δ cells indicating that Pmp3p could protect some MCC transporters against endocytosis and link this process to cation homeostasis. It is known that the arginine permease Can1 is degraded in

presence of an excess of arginine, so it would be interesting to analyze the comportment of Pmp3p in this case.

Besides Can1p, the co-immunoprecipitation experiment revealed plasma membrane transporters (Hxt3p, Itr1p, Zrt1p and Ctr1p) which could be closely linked to Pmp3p. Similarly, Pdr15p could be another transporter regulated by Pmp3p, because the proteomic approach highlighted its down-regulation in response to the deletion of *PMP3*. A lot of questions remain to be elucidated. For instance, how these transporters are regulated by Pmp3p and are they all localized in the MCC? In order to answer to these questions, it will be interesting to analyze the comportment of the known MCC transporters (Fur4p, Tat2p) and those identified here (Hxt3p, Itr1p, Zrt1p, Ctr1p and Pdr15p) in a *pmp3*Δ strain. Thanks to the fusion of two different fluorescent tags, it should be possible to determine whether these transporters are localized to the MCC and whether Pmp3p protects all of them against endocytosis or only some of them. It is also possible to follow the stability of these transporters in a *pmp3*Δ strain by pulse chase experiments. A model illustrating the function of Pmp3p is presented at the Figure 50.

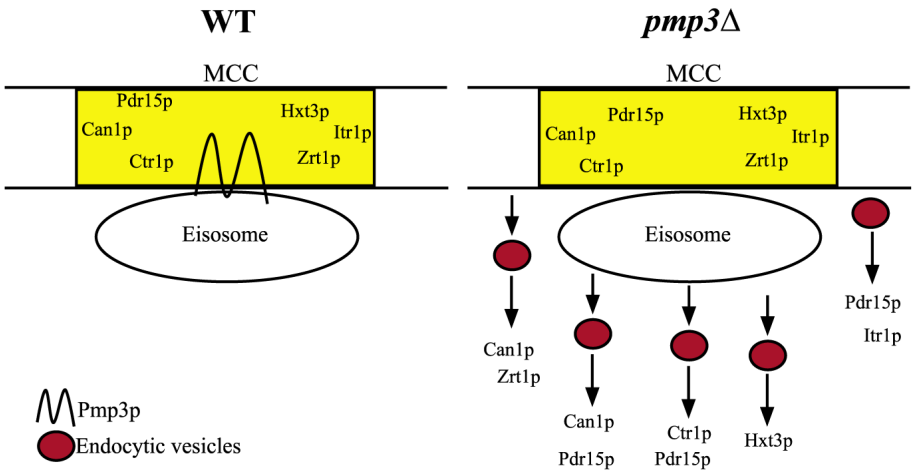

Figure 50. Proposed model for the function of Pmp3p.

Another interesting question is to know in which conditions Pmp3p fulfill its endocytic role. Knowing that the gene is not essential, that the *PMP3* genes in various organisms are induced by various stresses, the study of its expression level and its stability in various conditions (growing phase, stress,…) could give some interesting data. Do the three homologues of Pmp3p play a similar role in different sub-compartments ? Deletion of the C-terminal region of Sna2p redirects the protein to the plasma membrane and restores partially growth defect of *pmp3Δ* strain on hygromycin B (Henri-François Renard, personnal communication).

Another intruiging point is to know whether the MCC/eisosomes are sites of endocytosis or instead whether they protect against endocytosis. One way to answer this question is to block the endocytosis and check whether Can1p-GFP still colocalize with Pil1p-DsRed in a *pmp3*Δ strain. It would also be interesting to know the localization of Pmp3p in a *pil1*Δ strain.

It has been postulated that Pmp3p could interact with NSC1 and that several non specific transporters (Hxt3p, inositol and amino acid transporters…) would be involved in this low affinity transport of cations observed in the *trk1*Δ*trk2*Δ mutant. It is particularly interesting to note that we found in this study some of these transporters (Hxt3p and Itr1p) in close relation with Pmp3p. Further experiments based on patch clamp techniques will be necessary to confirm that NSC1 is composed of these transporters and to confirm the link with Pmp3p.

Beside this, the site-directed mutagenesis approach revealed that at least 9 conserved residues (F14, P17, G25, D29, L36, L39, P43, A48, Y50) are important for the function of Pmp3p. Among them, D29 is particularly important for the plasma membrane stabilization of the transporters (Hxt3p, Zrt1p, Itr1p…) responsible for the rhodamine 6G phenotype but not for the one responsible for the hygromycin phenotype. Moreover, Pmp3p exists in the membrane as an oligomeric form. We will much

better understand the impact of these residues if we can compare them with structural data of Pmp3p. The most direct approach would be to synthesize in vitro a polypeptide whose sequence corresponds to Pmp3p and then analyze it using nuclear magnetic resonance (NMR). This approach has already been used successfully to determine the structure of another proteolipid of the yeast plasma membrane, Pmp1p (Beswick et al., 1998).

MATERIALS AND METHODS

1. Strains and media

1.1. *Escherichia coli*

Escherichia coli JM109 (*rec*A1, *sup*E44, *end*A1, *hsd*R17, *gyr*A96, *rel*A1, *thi*, Δ(*lac-proAB*), F'[*trad36, proAB*$^{+}$, *lacI*^{q}, *lacZ*Δ*M15])* strain was used for plasmid amplification during sub-cloning and sequencing steps. Bacteria were cultured at 37°C in Luria-Bertani (LB) medium (1% (w/v) bactotryptone, 0.5% (w/v) yeast extract and 1% (w/v) NaCl), supplemented with 100 μg/ml ampicilin (Roche). Solid media were supplemented with 2% (w/v) Bacto agar.

1.2. *Saccharomyces cerevisiae*

Saccharomyces cerevisiae strains used in this study are listed in Table 6. Cells were transformed by the One-Step method developed by Chen et al. (1992). Yeast strains were grown at 30°C in rich YD medium (2% yeast extract and 2% glucose) or in YNB minimal medium (2% glucose and 0.7% yeast nitrogen base) supplemented with the appropriate amino acids and adenine required for plasmid maintenance. Solid media additionally contained 2% agar (Sigma).

Table 6. Strains used in this study.

Strain	Genotype	Source
W303-1B	*Matα ade2-1 can 1-100 leu 2-3 his 3-11 ura 3-1 trp 1-1*	(Wallis et al., 1989)
pmp3Δ ::URA3	W303-1B *pmp3Δ::URA3*	(Navarre and Goffeau, 2000)
HA-PMP3	W303-1B *pmp3Δ::HA-PMP3*	This work
PMP3-HA	W303-1B *pmp3Δ::PMP3-HA*	This work
Myc-PMP3	W303-1B *pmp3Δ::MYC-PMP3*	This work
PMP3-Myc	W303-1B *pmp3Δ::PMP3-MYC*	This work
His_6-PMP3	W303-1B *pmp3Δ:: His_6-PMP3*	This work
PMP3-His_6	W303-1B *pmp3Δ::PMP3-His_6*	This work
BY4741	*Mata his 3 leu 2 met15 ura 3*	Euroscarf
BY4742	*Matα his 3 leu 2 met15 ura 3*	Euroscarf
BY *pmp3Δ*	BY4741 *pmp3Δ:: KanMX*	Euroscarf
BY *pil1Δ*	BY4741 *pil1Δ:: KanMX*	Euroscarf
BY *lsp1Δ*	BY4741 *lsp1Δ:: KanMX*	Euroscarf
BY *hxt3Δ*	BY4741 *hxt3Δ:: KanMX*	Euroscarf
BY *ctr1Δ*	BY4741 *ctr1Δ:: KanMX*	Euroscarf
BY *itr1Δ*	BY4741 *itr1Δ:: KanMX*	Euroscarf
BY *zrt1Δ*	BY4741 *zrt1Δ:: KanMX*	Euroscarf
Can1-GFP	BY4742 CAN1::GFP::URA3	(Grossmann et al., 2008)
Can1-GFP pmp3Δ	BY4742 CAN1::GFP::URA3 *pmp3Δ*::K*anMX*	This work

2. DNA constructs

2.1. Strains

The promoter and 3' end regions of *PMP3* were amplified by the polymerase chain reaction (PCR) and cloned into the pTZ vector as *Hin*dIII-*Bam*HI and *Bam*HI-*Eco*RI fragments, respectively. Six *Bam*HI fragments containing the different tagged *PMP3* gene were generated by

PCR using PMP3-HA, HA-PMP3, PMP3-Myc, Myc-PMP3, PMP3-6His, 6His-PMP3, BamH1 and BamH2 oligonucleotides (Table 7) and cloned into the resulting centromeric pTZ::$PMP3_{PROM}$-$PMP3_{STOP}$ vector. These plasmids were restricted with *Eco*RI and the generated DNA was transformed into yeast cells. These fragments were used to transformed *pmp3*Δ, where *PMP3* is disrupted by the *URA3* marker. Loss of the *URA3* marker was monitored by plating one-tenth of an overnight culture in YD on solid YD medium containing 1 g/l of 5-fluoroorotic acid. The resistant cells were screened by PCR to make sure that tagged *PMP3* had replaced the *URA3* marker at the chromosomal *PMP3* locus. Moreover, the *Eco*RI fragment containing the 3' Myc tagged *PMP3* was cloned into the 2μ YEplac195 and the *Eco*RI fragment containing the 3' HA tagged *PMP3* was cloned into the 2μ YEplac181.

2.2. Plasmids

The plasmids used in this study are listed in Table 8. *Bam*HI fragment containing the *PMP3* gene and the 12 mutated *PMP3* genes were generated by PCR using BamH1, BamH2 and F14L,…, Y50L oligonucleotides and cloned into the resulting centromeric pTZ::$PMP3_{PROM}$-$PMP3_{STOP}$ vector. These plasmids were restricted with *Eco*RI and the generated DNA was cloned into the centromeric pRS316

vector, creating a series of construct coding for wild type or mutated version of Pmp3 under the control of its own promoter.

*Hin*dIII-*Age*I fragments containing the *PMP3* gene and the 12 mutated *PMP3* genes were generated by PCR using Hind, Age and F14L,…, Y50L oligonuclueotides and cloned into the centromeric pTL321 vector (derived from pRS416), creating a series of construct coding for 3' GFP wild type or mutated *PMP3* under the control of the *TPI1* promoter (Reggiori and Pelham, 2001).

*Spe*I-*Xho*I fragment containing the *PIL1* gene was generated by PCR and cloned into the centromeric pRS406 vector, creating a construct coding for a 5' GFP tagged *PIL1* under the control of the *SNA2* promoter.

The complete sequence of each construct was checked by sequencing. All enzymes for manipulation of DNA and Faststart High Fidelity PCR polymerase were from Roche Applied Science, except *Age*I enzyme, which was from New England Biolabs.

Table 7. Primers used in this study.

Oligos Name	Sequence (5'-3')[a,b]
BamH1	TAGT***GGATCC***ATGGATTCTGCCAAGATC
BamH2	GCAC***GGATCC***TTAATCTTGTAGGACAATGTA
PMP3-HA	GCAC***GGATCC***TTAGGCGTAGTCTGGGACATCGTATG GGTAATCTTGTAGGACAATGTA

HA-PMP3	TAGT***GGATCC***ATGTACCCATACGATGTCCCAGACTA CGCCGGTGGTGGTGATTCTGCCAAGATC
PMP3-Myc	GCAC***GGATCC***TTACAGATCTTCTTCGGAGATCAGTT TTTGTTCATCTTGTAGGACAATGTA
Myc-PMP3	TAGT***GGATCC***ATGGAACAAAAACTGATCTCCGAAG AAGATCTGGGTGGTGGTGATTCTGCCAAGATC
PMP3-6His	GCAC***GGATCC***TTAATGGTGATGGTGATGGTGATCTT GTAGGACAATGTA
6His-PMP3	TAGT***GGATCC***ATGCACCATCACCATCACCATGGTGG TGGTGATTCTGCCAAGATC
Hind	GCG***AAGCTT***ATGGATTCTGCCAAGATC
Age	GCA***ACCGGT***TAATCTTGTAGGACAATGTA
F14L	TAGTGGATCCATGGATTCTGCCAAGATCATTAACAT TATATTATCCCTTTTATTACCACCA
P16L	TTATCCCTTTTCTTATTACCAGTCGCCGTTTTT
P17L	TCCCTTTTCTTACCATTAGTCGCCGTTTTTCTA
A19L	TTCTTACCACCAGTCTTGGTTTTTCTAGCCCGT
V20L	TTACCACCAGTCGCCCTTTTTCTAGCCCGTGGG
G25L	GTTTTTCTAGCCCGTTTGTGGGGTACTGACTGT
D29L	GATATCCACTATACATAAAGTACCCCACCCACG
L36A	CCAAGCCAAAATGGTAGCAATGATATCCACTAT
L39A	GATATCCACTATACATAAAGTACCCCACCCACG
P43L	GCACGGATCCTTAATCTTGTAGGACAATGTACAATA AATATAGCATACCTAGGAACCA
A48L	GCACGGATCCTTAATCTTGTAGGACAATGTACAATA AATATAGCATACCTGGGAACCA
Y50L	GCACGGATCCTTAATCTTGTAGGACAATTAACAAGG CATATAGCATACC

[A] The restriction sites are in bold and in italic.
[B] The mutated codons are underlined.

Table 8. Plasmids used in this study.

Plasmid	Genotype	Source
pTZ19u-$PMP3_{prom}$-$PMP3_{term}$	lacZ, Amp^R, ori	Navarre and Goffeau, 2000
pRS316-PMP3	*CEN, URA3, PMP3*	This study
pRS316-PMP3(F14L)	*CEN, URA3, PMP3*	This study
pRS316-PMP3(P16L)	*CEN, URA3, PMP3*	This study
pRS316-PMP3(P17L)	*CEN, URA3, PMP3*	This study
pRS316-PMP3(A19L)	*CEN, URA3, PMP3*	This study
pRS316-PMP3(V20L)	*CEN, URA3, PMP3*	This study
pRS316-PMP3(G25L)	*CEN, URA3, PMP3*	This study
pRS316-PMP3(D29L)	*CEN, URA3, PMP3*	This study
pRS316-PMP3(L36A)	*CEN, URA3, PMP3*	This study
pRS316-PMP3(L39A)	*CEN, URA3, PMP3*	This study
pRS316-PMP3(P43L)	*CEN, URA3, PMP3*	This study
pRS316-PMP3(A48L)	*CEN, URA3, PMP3*	This study
pRS316-PMP3(Y50L)	*CEN, URA3, PMP3*	This study
YEplac195-PMP3-Myc	2μ, *URA3*, *PMP3-Myc*	This study
YEplac181-PMP3-HA	2μ, *LEU2*, *PMP3-HA*	This study
pRS416-PMP3-GFP	*CEN, URA3, TPI1-PMP3-GFP*	This study
pRS416-PMP3(F14L)-GFP	*CEN, URA3, TPI1-PMP3-GFP*	This study
pRS416-PMP3(P16L)-GFP	*CEN, URA3, TPI1-PMP3-GFP*	This study

pRS416-PMP3(P17L)-GFP	*CEN, URA3, TPI1-PMP3-GFP*	This study
pRS416-PMP3(A19L)-GFP	*CEN, URA3, TPI1-PMP3-GFP*	This study
pRS416-PMP3(V20L)-GFP	*CEN, URA3, TPI1-PMP3-GFP*	This study
pRS416-PMP3(G25L)-GFP	*CEN, URA3, TPI1-PMP3-GFP*	This study
pRS416-PMP3(D29L)-GFP	*CEN, URA3, TPI1-PMP3-GFP*	This study
pRS416-PMP3(L36A)-GFP	*CEN, URA3, TPI1-PMP3-GFP*	This study
pRS416-PMP3(L39A)-GFP	*CEN, URA3, TPI1-PMP3-GFP*	This study
pRS416-PMP3(P43L)-GFP	*CEN, URA3, TPI1-PMP3-GFP*	This study
pRS416-PMP3(A48L)-GFP	*CEN, URA3, TPI1-PMP3-GFP*	This study
pRS416-PMP3(Y50L)-GFP	*CEN, URA3, TPI1-PMP3-GFP*	This study
pRS406-GFP-PIL1	*CEN, URA3, SNA2-GFP-PIL1*	This study

3. Drug tests

Growth resistance to drug was assayed by spotting 10-fold dilutions of overnight cultures (OD_{600} of 1) onto the surface of a solid medium. Solid media were supplemented with hygromycin B (Sigma), rhodamine 6G (Sigma) and $CaCl_2$ (VWR international) as indicated. Plates were incubated for 2 to 3 days at 30°C.

4. Fluorescence microscopy

Yeast cultures at the exponential growth phase (OD_{600} of 1.2) were examined by epifluorescence microscopy using a Leica DMR microscope and a 100 x oil immersion objective. Excitation was obtained with a mercury HBO 103 w/2 lamp (OSRAM) and observation was performed using a GFP filter (Leica, excitation path 470/40 nm, emission path 525/50 nm). The images were taken with a DC200 camera (Leica) and analysed with the Leica IM1000 software.

5. Proteins

5.1. Plasma membrane preparation

5.1.1. Differential centrifugation

1.2 l late exponential phase cultures in YD or in YNB minimal medium were harvested by centrifugation and washed with H_2O. MBS breaking buffer (sorbitol 250 mM, $MgCl_2.6H_2O$ 1 mM, imidazole 50 mM, pH 7.5) supplemented with protease inhibitor cocktail (leupeptin, aprotinin, antipain, pepstatin and chemostatin, each at 2 μg/ml, Sigma) and 1 mM PMSF were added to the cells (15 ml of buffer per 10 g of harvested cells). Cells were lysed with glass beads at 4°C by agitation for 3 min, with intermittent cooling (once every 30 sec of agitation). After addition of 5 ml of MBS buffer, cell debris and glass beads were removed by centrifugation at 3000 rpm for 5 min at 4°C (2X). The resulting supernatant was centrifuged at 6000 rpm for 5 min at 4°C to give a nuclear membrane-enriched pellet. Then, the supernatant was centrifuged once more at 13000 rpm for 40 min at 4°C to obtain a plasma membrane-enriched pellet (C15/40), which was resuspended in 5 ml of MS suspension buffer ($MgCl_2.6H_2O$ 1 mM, imidazole 50 mM, pH 7.5).

5.1.2. Acid precipitation

Plasma membranes were purified from the C15/40 fraction by acid precipitation. Protein concentration of the C15/40 fraction was adjusted to 5 mg/ml with MS buffer, and the pH to 5.2, with 1 M acetic acid. The membrane suspension was then centrifuged at 6500 rpm for 3 min at 4°C to obtain the mitochondria-enriched pellet. After pH neutralization to 7.5 with 1 M NaOH the supernatant fraction was centrifuged at 15000 rpm for 40 min 4°C to obtain the plasma membranes which were resuspended in 500 µl of MS buffer.

5.2. Protein quantification

Protein concentration was determined by the Bradford method, which is based on the binding of Coomassie Blue G-250 (Sigma) to proteins (Bradford, 1976). As standards, 0 to 7 µg of bovine serum albumin (BSA, Sigma) were used. Absorbance was measured at 595 nm.

5.3. Membrane solubilization

Membrane proteins were solubilized with zwittergent 3-14 (Calbiochem) at a detergent/protein ratio of 10/1. After 30 min of agitation at 4°C, samples were centrifuged at 48000 rpm for 60 min. The supernatant was kept and membrane pellets were resuspended in 10 mM Tris-HCl (pH 7.5) with a syringe.

5.4. Protein separation and detection

5.4.1. SDS polyacrylamide gel electrophoresis (PAGE)

Proteins were incubated for 10 min in the Laemmli buffer (Tris-HCl 80 mM, pH 6.8, 2% SDS, 10% glycerol, 1% DTT, and 0.005% bromophenol blue) and separated in a 8% or 15% (w/v) SDS-polyacrylamide gel depending on the size of the protein analyzed. Electrophoresis was carried out at 100 V for 1 h. When the proteins entered the separating gel the voltage was increased to 160 V and the electrophoresis was continued for 1h.

After migration, gels were fixed in 50% ethanol, 2% H_3PO_4 for at least 3h at room temperature. After washing 3 times for 30 min in water, the gels were incubated for 1h in the staining solution (34% methanol, 17% (w/v) $(NH_4)_2SO_4$, 3% H_3PO_4). Then, Coomassie colloidal blue (Serva Blue G-250) was added to 0.07% (w/v) and incubated for 3 days. Excess dye was washed off with H_2O.

5.4.2. SDS polyacrylamide gel electrophoresis (Tris-Tricine)

The methodology described by Schäger and von Jagow (1987), has the advantage to separate the polypeptides of small sizes. Proteins were denaturated in the Laemmli buffer, electrophoresed and silver stained. The conditions used are those described for a concentration gel of 4% T-

3% C, a spacer of 10% T- 3% C and for a separating gel of 16.5% T- 3.3% C, where T corresponds to the total concentration in acrylamide/bis-acrylimide and C corresponds to the concentration in bis-acrylimide.

5.4.3. Western blot analysis

Proteins separated by SDS-PAGE were transferred onto a polyvinylidene difluoride (PVDF) membrane at 50 V for 20 min in 30 mM Tris, 240 mM glycine, 20% (v/v) methanol and 0.02% SDS. We used the BIO-RAD "wet" transfer system. After transfer, the membrane was washed three times for 5 min in Tris-buffered saline (TBS) buffer (Tris-HCl 20 mM, pH 7.5, NaCl 150 mM) supplemented with 0.1% Tween 80 and then incubated at room temperature for 30 min in TBS buffer supplemented with 3% (w/v) low fat dried milk and 0.5% (w/v) Tween 80. After washing three times for 5 min with TBS buffer, the membrane was incubated in TBS buffer supplemented with 0.5% low fat dried milk, 0.1% Tween 80, and the specific primary antibodies (Table 9). After washing twice for 10 min in TBS buffer, the membrane was incubated with secondary peroxidase-coupled antibodies (Table 9). After washing three times for 5 min with TBS buffer, the antigen-antibody complexes were detected by the enhanced chemiluminescence (Roche). The membrane was stripped with 0.5 N NaOH for 5 min and washed 5 min

with TBS buffer in order to remove bound antibodies before a second immunodetection.

Table 9. Primary and secondary antibodies used in this study.

Primary antibodies	Dilution and incubation time	Secondary antibodies	Dilution and incubation time
Anti-HA (Roche)	1/1000 2h	Anti-rat	1/10000 2h
Anti-Myc (Santa Cruz biotechnology)	1/1000 2h	Anti-rabbit	1/10000 2h
Anti-His_5 (Qiagen)	1/1000 2h	Anti-mouse	1/10000 2h
Anti-GFP (Roche)	1/5000 2h	Anti-mouse	1/10000 2h

5.5. Immunoprecipitation

Plasma membranes were solubilized with zwittergent 3-14 at a 1/10 protein/detergent ratio for 30 min at 4°C on a rotating mixer. Non-solubilized membranes were removed by centrifugation at 48000 rpm for 1 h at 4°C. To reduce background caused by non-specific adsorption of irrelevant proteins to protein G agarose beads (Roche Diagnostics Co.), we added 50 µl of protein G agarose beads to the solubilized plasma membranes and incubated 2 hours at 4°C on a rotating mixer. Then, immunoprecipitation was performed for 2 h at 4°C on a rotating mixer using rat anti-HA, mouse anti-GFP (Roche Diagnostics) or rabbit anti-Myc (Santa Cruz Biotechnology) antibodies, followed by 2 h incubation with protein G agarose beads. The beads were washed three times with

MS buffer (10 mM imidazole, 1 mM $MgCl_2$, pH 7.5) and the immunoprecipitated proteins eluted with sample buffer (Tris-HCl 80 mM pH 6.8, glycerol 10%, SDS 2%, Bromophenol Blue 0.005%). The stained protein band was manually excised and in-gel tryptic digest performed using standard protocols. The peptides generated were mixed with 2 mg/ml of alpha-cyano-4-hydroxycinnamic acid matrix and MS and MS/MS spectra acquired using an Applied Bisosystems 4800 MALDI TOF/TOF™ Analyzer spectrometer. MS and MS/MS queries were performed using the Applied Biosystems GPS Explorer™ 3.6 software working with the Matrix Science Ltd MASCOT® Database search engine v2.1 (Boston, USA). The National Center for Biotechnology Information database restricted to fungi was used. A 200 ppm precursor tolerance for MS spectra and a 0.1 Da fragment tolerance for MS/MS spectra were allowed. The selected charge state of + 1, one trypsin mis-cleavage, and modifications, consisting of methionine oxidation, cysteine carbamidomethylation, and acrylamide-modified cysteine, were used.

6. Immunofluorescence

Yeast cells grown to exponential growth phase were fixed by incubation for 10 min in 4% formaldehyde. They were then collected by centrifugation and resuspended for 2 h at RT in fixation buffer (0.1 M phosphate buffer, 0.5 mM $MgCl_2$, 3.7% formaldehyde, pH 6.5). They

were washed three times in washing buffer (0.1 M phosphate buffer, 1.2 M sorbitol), resuspended in 2 mL of washing buffer supplemented with 0.2 mg/mL Zymolyase 20 T (Seikagaku, Tokyo, Japan) and incubated for 15–30 min at 37°C. The resulting spheroplasts were washed twice in washing buffer and were spotted onto polylysine-coated slides for 5 min. They were then permeabilized by incubation in methanol at -20°C during 6' followed by incubation in aceton during 30''. The slides were incubated with PBS (50 mM potassium phosphate, pH 7.5 and 150 mM NaCl) supplemented with 0.5% Tween20 and 2% powder milk for 60' at room temperature. The slides were then incubated overnight at 4°C with the monoclonal anti-HA diluted 1:100 (clone 3F10) (Roche Diagnostics, Meylan, France) or 1:100 (polyclonal anti-GFP) in PBS supplemented with 0.2% powder milk. They were then washed three times in PBS and incubated with $Alexa_{633}$-labeled goat anti-mouse IgG (Molecular Probes) and fluorescein isothiocyanate (FITC)-labeled goat anti-rat IgG (Pierce) diluted 1:100 for 60 min. Optically sectioned images were acquired by confocal laser scanning microscopy using a Zeiss LSM 710 confocal microscope and analyzed using ZEN 2008.

7. Endocytosis assays

For monitoring endocytosis by uptake of FM4-64 (Invitrogen), the cells were grown to exponential phase in YD medium to an OD of 1 to 1.5 and

centrifuged at 6000 rpm for 1 min. All but 100 µl of the medium was removed, and then 1 µl of FM4-64 (16mM) was added to the pellet and the remaining medium in the tube, and the tubes vortexed and incubated for 15 min at 4°C. The cells were washed twice with fresh medium and centrifuged at 10000 rpm for 1 min, and then the supernatant was discarded and the cells were resuspended in 1 ml of fresh medium and incubated for different times at 30 °C. FM4-64 uptake was stopped by the addition of 10 mM NaN_3 and 10 mM NaF. Fluorescence was observed with a Texas red filter. Yeast cultures were examined by epifluorescence microscopy using a Leica DMR microscope and a 100 x oil immersion objective.

8. iTRAQ analysis

8.1. iTRAQ labeling

iTRAQ technique (Applied biosystems) uses amine specific isobaric reagents that label the primary amines from four different states of samples. In this study we used two isobaric tags for labeling of peptides coming from the WT strain and the strain deleted for *PMP3*. 100 µg of proteins from purified plasma membrane fractions were solubilized with 2% rapigest (Waters), then reduced with 5mM DTT, blocked by 15 mM iodoacetamide and digested with trypsin (1 µg/100 µg proteins). The detergent was removed by acidic lysis (trifluoroacetic acid 0,5%) and the

iTRAQ labeling was performed according to the manufacturer's protocol (Applied Biosystems).

8.2. Reverse phase chromatography

Reverse-phase separation of peptides was completed on a C18 PepMap100 (3μm, 100Å) (Dionex). Before separation sample was desalted using pre-column. Gradient solution A contained: 0.1 % trifluoroacetic acid (TFA), 5% acetonitrile (ACN) and gradient solution B: 0.085 % TFA and 80 % ACN. The eluting peptides were mixed with α–cyano-4-hydroxycinnamic acid matrix, 2 mg/ml (solvent: 70% ACN, 0.1 % TFA) and spotted directly onto a maldi plate using a Probot system (LC Packings Amersham).

8.3. Mass spectrometry analysis and protein identification

Peptides were analyzed with a MALDI-TOF/TOF ABI 4800 mass spectrometer (Applied Biosystems). Identification of proteins was carried using Protein™ pilot Software. It allows identifying proteins from database searches of mass spectrometry data using two database searching algorithms: the Paragon™ Algorithm and the Mascot Algorithm. For searches using the Paragon Algorithm, the searches results were further processed by the Pro Group™ Algorithm to determine the minimal set of justifiable identified proteins. The peptide confidence

for each peptide was converted to Prot Score units. For each detected protein, the Pro Group™ Algorithm calculates the Total Prot Score. Proteins were assigned to subcellular localizations, based on SGD annotations and Uniprot Database.

8.4. Quantification of relative change

The Paragon™ Algorithm was used to determine relative protein levels. The quantification information was obtained automatically from the peak areas of the reporter ions from the mass spectra. For each protein ratio reported in the Pro Group™ Algorithm Results, the program calculates a p-value, the certainty that the observed change is real. All ratios for which $p<0.05$ were regarded as significant.

REFERENCES

Addison, R. (1986) Primary structure of the Neurospora plasma membrane H+-ATPase deduced from the gene sequence. Homology to Na+/K+-, Ca2+-, and K+-ATPase. *J Biol Chem*, **261**, 14896-14901.

Agarwal, A.K., Rogers, P.D., Baerson, S.R., Jacob, M.R., Barker, K.S., Cleary, J.D., Walker, L.A., Nagle, D.G. and Clark, A.M. (2003) Genome-wide expression profiling of the response to polyene, pyrimidine, azole, and echinocandin antifungal agents in Saccharomyces cerevisiae. *J Biol Chem*, **278**, 34998-35015.

Aggarwal, K., Choe, L.H. and Lee, K.H. (2006) Shotgun proteomics using the iTRAQ isobaric tags. *Brief Funct Genomic Proteomic*, **5**, 112-120.

Alepuz, P.M., Cunningham, K.W. and Estruch, F. (1997) Glucose repression affects ion homeostasis in yeast through the regulation of the stress-activated ENA1 gene. *Mol Microbiol*, **26**, 91-98.

Alvarez, F.J., Douglas, L.M. and Konopka, J.B. (2007) Sterol-rich plasma membrane domains in fungi. *Eukaryot Cell*, **6**, 755-763.

Alvarez, F.J., Douglas, L.M., Rosebrock, A. and Konopka, J.B. (2008) The Sur7 protein regulates plasma membrane organization and prevents intracellular cell wall growth in Candida albicans. *Mol Biol Cell*, **19**, 5214-5225.

Anderson, R.G. and Jacobson, K. (2002) A role for lipid shells in targeting proteins to caveolae, rafts, and other lipid domains. *Science*, **296**, 1821-1825.

Aouida, M., Leduc, A., Poulin, R. and Ramotar, D. (2005) AGP2 encodes the major permease for high affinity polyamine import in Saccharomyces cerevisiae. *J Biol Chem*, **280**, 24267-24276.

Aouida, M., Leduc, A., Wang, H. and Ramotar, D. (2004a) Characterization of a transport and detoxification pathway for the antitumour drug bleomycin in Saccharomyces cerevisiae. *Biochem J*, **384**, 47-58.

Aouida, M., Page, N., Leduc, A., Peter, M. and Ramotar, D. (2004b) A genome-wide screen in Saccharomyces cerevisiae reveals altered transport as a mechanism of resistance to the anticancer drug bleomycin. *Cancer Res*, **64**, 1102-1109.

Aouida, M. and Ramotar, D. (2006) Bleomycin holds the key for improved anticancer therapy. *Cancer Therapy*, **4**, 171-182.

Aronova, S., Wedaman, K., Aronov, P.A., Fontes, K., Ramos, K., Hammock, B.D. and Powers, T. (2008) Regulation of ceramide biosynthesis by TOR complex 2. *Cell Metab*, **7**, 148-158.

Auer, M., Scarborough, G.A. and Kuhlbrandt, W. (1998) Three-dimensional map of the plasma membrane H+-ATPase in the open conformation. *Nature*, **392**, 840-843.

Axelsen, K.B. and Palmgren, M.G. (1998) Evolution of substrate specificities in the P-type ATPase superfamily. *J Mol Evol*, **46**, 84-101.

Bagnat, M., Chang, A. and Simons, K. (2001) Plasma membrane proton ATPase Pma1p requires raft association for surface delivery in yeast. *Mol Biol Cell*, **12**, 4129-4138.

Bagnat, M., Keranen, S., Shevchenko, A. and Simons, K. (2000) Lipid rafts function in biosynthetic delivery of proteins to the cell surface in yeast. *Proc Natl Acad Sci U S A*, **97**, 3254-3259.

Bagnat, M. and Simons, K. (2002) Lipid rafts in protein sorting and cell polarity in budding yeast Saccharomyces cerevisiae. *Biol Chem*, **383**, 1475-1480.

Banuelos, M.A., Sychrova, H., Bleykasten-Grosshans, C., Souciet, J.L. and Potier, S. (1998) The Nha1 antiporter of Saccharomyces cerevisiae mediates sodium and potassium efflux. *Microbiology*, **144**, 2749-2758.

Benito, B., Quintero, F.J. and Rodriguez-Navarro, A. (1997) Overexpression of the sodium ATPase of Saccharomyces cerevisiae: conditions for phosphorylation from ATP and Pi. *Biochim Biophys Acta*, **1328**, 214-226.

Berchtold, D. and Walther, T.C. (2009) TORC2 plasma membrane localization is essential for cell viability and restricted to a distinct domain. *Mol Biol Cell*, **20**, 1565-1575.

Bertl, A., Bihler, H., Reid, J.D., Kettner, C. and Slayman, C.L. (1998) Physiological characterization of the yeast plasma membrane outward rectifying K+ channel, DUK1 (TOK1), in situ. *J Membr Biol*, **162**, 67-80.

Bertl, A., Ramos, J., Ludwig, J., Lichtenberg-Frate, H., Reid, J., Bihler, H., Calero, F., Martinez, P. and Ljungdahl, P.O. (2003) Characterization of potassium transport in wild-type and isogenic yeast strains carrying all combinations of trk1, trk2 and tok1 null mutations. *Mol Microbiol*, **47**, 767-780.

Bertl, A., Slayman, C.L. and Gradmann, D. (1993) Gating and conductance in an outward-rectifying K+ channel from the plasma membrane of Saccharomyces cerevisiae. *J Membr Biol*, **132**, 183-199.

Beswick, V., Roux, M., Navarre, C., Coic, Y.M., Huynh-Dinh, T., Goffeau, A., Sanson, A. and Neumann, J.M. (1998) 1H- and 2H-NMR studies of a fragment of PMP1, a regulatory subunit associated with the yeast plasma membrane H(+)-ATPase. Conformational properties and lipid-peptide interactions. *Biochimie*, **80**, 451-459.

Bihler, H., Slayman, C.L. and Bertl, A. (1998) NSC1: a novel high-current inward rectifier for cations in the plasma membrane of Saccharomyces cerevisiae. *FEBS Lett*, **432**, 59-64.

Bihler, H., Slayman, C.L. and Bertl, A. (2002) Low-affinity potassium uptake by Saccharomyces cerevisiae is mediated by NSC1, a calcium-blocked non-specific cation channel. *Biochim Biophys Acta*, **1558**, 109-118.

Borochov, H. and Shinitzky, M. (1976) Vertical displacement of membrane proteins mediated by changes in microviscosity. *Proc Natl Acad Sci U S A*, **73**, 4526-4530.

Bowers, K., Levi, B.P., Patel, F.I. and Stevens, T.H. (2000) The sodium/proton exchanger Nhx1p is required for endosomal protein trafficking in the yeast Saccharomyces cerevisiae. *Mol Biol Cell*, **11**, 4277-4294.

Bradford, M.M. (1976) A rapid and sensitive method for the quantitation of microgram quantities of protein utilizing the principle of protein-dye binding. *Anal Biochem*, **72**, 248-254.

Brett, C.L., Donowitz, M. and Rao, R. (2005a) Evolutionary origins of eukaryotic sodium/proton exchangers. *Am J Physiol Cell Physiol*, **288**, C223-239.

Brett, C.L., Tukaye, D.N., Mukherjee, S. and Rao, R. (2005b) The yeast endosomal Na+K+/H+ exchanger Nhx1 regulates cellular pH to control vesicle trafficking. *Mol Biol Cell*, **16**, 1396-1405.

Brown, D.A. and London, E. (1998) Functions of lipid rafts in biological membranes. *Annu Rev Cell Dev Biol*, **14**, 111-136.

Brown, D.A. and Rose, J.K. (1992) Sorting of GPI-anchored proteins to glycolipid-enriched membrane subdomains during transport to the apical cell surface. *Cell*, **68**, 533-544.

Bryant, N.J. and Stevens, T.H. (1998) Vacuole biogenesis in Saccharomyces cerevisiae: protein transport pathways to the yeast vacuole. *Microbiol Mol Biol Rev*, **62**, 230-247.

Cagnac, O., Leterrier, M., Yeager, M. and Blumwald, E. (2007) Identification and characterization of Vnx1p, a novel type of vacuolar monovalent cation/H+ antiporter of Saccharomyces cerevisiae. *J Biol Chem*, **282**, 24284-24293.

Casey, P.J. (1995) Protein lipidation in cell signaling. *Science*, **268**, 221-225.

Catty, P., de Kerchove d'Exaerde, A. and Goffeau, A. (1997) The complete inventory of the yeast Saccharomyces cerevisiae P-type transport ATPases. *FEBS Lett*, **409**, 325-332.

Chang-Qing, Z., Shunsaku, N., Shenkui, L. and Tetsuo, T. (2008) Characterization of two plasma membrane protein 3 genes (PutPMP3) from the alkali grass, Puccinellia tenuiflora, and functional comparison of the rice homologues, OsLti6a/b from rice. *BMB Rep*, **41**, 448-454.

Chen, D.C., Yang, B.C. and Kuo, T.T. (1992) One-step transformation of yeast in stationary phase. *Curr Genet*, **21**, 83-84.

Crespo, J.L., Daicho, K., Ushimaru, T. and Hall, M.N. (2001) The GATA transcription factors GLN3 and GAT1 link TOR to salt stress in Saccharomyces cerevisiae. *J Biol Chem*, **276**, 34441-34444.

Danielli, J.F. and Davson H. (1935) A contribution to the theory of permeability of thin films. *J Cell Comp Physiol*, **5**, 495-508.

Daquinag, A., Fadri, M., Jung, S.Y., Qin, J. and Kunz, J. (2007) The yeast PH domain proteins Slm1 and Slm2 are targets of sphingolipid signaling during the response to heat stress. *Mol Cell Biol*, **27**, 633-650.

Daum, G., Lees, N.D., Bard, M. and Dickson, R. (1998) Biochemistry, cell biology and molecular biology of lipids of Saccharomyces cerevisiae. *Yeast*, **14**, 1471-1510.

deHart, A.K., Schnell, J.D., Allen, D.A. and Hicke, L. (2002) The conserved Pkh-Ypk kinase cascade is required for endocytosis in yeast. *J Cell Biol*, **156**, 241-248.

deHart, A.K., Schnell, J.D., Allen, D.A., Tsai, J.Y. and Hicke, L. (2003) Receptor internalization in yeast requires the Tor2-Rho1 signaling pathway. *Mol Biol Cell*, **14**, 4676-4684.

Deng, C., Xiong, X. and Krutchinsky, A.N. (2009) Unifying fluorescence microscopy and mass spectrometry for studying protein complexes in cells. *Mol Cell Proteomics*, **8**, 1413-1423.

Dickson, R.C. (2008) Thematic review series: sphingolipids. New insights into sphingolipid metabolism and function in budding yeast. *J Lipid Res*, **49**, 909-921.

Dufour, J.P. and Goffeau, A. (1978) Solubilization by lysolecithin and purification of the plasma membrane ATPase of the yeast Schizosaccharomyces pombe. *J Biol Chem*, **253**, 7026-7032.

Dupre, S. and Haguenauer-Tsapis, R. (2003) Raft partitioning of the yeast uracil permease during trafficking along the endocytic pathway. *Traffic*, **4**, 83-96.

Durell, S.R. and Guy, H.R. (1999) Structural models of the KtrB, TrkH, and Trk1,2 symporters based on the structure of the KcsA K(+) channel. *Biophys J*, **77**, 789-807.

Eisenkolb, M., Zenzmaier, C., Leitner, E. and Schneiter, R. (2002) A specific structural requirement for ergosterol in long-chain fatty acid synthesis mutants important for maintaining raft domains in yeast. *Mol Biol Cell*, **13**, 4414-4428.

Engqvist-Goldstein, A.E. and Drubin, D.G. (2003) Actin assembly and endocytosis: from yeast to mammals. *Annu Rev Cell Dev Biol*, **19**, 287-332.

Eraso, P. and Gancedo, C. (1987) Activation of yeast plasma membrane ATPase by acid pH during growth. *FEBS Lett*, **224**, 187-192.

Erez, O. and Kahana, C. (2001) Screening for modulators of spermine tolerance identifies Sky1, the SR protein kinase of Saccharomyces cerevisiae, as a regulator of polyamine transport and ion homeostasis. *Mol Cell Biol*, **21**, 175-184.

Erez, O. and Kahana, C. (2002) Deletions of SKY1 or PTK2 in the Saccharomyces cerevisiae trk1Deltatrk2Delta mutant cells exert dual effect on ion homeostasis. *Biochem Biophys Res Commun*, **295**, 1142-1149.

Fairman, C., Zhou, X. and Kung, C. (1999) Potassium uptake through the TOK1 K+ channel in the budding yeast. *J Membr Biol*, **168**, 149-157.

Friant, S., Lombardi, R., Schmelzle, T., Hall, M.N. and Riezman, H. (2001) Sphingoid base signaling via Pkh kinases is required for endocytosis in yeast. *EMBO J*, **20**, 6783-6792.

Frohlich, F., Moreira, K., Aguilar, P.S., Hubner, N.C., Mann, M., Walter, P. and Walther, T.C. (2009) A genome-wide screen for genes affecting eisosomes reveals Nce102 function in sphingolipid signaling. *J Cell Biol*, **185**, 1227-1242.

Frye, L.D. and Edidin M. (1970) The rapid intermixing of cell surface antigens after formation of mouse–human heterokaryons. *J. Cell Sci.*, **7**, 319–335.

Furuse, M. and Tsukita, S. (2006) Claudins in occluding junctions of humans and flies. *Trends Cell Biol*, **16**, 181-188.

Gaber, R.F., Styles, C.A. and Fink, G.R. (1988) TRK1 encodes a plasma membrane protein required for high-affinity potassium transport in Saccharomyces cerevisiae. *Mol Cell Biol*, **8**, 2848-2859.

Gaigg, B., Timischl, B., Corbino, L. and Schneiter, R. (2005) Synthesis of sphingolipids with very long chain fatty acids but not ergosterol is required for routing of newly synthesized plasma membrane ATPase to the cell surface of yeast. *J Biol Chem*, **280**, 22515-22522.

Garciadeblas, B., Rubio, F., Quintero, F.J., Banuelos, M.A., Haro, R. and Rodriguez-Navarro, A. (1993) Differential expression of two genes encoding isoforms of the ATPase involved in sodium efflux in Saccharomyces cerevisiae. *Mol Gen Genet*, **236**, 363-368.

Gaxiola, R.A., Rao, R., Sherman, A., Grisafi, P., Alper, S.L. and Fink, G.R. (1999) The Arabidopsis thaliana proton transporters, AtNhx1 and Avp1, can function in cation detoxification in yeast. *Proc Natl Acad Sci U S A*, **96**, 1480-1485.

Ghislain, M., Schlesser, A. and Goffeau, A. (1987) Mutation of a conserved glycine residue modifies the vanadate sensitivity of the plasma membrane H+-ATPase from Schizosaccharomyces pombe. *J Biol Chem*, **262**, 17549-17555.

Ghislain, M., de Sadeleer, M. and Goffeau, A. (1992) Altered plasma membrane H^+-ATPase from the Dio-9-resistant pma1-2 mutant of *Schizosaccharomyces pombe*. *Eur. J. Biochem.*, **209**, 275–279.

Girao, H., Geli, M.I. and Idrissi, F.Z. (2008) Actin in the endocytic pathway: from yeast to mammals. *FEBS Lett*, **582**, 2112-2119.

Goddard, N.J., Dunn, M.A., Zhang, L., White, A.J., Jack, P.L. and Hughes, M.A. (1993) Molecular analysis and spatial expression pattern of a low-temperature-specific barley gene, blt101. *Plant Mol Biol*, **23**, 871-879.

Goffeau, A. and de Meis, L. (1990) Effects of phosphate and hydrophobic molecules on two mutations in the beta-strand sector of the H(+)-ATPase from the yeast plasma membrane. *J Biol Chem*, **265**, 15503-15505.

Goffeau, A. and Dufour, J.P. (1988) Plasma membrane ATPase from the yeast Saccharomyces cerevisiae. *Methods Enzymol*, **157**, 528-533.

Gomez, M.J., Luyten, K. and Ramos, J. (1996) The capacity to transport potassium influences sodium tolerance in Saccharomyces cerevisiae. *FEMS Microbiol Lett*, **135**, 157-160.

Goossens, A., de La Fuente, N., Forment, J., Serrano, R. and Portillo, F. (2000) Regulation of yeast H(+)-ATPase by protein kinases belonging to a family dedicated to activation of plasma membrane transporters. *Mol Cell Biol*, **20**, 7654-7661.

Grandori, R. and Carey, J. (1994) Six new candidate members of the alpha/beta twisted open-sheet family detected by sequence similarity to flavodoxin. *Protein Sci*, **3**, 2185-2193.

Grosshans, B.L., Grotsch, H., Mukhopadhyay, D., Fernandez, I.M., Pfannstiel, J., Idrissi, F.Z., Lechner, J., Riezman, H. and Geli, M.I. (2006) TEDS site phosphorylation of the yeast myosins I is required for ligand-induced but not for constitutive endocytosis of the G protein-coupled receptor Ste2p. *J Biol Chem*, **281**, 11104-11114.

Grossmann, G., Malinsky, J., Stahlschmidt, W., Loibl, M., Weig-Meckl, I., Frommer, W.B., Opekarova, M. and Tanner, W. (2008) Plasma membrane microdomains regulate turnover of transport proteins in yeast. *J Cell Biol*, **183**, 1075-1088.

Grossmann, G., Opekarova, M., Malinsky, J., Weig-Meckl, I. and Tanner, W. (2007) Membrane potential governs lateral segregation of plasma membrane proteins and lipids in yeast. *EMBO J*, **26**, 1-8.

Grossmann, G., Opekarova, M., Novakova, L., Stolz, J. and Tanner, W. (2006) Lipid raft-based membrane compartmentation of a plant transport protein expressed in Saccharomyces cerevisiae. *Eukaryot Cell*, **5**, 945-953.

Guan, X.L., Souza, C.M., Pichler, H., Dewhurst, G., Schaad, O., Kajiwara, K., Wakabayashi, H., Ivanova, T., Castillon, G.A., Piccolis, M., Abe, F., Loewith, R., Funato, K., Wenk, M.R. and Riezman, H. (2009) Functional interactions between sphingolipids and sterols in biological membranes regulating cell physiology. *Mol Biol Cell*, **20**, 2083-2095.

Hager, K.M., Mandala, S.M., Davenport, J.W., Speicher, D.W., Benz, E.J., Jr. and Slayman, C.W. (1986) Amino acid sequence of the plasma membrane ATPase of Neurospora crassa: deduction from genomic and cDNA sequences. *Proc Natl Acad Sci U S A*, **83**, 7693-7697.

Halachmi, D. and Eilam, Y. (1996) Elevated cytosolic free Ca2+ concentrations and massive Ca2+ accumulation within vacuoles, in yeast mutant lacking PMR1, a homolog of Ca2+ -ATPase. *FEBS Lett*, **392**, 194-200.

Hall, S.E., Roberts, K. and Vaidehi, N. (2009) Position of helical kinks in membrane protein crystal structures and the accuracy of computational prediction. *J Mol Graph Model*, **27**, 944-950.

Hancock, J.F. (2006) Lipid rafts: contentious only from simplistic standpoints. *Nat Rev Mol Cell Biol*, **7**, 456-462.

Haro, R., Garciadeblas, B. and Rodriguez-Navarro, A. (1991) A novel P-type ATPase from yeast involved in sodium transport. *FEBS Lett*, **291**, 189-191.

Haro, R. and Rodriguez-Navarro, A. (2002) Molecular analysis of the mechanism of potassium uptake through the TRK1 transporter of Saccharomyces cerevisiae. *Biochim Biophys Acta*, **1564**, 114-122.

Haro, R. and Rodriguez-Navarro, A. (2003) Functional analysis of the M2(D) helix of the TRK1 potassium transporter of Saccharomyces cerevisiae. *Biochim Biophys Acta*, **1613**, 1-6.

Hearn, J.D., Lester, R.L. and Dickson, R.C. (2003) The uracil transporter Fur4p associates with lipid rafts. *J Biol Chem*, **278**, 3679-3686.

Heberle, F.A., Buboltz, J.T., Stringer, D. and Feigenson, G.W. (2005) Fluorescence methods to detect phase boundaries in lipid bilayer mixtures. *Biochim Biophys Acta*, **1746**, 186-192.

Heitman, J., Movva, N.R. and Hall, M.N. (1991) Targets for cell cycle arrest by the immunosuppressant rapamycin in yeast. *Science*, **253**, 905-909.

Homann, U., Meckel, T., Hewing, J., Hutt, M.T. and Hurst, A.C. (2007) Distinct fluorescent pattern of KAT1::GFP in the plasma membrane of Vicia faba guard cells. *Eur J Cell Biol*, **86**, 489-500.

Inada, M., Ueda, A., Shi, W. and Takabe, T. (2005) A stress-inducible plasma membrane protein 3 (AcPMP3) in a monocotyledonous halophyte, Aneurolepidium chinense, regulates cellular Na(+) and K(+) accumulation under salt stress. *Planta*, **220**, 395-402.

Inagaki, M., Schmelzle, T., Yamaguchi, K., Irie, K., Hall, M.N. and Matsumoto, K. (1999) PDK1 homologs activate the Pkc1-mitogen-activated protein kinase pathway in yeast. *Mol Cell Biol*, **19**, 8344-8352.

Ipsen, J.H., Karlstrom, G., Mouritsen, O.G., Wennerstrom, H. and Zuckermann, M.J. (1987) Phase equilibria in the phosphatidylcholine-cholesterol system. *Biochim Biophys Acta*, **905**, 162-172.

Iwaki, T., Higashida, Y., Tsuji, H., Tamai, Y. and Watanabe, Y. (1998) Characterization of a second gene (ZSOD22) of Na+/H+ antiporter from salt-tolerant yeast Zygosaccharomyces rouxii and functional expression of ZSOD2 and ZSOD22 in Saccharomyces cerevisiae. *Yeast*, **14**, 1167-1174.

Jacinto, E., Loewith, R., Schmidt, A., Lin, S., Ruegg, M.A., Hall, A. and Hall, M.N. (2004) Mammalian TOR complex 2 controls the actin cytoskeleton and is rapamycin insensitive. *Nat Cell Biol*, **6**, 1122-1128.

Jia, Z.P., McCullough, N., Martel, R., Hemmingsen, S. and Young, P.G. (1992) Gene amplification at a locus encoding a putative Na+/H+ antiporter confers sodium and lithium tolerance in fission yeast. *EMBO J*, **11**, 1631-1640.

Johnson, A.S., van Horck, S. and Lewis, P.J. (2004) Dynamic localization of membrane proteins in Bacillus subtilis. *Microbiology*, **150**, 2815-2824.

Kadurin, I., Huber, S. and Grunder, S. (2009) A single conserved proline residue determines the membrane topology of stomatin. *Biochem J*, **418**, 587-594.

Ketchum, K.A., Joiner, W.J., Sellers, A.J., Kaczmarek, L.K. and Goldstein, S.A. (1995) A new family of outwardly rectifying potassium channel proteins with two pore domains in tandem. *Nature*, **376**, 690-695.

Kinclova, O., Ramos, J., Potier, S. and Sychrova, H. (2001) Functional study of the Saccharomyces cerevisiae Nha1p C-terminus. *Mol Microbiol*, **40**, 656-668.

Klionsky, D.J., Herman, P.K. and Emr, S.D. (1990) The fungal vacuole: composition, function, and biogenesis. *Microbiol Rev*, **54**, 266-292.

Ko, C.H., Buckley, A.M. and Gaber, R.F. (1990) TRK2 is required for low affinity K+ transport in Saccharomyces cerevisiae. *Genetics*, **125**, 305-312.

Ko, C.H. and Gaber, R.F. (1991) TRK1 and TRK2 encode structurally related K+ transporters in Saccharomyces cerevisiae. *Mol Cell Biol*, **11**, 4266-4273.

Kodama, Y., Omura, F., Takahashi, K., Shirahige, K. and Ashikari, T. (2002) Genome-wide expression analysis of genes affected by amino acid sensor Ssy1p in Saccharomyces cerevisiae. *Curr Genet*, **41**, 63-72.

Koike, M., Sutoh, K., Kawakami, A., Torada, A., Oono, K. and Imai, R. (2005) Molecular characterization of a cold-induced plasma membrane protein gene from wheat. *Mol Genet Genomics*, **274**, 445-453.

Kolaczkowski, M., van der Rest, M., Cybularz-Kolaczkowska, A., Soumillion, J.P., Konings, W.N. and Goffeau, A. (1996) Anticancer drugs, ionophoric peptides, and steroids as substrates of the yeast multidrug transporter Pdr5p. *J Biol Chem*, **271**, 31543-31548.

Korzeniowski, M., Kwiatkowska, K. and Sobota, A. (2003) Insights into the association of FcgammaRII and TCR with detergent-resistant membrane domains: isolation of the domains in detergent-free density gradients facilitates membrane fragment reconstitution. *Biochemistry*, **42**, 5358-5367.

Kubler, E., Dohlman, H.G. and Lisanti, M.P. (1996) Identification of Triton X-100 insoluble membrane domains in the yeast Saccharomyces cerevisiae. Lipid requirements for targeting of heterotrimeric G-protein subunits. *J Biol Chem*, **271**, 32975-32980.

Kunz, J., Henriquez, R., Schneider, U., Deuter-Reinhard, M., Movva, N.R. and Hall, M.N. (1993) Target of rapamycin in yeast, TOR2, is an essential phosphatidylinositol kinase homolog required for G1 progression. *Cell*, **73**, 585-596.

Lagerholm, B.C., Weinreb, G.E., Jacobson, K. and Thompson, N.L. (2005) Detecting microdomains in intact cell membranes. *Annu Rev Phys Chem*, **56**, 309-336.

Lauwers, E. and Andre, B. (2006) Association of yeast transporters with detergent-resistant membranes correlates with their cell-surface location. *Traffic*, **7**, 1045-1059.

Lauwers, E., Grossmann, G. and Andre, B. (2007) Evidence for coupled biogenesis of yeast Gap1 permease and sphingolipids: essential role in transport activity and normal control by ubiquitination. *Mol Biol Cell*, **18**, 3068-3080.

Lee, J., Godon, C., Lagniel, G., Spector, D., Garin, J., Labarre, J. and Toledano, M.B. (1999) Yap1 and Skn7 control two specialized oxidative stress response regulons in yeast. *J Biol Chem*, **274**, 16040-16046.

Lee, M.C., Hamamoto, S. and Schekman, R. (2002) Ceramide biosynthesis is required for the formation of the oligomeric H+-ATPase Pma1p in the yeast endoplasmic reticulum. *J Biol Chem*, **277**, 22395-22401.

Lentzen, H., Arreguin, M., Kappeli, O., Fiechter, A. and Fuhrmann, G.F. (1987) Bioregulation of yeast plasma membrane ATPase and acetyl transferase (CAT) activity at defined metabolic states. *J. Biotechnol.*, **6**, 281–291.

Lesage, F., Guillemare, E., Fink, M., Duprat, F., Lazdunski, M., Romey, G. and Barhanin, J. (1996) A pH-sensitive yeast outward rectifier K+ channel with two pore domains and novel gating properties. *J Biol Chem*, **271**, 4183-4187.

Lisanti, M.P. and Rodriguez-Boulan, E. (1990) Glycophospholipid membrane anchoring provides clues to the mechanism of protein sorting in polarized epithelial cells. *Trends Biochem Sci*, **15**, 113-118.

Liu, K., Zhang, X., Lester, R.L. and Dickson, R.C. (2005) The sphingoid long chain base phytosphingosine activates AGC-type protein kinases in Saccharomyces cerevisiae including Ypk1, Ypk2, and Sch9. *J Biol Chem*, **280**, 22679-22687.

Lopez-Villar, E., Monteoliva, L., Larsen, M.R., Sachon, E., Shabaz, M., Pardo, M., Pla, J., Gil, C., Roepstorff, P. and Nombela, C. (2006) Genetic and proteomic evidences support the localization of yeast enolase in the cell surface. *Proteomics*, **6**, S107-118.

Luo, G., Gruhler, A., Liu, Y., Jensen, O.N. and Dickson, R.C. (2008) The sphingolipid long-chain base-Pkh1/2-Ypk1/2 signaling pathway regulates eisosome assembly and turnover. *J Biol Chem*, **283**, 10433-10444.

Lutsenko, S. and Kaplan, J.H. (1995) Organization of P-type ATPases: significance of structural diversity. *Biochemistry*, **34**, 15607-15613.

Madrid, R., Gomez, M.J., Ramos, J. and Rodriguez-Navarro, A. (1998) Ectopic potassium uptake in trk1 trk2 mutants of Saccharomyces cerevisiae correlates with a highly hyperpolarized membrane potential. *J Biol Chem*, **273**, 14838-14844.

Malinska, K., Malinsky, J., Opekarova, M. and Tanner, W. (2003) Visualization of protein compartmentation within the plasma membrane of living yeast cells. *Mol Biol Cell*, **14**, 4427-4436.

Malinska, K., Malinsky, J., Opekarova, M. and Tanner, W. (2004) Distribution of Can1p into stable domains reflects lateral protein segregation within the plasma membrane of living S. cerevisiae cells. *J Cell Sci*, **117**, 6031-6041.

Malpartida, F. and Serrano, R. (1980) Purification of the yeast plasma membrane ATPase solubilized with a novel zwitterionic detergent. *FEBS Lett*, **111**, 69-72.

Maresova, L., Muend, S., Zhang, Y.Q., Sychrova, H. and Rao, R. (2009) Membrane hyperpolarization drives cation influx and fungicidal activity of amiodarone. *J Biol Chem*, **284**, 2795-2802.

Maresova, L. and Sychrova, H. (2005) Physiological characterization of Saccharomyces cerevisiae kha1 deletion mutants. *Mol Microbiol*, **55**, 588-600.

Maresova, L., Urbankova, E., Gaskova, D. and Sychrova, H. (2006) Measurements of plasma membrane potential changes in Saccharomyces cerevisiae cells reveal the importance of the Tok1 channel in membrane potential maintenance. *FEMS Yeast Res*, **6**, 1039-1046.

Martin, S.W. and Konopka, J.B. (2004) Lipid raft polarization contributes to hyphal growth in Candida albicans. *Eukaryot Cell*, **3**, 675-684.

Matsumoto, K., Kusaka, J., Nishibori, A. and Hara, H. (2006) Lipid domains in bacterial membranes. *Mol Microbiol*, **61**, 1110-1117.

Medina, J., Ballesteros, M.L. and Salinas, J. (2007) Phylogenetic and functional analysis of Arabidopsis RCI2 genes. *J Exp Bot*, **58**, 4333-4346.

Medina, J., Catala, R. and Salinas, J. (2001) Developmental and stress regulation of RCI2A and RCI2B, two cold-inducible genes of arabidopsis encoding highly conserved hydrophobic proteins. *Plant Physiol*, **125**, 1655-1666.

Megha, Bakht, O. and London, E. (2006) Cholesterol precursors stabilize ordinary and ceramide-rich ordered lipid domains (lipid rafts) to different degrees. Implications for the Bloch hypothesis and sterol biosynthesis disorders. *J Biol Chem*, **281**, 21903-21913.

Michel, B., Lozano, C., Rodriguez, M., Coria, R., Ramirez, J. and Pena, A. (2006) The yeast potassium transporter TRK2 is able to substitute for TRK1 in its biological function under low K and low pH conditions. *Yeast*, **23**, 581-589.

Mitsui, K., Hatakeyama, K., Matsushita, M. and Kanazawa, H. (2009) Saccharomyces cerevisiae Na+/H+ antiporter Nha1p associates with lipid rafts and requires sphingolipid for stable localization to the plasma membrane. *J Biochem*, **145**, 709-720.

Mitsuya, S., Taniguchi, M., Miyake, H. and Takabe, T. (2005) Disruption of RCI2A leads to over-accumulation of Na+ and increased salt sensitivity in Arabidopsis thaliana plants. *Planta*, **222**, 1001-1009.

Moor, H. and Mühlethaler, K. (1963) Fine structure in frozen-etched yeast cells. *J. Cell Biol.*, **17**, 609-628.

Morais-Cabral, J.H., Zhou, Y. and MacKinnon, R. (2001) Energetic optimization of ion conduction rate by the K+ selectivity filter. *Nature*, **414**, 37-42.

Moreira, K.E., Walther, T.C., Aguilar, P.S. and Walter, P. (2009) Pil1 controls eisosome biogenesis. *Mol Biol Cell*, **20**, 809-818.

Morsomme, P., Slayman, C.W. and Goffeau, A. (2000) Mutagenic study of the structure, function and biogenesis of the yeast plasma membrane H(+)-ATPase. *Biochim Biophys Acta*, **1469**, 133-157.

Morsy, M.R., Almutairi, A.M., Gibbons, J., Yun, S.J. and de Los Reyes, B.G. (2005) The OsLti6 genes encoding low-molecular-weight membrane proteins are differentially expressed in rice cultivars with contrasting sensitivity to low temperature. *Gene*, **344**, 171-180.

Mouritsen, O.G. and Jorgensen, K. (1997) Small-scale lipid-membrane structure: simulation versus experiment. *Curr Opin Struct Biol*, **7**, 518-527.

Mulet, J.M., Leube, M.P., Kron, S.J., Rios, G., Fink, G.R. and Serrano, R. (1999) A novel mechanism of ion homeostasis and salt tolerance in yeast: the Hal4 and Hal5 protein kinases modulate the Trk1-Trk2 potassium transporter. *Mol Cell Biol*, **19**, 3328-3337.

Munro, S. (2003) Lipid rafts: elusive or illusive? *Cell*, **115**, 377-388.

Nass, R., Cunningham, K.W. and Rao, R. (1997) Intracellular sequestration of sodium by a novel Na+/H+ exchanger in yeast is enhanced by mutations in the plasma membrane H+-ATPase. Insights into mechanisms of sodium tolerance. *J Biol Chem*, **272**, 26145-26152.

Nass, R. and Rao, R. (1998) Novel localization of a Na+/H+ exchanger in a late endosomal compartment of yeast. Implications for vacuole biogenesis. *J Biol Chem*, **273**, 21054-21060.

Navarre, C., Catty, P., Leterme, S., Dietrich, F. and Goffeau, A. (1994) Two distinct genes encode small isoproteolipids affecting plasma membrane H(+)-ATPase activity of Saccharomyces cerevisiae. *J Biol Chem*, **269**, 21262-21268.

Navarre, C., Ghislain, M., Leterme, S., Ferroud, C., Dufour, J.P. and Goffeau, A. (1992) Purification and complete sequence of a small proteolipid associated with the plasma membrane H(+)-ATPase of Saccharomyces cerevisiae. *J Biol Chem*, **267**, 6425-6428.

Navarre, C. and Goffeau, A. (2000) Membrane hyperpolarization and salt sensitivity induced by deletion of PMP3, a highly conserved small protein of yeast plasma membrane. *EMBO J*, **19**, 2515-2524.

Nichols, C.B., Fraser, J.A. and Heitman, J. (2004) PAK kinases Ste20 and Pak1 govern cell polarity at different stages of mating in Cryptococcus neoformans. *Mol Biol Cell*, **15**, 4476-4489.

Nuoffer, C., Jeno, P., Conzelmann, A. and Riezman, H. (1991) Determinants for glycophospholipid anchoring of the Saccharomyces cerevisiae GAS1 protein to the plasma membrane. *Mol Cell Biol*, **11**, 27-37.

Nylander, M., Heino, P., Helenius, E., Palva, E.T., Ronne, H. and Welin, B.V. (2001) The low-temperature- and salt-induced RCI2A gene of Arabidopsis complements the sodium sensitivity caused by a deletion of the homologous yeast gene SNA1. *Plant Mol Biol*, **45**, 341-352.

Oh, C.S., Toke, D.A., Mandala, S. and Martin, C.E. (1997) ELO2 and ELO3, homologues of the Saccharomyces cerevisiae ELO1 gene, function in fatty acid elongation and are required for sphingolipid formation. *J Biol Chem*, **272**, 17376-17384.

Ohgaki, R., Nakamura, N., Mitsui, K. and Kanazawa, H. (2005) Characterization of the ion transport activity of the budding yeast Na+/H+ antiporter, Nha1p, using isolated secretory vesicles. *Biochim Biophys Acta*, **1712**, 185-196.

Okorokov, L.A., Lichko, L.P. and Kulaev, I.S. (1980) Vacuoles: main compartments of potassium, magnesium, and phosphate ions in Saccharomyces carlsbergenis cells. *J Bacteriol*, **144**, 661-665.

Panaretou, B. and Piper, P.W. (1992) The plasma membrane of yeast acquires a novel heat-shock protein (hsp30) and displays a decline in proton-pumping ATPase levels in response to both heat shock and the entry to stationary phase. *Eur J Biochem*, **206**, 635-640.

Pedersen, P.L., and Carafoli, E. (1987) Ion motive ATPase. I. Ubiquity, properties, and significance to cell function. *Trends in Biochemical Sciences*, **12**, 146-150.

Pegg, A.E. and McCann, P.P. (1982) Polyamine metabolism and function. *Am J Physiol*, **243**, C212-221.

Pena, A., Cinco, G., Gomez-Puyou, A. and Tuena, M. (1972) Effect of the pH of the incubation medium on glycolysis and respiration in Saccharomyces cerevisiae. *Arch Biochem Biophys*, **153**, 413-425.

Pena, A., Cinco, G., Puyou, A.G. and Tuena, M. (1969) Studies on the mechanism of the stimulation of glycolysis and respiration by K+ in Saccharomyces cerevisiae. *Biochim Biophys Acta*, **180**, 1-8.

Pike, L.J. (2003) Lipid rafts: bringing order to chaos. *J Lipid Res*, **44**, 655-667.

Pokrzywa, W., Guerriat, B., Dodzian, J. and Morsomme, P. (2009) Dual sorting of the Saccharomyces cerevisiae vacuolar protein Sna4p. *Eukaryot Cell*, **8**, 278-286.

Porat, Z., Wender, N., Erez, O. and Kahana, C. (2005) Mechanism of polyamine tolerance in yeast: novel regulators and insights. *Cell Mol Life Sci*, **62**, 3106-3116.

Portillo, F., de Larrinoa, I.F. and Serrano, R. (1989) Deletion analysis of yeast plasma membrane H+-ATPase and identification of a regulatory domain at the carboxyl-terminus. *FEBS Lett*, **247**, 381-385.

Powell, B., Graham, L.A. and Stevens, T.H. (2000) Molecular characterization of the yeast vacuolar H+-ATPase proton pore. *J Biol Chem*, **275**, 23654-23660.

Prior, C., Potier, S., Souciet, J.L. and Sychrova, H. (1996) Characterization of the NHA1 gene encoding a Na+/H+-antiporter of the yeast Saccharomyces cerevisiae. *FEBS Lett*, **387**, 89-93.

Ramirez, J., Ramirez, O., Saldana, C., Coria, R. and Pena, A. (1998) A Saccharomyces cerevisiae mutant lacking a K+/H+ exchanger. *J Bacteriol*, **180**, 5860-5865.

Ramos, J., Haro, R. and Rodriguez-Navarro, A. (1990) Regulation of potassium fluxes in Saccharomyces cerevisiae. *Biochim Biophys Acta*, **1029**, 211-217.

Rath, A. and Deber, C.M. (2008) Surface recognition elements of membrane protein oligomerization. *Proteins*, **70**, 786-793.

Reggiori, F. and Pelham, H.R. (2001) Sorting of proteins into multivesicular bodies: ubiquitin-dependent and -independent targeting. *EMBO J*, **20**, 5176-5186.

Reid, J.D., Lukas, W., Shafaatian, R., Bertl, A., Scheurmann-Kettner, C., Guy, H.R. and North, R.A. (1996) The S. cerevisiae outwardly-rectifying potassium channel (DUK1) identifies a new family of channels with duplicated pore domains. *Receptors Channels*, **4**, 51-62.

Renard, H.F., Demaegdt, D., Guerriat, B. and Morsomme, P. (2010) Efficient ER exit and vacuole targeting of yeast Sna2p require two tyrosine-based sorting motifs. *Traffic*, Submitted.

Rietveld, A. and Simons, K. (1998) The differential miscibility of lipids as the basis for the formation of functional membrane rafts. *Biochim Biophys Acta*, **1376**, 467-479.

Robl, I., Grassl, R., Tanner, W. and Opekarova, M. (2000) Properties of a reconstituted eukaryotic hexose/proton symporter solubilized by structurally related non-ionic detergents: specific requirement of phosphatidylcholine for permease stability. *Biochim Biophys Acta*, **1463**, 407-418.

Rodriguez-Navarro, A. (2000) Potassium transport in fungi and plants. *Biochim Biophys Acta*, **1469**, 1-30.

Rodriguez-Navarro, A. and Ramos, J. (1984) Dual system for potassium transport in Saccharomyces cerevisiae. *J Bacteriol*, **159**, 940-945.

Roller, A., Natura, G., Bihler, H., Slayman, C.L. and Bertl, A. (2008) Functional consequences of leucine and tyrosine mutations in the dual pore motifs of the yeast K(+) channel, Tok1p. *Pflugers Arch*, **456**, 883-896.

Ross, P.L., Huang, Y.N., Marchese, J.N., Williamson, B., Parker, K., Hattan, S., Khainovski, N., Pillai, S., Dey, S., Daniels, S., Purkayastha, S., Juhasz, P., Martin, S., Bartlet-Jones, M., He, F., Jacobson, A. and Pappin, D.J. (2004) Multiplexed protein quantitation in Saccharomyces cerevisiae using amine-reactive isobaric tagging reagents. *Mol Cell Proteomics*, **3**, 1154-1169.

Rudolph, H.K., Antebi, A., Fink, G.R., Buckley, C.M., Dorman, T.E., LeVitre, J., Davidow, L.S., Mao, J.I. and Moir, D.T. (1989) The yeast secretory pathway is perturbed by mutations in PMR1, a member of a Ca2+ ATPase family. *Cell*, **58**, 133-145.

Ruiz, A. and Arino, J. (2007) Function and regulation of the Saccharomyces cerevisiae ENA sodium ATPase system. *Eukaryot Cell*, **6**, 2175-2183.

Sansom, M.S. and Weinstein, H. (2000) Hinges, swivels and switches: the role of prolines in signalling via transmembrane alpha-helices. *Trends Pharmacol Sci*, **21**, 445-451.

Sargiacomo, M., Sudol, M., Tang, Z. and Lisanti, M.P. (1993) Signal transducing molecules and glycosyl-phosphatidylinositol-linked proteins form a caveolin-rich insoluble complex in MDCK cells. *J Cell Biol*, **122**, 789-807.

Sauer, N., Friedlander, K. and Graml-Wicke, U. (1990) Primary structure, genomic organization and heterologous expression of a glucose transporter from Arabidopsis thaliana. *EMBO J*, **9**, 3045-3050.

Schagger, H. and von Jagow, G. (1987) Tricine-sodium dodecyl sulfate-polyacrylamide gel electrophoresis for the separation of proteins in the range from 1 to 100 kDa. *Anal Biochem*, **166**, 368-379.

Schimerlik, M.I. (2001) Overview of membrane protein solubilization. *Curr Protoc Neurosci*, **Chapter**, Unit 5.9.

Schlesser, A., Ulaszewski, S., Ghislain, M. and Goffeau, A. (1988) A second transport ATPase gene in Saccharomyces cerevisiae. *J Biol Chem*, **263**, 19480-19487.

Seron, K., Blondel, M.O., Haguenauer-Tsapis, R. and Volland, C. (1999) Uracil-induced down-regulation of the yeast uracil permease. *J Bacteriol*, **181**, 1793-1800.

Serrano, R. (1983) Purification and reconstitution of the proton-pumping ATPase of fungal and plant plasma membranes. *Arch Biochem Biophys*, **227**, 1-8.

Serrano, R. (1988) Structure and function of proton translocating ATPase in plasma membranes of plants and fungi. *Biochim Biophys Acta*, **947**, 1-28.

Serrano, R. (1996) Salt tolerance in plants and microorganisms: toxicity targets and defense responses. *Int Rev Cytol*, **165**, 1-52.

Serrano, R., Kielland-Brandt, M.C. and Fink, G.R. (1986) Yeast plasma membrane ATPase is essential for growth and has homology with (Na+ + K+), K+- and Ca2+-ATPases. *Nature*, **319**, 689-693.

Severs, N.J. (1997) Cholesterol cytochemistry in cell biology and disease. *Subcell Biochem*, **28**, 477-505.

Shogomori, H. and Brown, D.A. (2003) Use of detergents to study membrane rafts: the good, the bad, and the ugly. *Biol Chem*, **384**, 1259-1263.

Simons, K. and Ikonen, E. (1997) Functional rafts in cell membranes. *Nature*, **387**, 569-572.

Simons, K. and van Meer, G. (1988) Lipid sorting in epithelial cells. *Biochemistry*, **27**, 6197-6202.

Singer, S.J. and Nicolson, G.L. (1972) The fluid mosaic model of the structure of cell membranes. *Science*, **175**, 720-731.

Sivadon, P., Peypouquet, M.F., Doignon, F., Aigle, M. and Crouzet, M. (1997) Cloning of the multicopy suppressor gene SUR7: evidence for a functional relationship between the yeast actin-binding protein Rvs167 and a putative membranous protein. *Yeast*, **13**, 747-761.

Soong, T.W., Yong, T.F., Ramanan, N. and Wang, Y. (2000) The Candida albicans antiporter gene CNH1 has a role in Na+ and H+ transport, salt tolerance, and morphogenesis. *Microbiology*, **146**, 1035-1044.

Soulard, A., Cohen, A. and Hall, M.N. TOR signaling in invertebrates.

Stawiecka-Mirota, M., Pokrzywa, W., Morvan, J., Zoladek, T., Haguenauer-Tsapis, R., Urban-Grimal, D. and Morsomme, P. (2007) Targeting of Sna3p to the endosomal pathway depends on its interaction with Rsp5p and multivesicular body sorting on its ubiquitylation. *Traffic*, **8**, 1280-1296.

Stradalova, V., Stahlschmidt, W., Grossmann, G., Blazikova, M., Rachel, R., Tanner, W. and Malinsky, J. (2009) Furrow-like invaginations of the yeast plasma membrane correspond to membrane compartment of Can1. *J Cell Sci*, **122**, 2887-2894.

Sun, Y., Taniguchi, R., Tanoue, D., Yamaji, T., Takematsu, H., Mori, K., Fujita, T., Kawasaki, T. and Kozutsumi, Y. (2000) Sli2 (Ypk1), a homologue of mammalian protein kinase SGK, is a downstream kinase in the sphingolipid-mediated signaling pathway of yeast. *Mol Cell Biol*, **20**, 4411-4419.

Sutter, J.U., Campanoni, P., Tyrrell, M. and Blatt, M.R. (2006) Selective mobility and sensitivity to SNAREs is exhibited by the Arabidopsis KAT1 K+ channel at the plasma membrane. *Plant Cell*, **18**, 935-954.

Sychrova, H. (2004) Yeast as a model organism to study transport and homeostasis of alkali metal cations. *Physiol Res*, **53**, S91-98.

Sychrova, H., Ramirez, J. and Pena, A. (1999) Involvement of Nha1 antiporter in regulation of intracellular pH in Saccharomyces cerevisiae. *FEMS Microbiol Lett*, **171**, 167-172.

Tian, T., Harding, A., Inder, K., Plowman, S., Parton, R.G. and Hancock, J.F. (2007) Plasma membrane nanoswitches generate high-fidelity Ras signal transduction. *Nat Cell Biol*, **9**, 905-914.

Toret, C.P. and Drubin, D.G. (2006) The budding yeast endocytic pathway. *J Cell Sci*, **119**, 4585-4587.

Toulmay, A. and Schneiter, R. (2007) Lipid-dependent surface transport of the proton pumping ATPase: a model to study plasma membrane biogenesis in yeast. *Biochimie*, **89**, 249-254.

Uchida, E., Ohsumi, Y. and Anraku, Y. (1988) Purification of yeast vacuolar membrane H+-ATPase and enzymological discrimination of three ATP-driven proton pumps in Saccharomyces cerevisiae. *Methods Enzymol*, **157**, 544-562.

Uemura, T., Kashiwagi, K. and Igarashi, K. (2007) Polyamine uptake by DUR3 and SAM3 in Saccharomyces cerevisiae. *J Biol Chem*, **282**, 7733-7741.

Uemura, T., Tachihara, K., Tomitori, H., Kashiwagi, K. and Igarashi, K. (2005) Characteristics of the polyamine transporter TPO1 and regulation of its activity and cellular localization by phosphorylation. *J Biol Chem*, **280**, 9646-9652.

Umebayashi, K. and Nakano, A. (2003) Ergosterol is required for targeting of tryptophan permease to the yeast plasma membrane. *J Cell Biol*, **161**, 1117-1131.

Vallejo, C.G. and Serrano, R. (1989) Physiology of mutants with reduced expression of plasma membrane H+-ATPase. *Yeast*, **5**, 307-319.

Van Dyck, L., Petretski, J.H., Wolosker, H., Rodrigues Junior, G., Schlesser, A., Ghislain, M. and Goffeau, A. (1990) Molecular and biochemical characterization of the Dio-9-resistant pma1-1 mutation of the H(+)-ATPase from Saccharomyces cerevisiae. *Eur J Biochem*, **194**, 785-790.

van Meer, G. and Simons, K. (1982) Viruses budding from either the apical or the basolateral plasma membrane domain of MDCK cells have unique phospholipid compositions. *EMBO J*, **1**, 847-852.

Vargas, R.C., Garcia-Salcedo, R., Tenreiro, S., Teixeira, M.C., Fernandes, A.R., Ramos, J. and Sa-Correia, I. (2007) Saccharomyces cerevisiae multidrug resistance transporter Qdr2 is implicated in potassium uptake, providing a physiological advantage to quinidine-stressed cells. *Eukaryot Cell*, **6**, 134-142.

Vergani, P. and Blatt, M.R. (1999) Mutations in the yeast two pore K+ channel YKC1 identify functional differences between the pore domains. *FEBS Lett*, **458**, 285-291.

Wachtler, V., Rajagopalan, S. and Balasubramanian, M.K. (2003) Sterol-rich plasma membrane domains in the fission yeast Schizosaccharomyces pombe. *J Cell Sci*, **116**, 867-874.

Wallis, J.W., Chrebet, G., Brodsky, G., Rolfe, M. and Rothstein, R. (1989) A hyper-recombination mutation in S. cerevisiae identifies a novel eukaryotic topoisomerase. *Cell*, **58**, 409-419.

Walther, T.C., Aguilar, P.S., Frohlich, F., Chu, F., Moreira, K., Burlingame, A.L. and Walter, P. (2007) Pkh-kinases control eisosome assembly and organization. *EMBO J*, **26**, 4946-4955.

Walther, T.C., Brickner, J.H., Aguilar, P.S., Bernales, S., Pantoja, C. and Walter, P. (2006) Eisosomes mark static sites of endocytosis. *Nature*, **439**, 998-1003.

Wang, Q. and Chang, A. (2002) Sphingoid base synthesis is required for oligomerization and cell surface stability of the yeast plasma membrane ATPase, Pma1. *Proc Natl Acad Sci U S A*, **99**, 12853-12858.

Watanabe, Y., Miwa, S. and Tamai, Y. (1995) Characterization of Na+/H(+)-antiporter gene closely related to the salt-tolerance of yeast Zygosaccharomyces rouxii. *Yeast*, **11**, 829-838.

Wieland, J., Nitsche, A.M., Strayle, J., Steiner, H. and Rudolph, H.K. (1995) The PMR2 gene cluster encodes functionally distinct isoforms of a putative Na+ pump in the yeast plasma membrane. *EMBO J*, **14**, 3870-3882.

Wolfger, H., Mamnun, Y.M. and Kuchler, K. (2004) The yeast Pdr15p ATP-binding cassette (ABC) protein is a general stress response factor implicated in cellular detoxification. *J Biol Chem*, **279**, 11593-11599.

Wright, M.B., Ramos, J., Gomez, M.J., Moulder, K., Scherrer, M., Munson, G. and Gaber, R.F. (1997) Potassium transport by amino acid permeases in Saccharomyces cerevisiae. *J Biol Chem*, **272**, 13647-13652.

Xu, X., Bittman, R., Duportail, G., Heissler, D., Vilcheze, C. and London, E. (2001) Effect of the structure of natural sterols and sphingolipids on the formation of ordered sphingolipid/sterol domains (rafts). Comparison of cholesterol to plant, fungal, and disease-associated sterols and comparison of sphingomyelin, cerebrosides, and ceramide. *J Biol Chem*, **276**, 33540-33546.

Yale, J. and Bohnert, H.J. (2001) Transcript expression in Saccharomyces cerevisiae at high salinity. *J Biol Chem*, **276**, 15996-16007.

Young, M.E., Karpova, T.S., Brugger, B., Moschenross, D.M., Wang, G.K., Schneiter, R., Wieland, F.T. and Cooper, J.A. (2002) The Sur7p family defines novel cortical domains in Saccharomyces cerevisiae, affects sphingolipid metabolism, and is involved in sporulation. *Mol Cell Biol*, **22**, 927-934.

Zanolari, B., Friant, S., Funato, K., Sutterlin, C., Stevenson, B.J. and Riezman, H. (2000) Sphingoid base synthesis requirement for endocytosis in Saccharomyces cerevisiae. *EMBO J*, **19**, 2824-2833.

Zhang, X., Lester, R.L. and Dickson, R.C. (2004) Pil1p and Lsp1p negatively regulate the 3-phosphoinositide-dependent protein kinase-like kinase Pkh1p and downstream signaling pathways Pkc1p and Ypk1p. *J Biol Chem*, **279**, 22030-22038.

Zhou, X.L., Vaillant, B., Loukin, S.H., Kung, C. and Saimi, Y. (1995) YKC1 encodes the depolarization-activated K+ channel in the plasma membrane of yeast. *FEBS Lett*, **373**, 170-176.

Zhou, Y., Morais-Cabral, J.H., Kaufman, A. and MacKinnon, R. (2001) Chemistry of ion coordination and hydration revealed by a K+ channel-Fab complex at 2.0 A resolution. *Nature*, **414**, 43-48.

ANNEXES

Annex 1. Chemical structure of different molecules.

Amine specific isobaric reagents

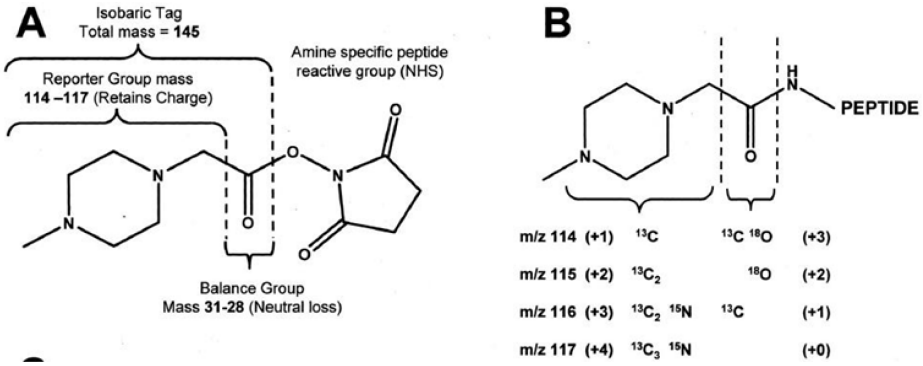

Bleomycin

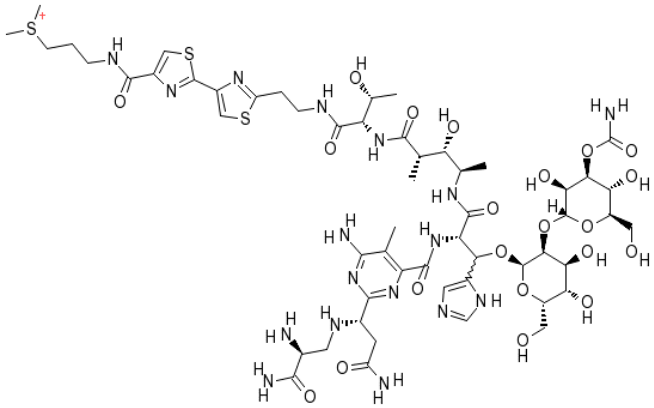

Filipin

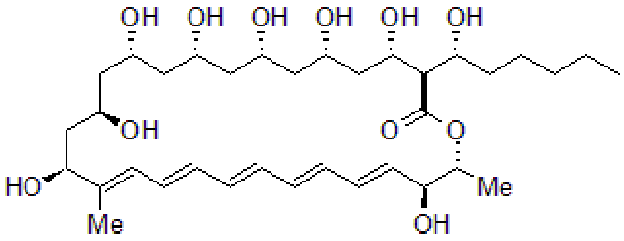

Hygromycin B

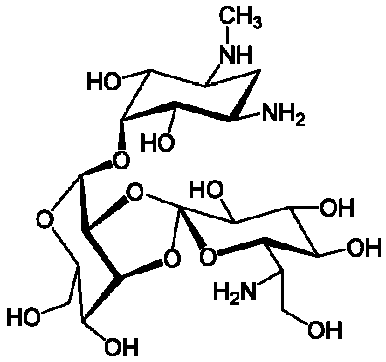

Rhodamine 6G

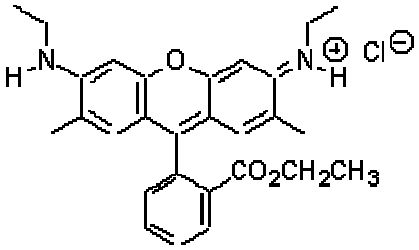

Spermine

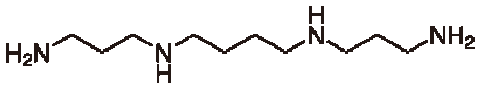

Tag HA : YPYDVPDYA
Tag myc: EQKLISEEDL

Annex 2. Proteins identified in the yeast PM fraction.

Standard Name	Systematic Name	Description summary	TMD	Score	Peptide	Sequence coverage (%)	Location
Transport							
PMA1	YGL008C	Proton transporter	10	1159	26	29	PM
PMA2	YPL036W	Proton transporter	10	772	18	22	PM
HXT7	YDR342C	Glucose transporter	11	595	6	16	PM
HXT6	YDR343C	Glucose transporter	11	489	6	16	PM
VDAC1	YNL055C	Mitochondrial porin	0	247	6	30	Mt
THI7	YLR237W	Thiamine transporter	12	205	8	11	PM
NRT1	YOR071C	Nicotinamide riboside transporter	10	190	7	11	PM
MEP2	YNL142W	Ammonium transporter	11	153	2	9	PM
ADY2	YCR010C	Acetate transporter	5	139	3	19	PM
MIR1	YJR077C	Mitochondrial phosphate transporter	0	129	6	21	Mt
JEN1	YKL217W	Lactate transporter	12	112	3	13	PM
HXT3	YDR345C	Glucose transporter	11	86	5	12	PM
PET9	YBL030C	Mitochondrial ADP/ATP transporter	3	83	7	11	Mt
YOR1	YGR281W	Multidrug transporter	11	81	13	14	PM

Standard Name	Systematic Name	Description summary	TMD	Score	Peptide	Sequence coverage (%)	Location
HXT4	YHR092C	Glucose transporter	11	76	5	9	PM
HXT2	YMR011W	Glucose transporter	12	72	7	12	PM
GAL2	YLR081W	Galactose transporter	12	71	3	8	PM
PNS1	YOR161C	Similar to a choline transporter (*T.californica*)	10	59	2	6	PM
HXT15	YDL245C	Protein of unknown function with similarity to hexose transporter	12	56	3	7	PM
HXT13	YEL069C	Hexose transporter	12	56	2	5	PM
MEP3	YPR138C	Ammonium transporter	11	56	2	7	PM
TFP1	YDL185W	Subunit of vacuolar proton transporter	0	56	13	6	Vac
AAC3	YBR085W	Mitochondrial ADP/ATP transporter	4	55	4	16	Mt
AAC1	YMR056C	Mitochondrial ADP/ATP transporter	4	55	2	7	Mt
VMA5	YKL080W	Subunit of vacuolar proton transporter	0	53	3	12	Vac
SNQ2	YDR011W	Multidrug transporter	12	50	11	10	PM
MEP1	YGR121C	Ammonium transporter	11	49	2	7	PM
HXT5	YHR096C	Hexose transporter	11	49	4	10	PM
PTR2	YKR093W	Di- and tri-peptides transporter	11	48	6	15	PM
VMA2	YBR127C	Subunit of vacuolar proton transporter	0	47	10	28	Vac
VPH1	YOR270C	Subunit of vacuolar proton transporter	7	46	4	8	Vac
HXT1	YHR094C	Glucose transporter	11	45	4	9	PM
HXT9	YJL219W	Putative hexose transporter	11	45	2	4	PM
HXT10	YFL011W	Putative hexose transporter	11	45	3	8	PM
HXT8	YJL214W	Protein of unknown function with similarity to hexose transporter	10	45	2	5	PM
FPS1	YLL043W	Glycerol transporter	5	39	3	5	PM
ENA1	YDR040C	Sodium transporter	10	38	6	8	PM
VMA13	YPR036W	Subunit of vacuolar proton transporter	0	37	3	10	Vac

Standard Name	Systematic Name	Description summary	TMD	Score	Peptide	Sequence coverage (%)	Location
THI73	YLR004C	Putative carboxylic acid transporter	12	36	2	6	PM
VMA6	YLR447	Subunit of vacuolar proton transporter	0	34	5	23	Vac
TOM70	YNL121C	Translocase of the mitochondrial membrane	1	34	2	6	Mt
PDR5	YOR153W	Multidrug transporter	14	33	12	12	PM
TPO3	YPR156C	Polyamine transporter	12	30	2	6	PM
PDR15	YDR406W	Multidrug transporter	12	29	6	8	PM
PDR12	YPL058C	Multidrug transporter	11	25	4	7	PM
THI72	YOR192C	Thiamine transporter	10	24	3	6	PM
TPO4	YOR273C	Polyamine transporter	11	24	3	6	PM
Signaling							
PIL1	YGR086C	Primary component of eisosomes	0	463	9	13	Cyt, PM
YCK2	YNL154C	Casein kinase	0	143	8	21	PM
LSP1	YPL004C	Primary component of eisosomes	0	119	3	13	Cyt, PM
RAS2	YNL098C	GTP-binding protein	0	61	3	15	PM
MID2	YLR332W	Sensor for cell wall	1	58	1	3	PM
YPT7	YML001W	GTP-binding protein of the rab family	0	57	2	18	Vac
BCY1	YIL033C	Component of a signaling pathway	0	56	6	23	PM, Cyt, Nuc
SUR7	YML052W	Component of eisosomes	4	42	6	17	PM
YCK1	YHR135C	Casein kinase	0	37	5	15	PM
BEM2	YER155C	Rho GTPase-activating protein	0	29	6	3	Mt
RHO5	YNL180C	GTPase of the Rho/Rac subfamily	0	28	2	11	Cyt, Nuc
Cell wall							
GAS1	YMR307W	Beta-1,3-glucanosyltransferase	0	214	7	17	PM
FMP45	YDL222C	Required for viability in stationary phase	4	172	4	21	Mit, PM

Standard Name	Systematic Name	Description summary	TMD	Score	Peptide	Sequence coverage (%)	Location
FKS1	YLR342W	Involved in cell wall synthesis	13	58	15	10	PM
ECM33	YBR078W	GPI-anchored protein involved in apical budding	2	54	3	6	PM
GAS5	YOL030W	Beta-1,3-glucanosyltransferase	0	43	3	5	PM, Wall
DCW1	YKL046C	GPI-anchored protein	1	30	2	6	PM
Stress							
SSA1	YAL005C	ATPase involved in protein folding	0	288	10	19	Various
SSA2	YLL024C	Heat shock protein	0	282	9	25	Various
SSA3	YBL075C	Heat shock protein	0	164	7	14	Cyt
MRH1	YDR033W	Protein related to Hsp30p	7	126	3	12	PM
HSP30	YCR021C	Protein negatively regulates Pma1p	7	123	5	27	PM
SSA4	YER103W	Heat shock protein	0	70	5	10	Cyt
HSP104	YLL026W	Heat shock protein	0	51	12	16	Cyt
HSP78	YDR258C	Mitochondrial chaperone	0	33	12	19	Mt
SSC1	YJR045C	Hsp70 family ATPase	0	29	8	19	Mt
MSN1	YOL116W	Transcriptional activator	0	26	2	5	Nuc
HSC82	YMR186W	Cytoplasmic chaperone	0	26	3	6	Cyt
PST2	YDR032C	Induced by oxidative stress	0	25	2	30	PM, Mt
Targeting/ Vesicular transport							
SSO2	YMR183C	Plasma membrane t-SNARE	1	93	4	18	PM
SAR1	YPL218W	Component of COPII coat of vesicles	0	64	6	47	ER
VPS1	YKR001C	GTPase required for vacuolar sorting	0	52	7	11	Cyt
SEC23	YPR181C	GTPase-activating protein	0	48	8	14	Cyt
ARF1	YDL192W	GTPase of the Ras superfamily	0	48	4	22	Cyt

Standard Name	Systematic Name	Description summary	TMD	Score	Peptide	Sequence coverage (%)	Location
SEC21	YNL287W	Subunit of coatomer	0	35	5	9	ER
SEC31	YDL195W	Component of COPII coat of vesicles	0	27	5	4	ER
Biosynthesis/ degradation							
EFT1	YOR133W	Elongation factor 2	0	586	21	35	Rib
TEF1	YPR080W	Translational elongation factor	0	438	11	35	Rib
SSB2	YNL209W	Cytoplasmic ATPase	0	425	13	20	Cyt
TEF4	YKL081W	Translational elongation factor	0	300	7	22	Rib
YEF3	YLR249W	Translational elongation factor 3	0	258	19	27	Rib
SUB2	YDL084W	Member of the DEAD-box RNA helicase	0	193	10	37	Nuc
NOP56	YLR197W	Direct 2'-O-methylation of pre-rRNA	0	177	10	33	Nuc
RPG1	YBR079C	Translation initiation factor	0	138	15	25	Rib
DED1	YOR240W	Member of the DEAD-box RNA helicase	0	116	14	34	Cyt
NSR1	YGR159C	Ribosome biogenesis	0	97	4	20	Nuc
HEF3	YNL014W	Translational elongation factor	0	84	7	10	Rib
ZUO1	YGR285C	Cytosolic ribosome-associated chaperone	0	81	7	24	Rib
TUF1	YOR187W	Mitochondrial translation elongation factor	0	79	4	17	Mt
NOP58	YOR310C	Protein involved in pre-rRNA processing	0	79	4	12	Nuc
SSB1/HSP75	YDL229W	ATPase that is a ribosome-associated molecular chaperone	0	78	3	6	Cyt
CAM1	YPL048W	Similarity to translational cofactor EF-1	0	70	6	18	Rib
NOP1	YDL014W	Subunit processome complex	0	68	7	29	Rib

Standard Name	Systematic Name	Description summary	TMD	Score	Peptide	Sequence coverage (%)	Location
SPT5	YML010W	Protein involved in the regulating Pol I and Pol II transcription	0	58	15	21	Nuc
ACO1	YLR304C	Mitochondrial genome maintenance	0	57	9	17	Mt
SSZ1	YHR064C	Hsp70 protein	0	56	2	5	Cyt
SIS1	YNL007C	Co-chaperone	0	53	5	17	Rib
TIF1	YKR059W	Translation initiation factor	0	44	8	25	Rib
ARC1	YGL105W	Protein that binds tRNA	0	44	3	5	Cyt
RSP5	YER125W	Ligase involved in ubiquitin-mediated protein degradation	0	43	9	15	Various
ARB1	YER036C	Involved in Ribosome Biogenesis	0	43	5	12	Rib
NIP1	YMR309C	Translation initiation factor	0	41	6	11	Rib
ATP1	YBL099W	ATP synthesis	0	38	6	16	Mt
CLU1	YMR012W	Translation initiation factor	0	36	8	13	Rib
PRT1	YOR361C	Translation initiation factor	0	34	9	15	Rib
RPC34	YNR003C	RNA polymerase III subunit	0	33	3	16	Cyt
SPT16	YGL207W	Subunit of the heterodimeric FACT complex	0	32	8	13	Nuc
ERG1	YGR175C	ERGosterol biosynthesis	2	31	5	13	ER
YDJ1	YNL064C	Protein chaperone	0	29	7	27	Cyt
DBP3	YGL078C	RNA helicase	0	29	3	9	Nuc
CDC48	YDL126C	ATPase in ER, nuclear membrane and cytosol	0	28	5	8	Various
TIF3	YPR163C	Translation initiation factor	0	27	3	8	Rib
SNU13	YEL026W	RNA binding protein	0	27	2	26	Nuc
KAR2	YJL034W	ATPase involved in protein import into the ER	1	27	3	7	ER
PRP43	YGL120C	RNA helicase	0	27	9	16	Rib
TIF45	YOL139C	Translation initiation factor	0	26	4	21	Rib

Standard Name	Systematic Name	Description summary	TMD	Score	Peptide	Sequence coverage (%)	Location
PEP4	YPL154C	Vacuolar aspartyl protease	0	25	2	7	Vac
Metabolism							
ACS2	YLR153C	Acetyl-coA synthetase isoform	0	309	11	25	Cyt
PDC5	YLR134W	Pyruvate decarboxylase	0	122	6	17	Nuc
HXK1	YFR053C	Hexokinase	0	120	11	30	Cyt
CDC19	YAL038W	Pyruvate kinase	0	109	9	19	Cyt
LYS20	YDL182W	Homocitrate synthase	0	105	8	25	Nuc
LYS21	YDL131W	Homocitrate synthase	0	105	8	21	Nuc
FPR4	YLR449W	Peptidyl-prolyl cis-trans isomerase	0	83	3	13	Nuc
ILV1	YER086W	Threonine deaminase	0	74	10	27	Mit
PDC1	YLR044C	Pyruvate decarboxylase	0	74	9	29	Cyt
FBA1	YKL060C	Fructose 1,6-bisphosphate aldolase	0	73	2	9	Cyt
PDC6	YGR087C	Pyruvate decarboxylase	0	71	4	11	Cyt
FET3	YMR058W	Integral membrane multicopper oxidases	1	70	2	7	PM
ILV2	YMR108W	Acetolactate synthase	0	62	8	21	Mt
ENO2	YHR174W	Enolase II	0	59	3	10	Cyt
CBF5	YLR175W	Pseudouridine synthase	0	54	5	15	Nuc
HXK2	YGL253W	Hexokinase	0	46	3	13	Nuc
GLK1	YCL040W	Glucokinase	0	45	6	19	Cyt
FAS1	YKL182W	Beta subunit of fatty acid synthetase	0	45	12	9	Cyt
QCR7	YDR529C	Mitochondrial inner membrane electron transport chain	0	45	4	47	Mt
AKL1	YBR059C	Ser-Thr protein kinase	0	43	7	10	Cyt
NDE1	YMR145C	Mitochondrial external NADH dehydrogenase	0	43	4	13	Mt
PGK1	YCR012W	3-phosphoglycerate kinase	0	42	6	20	Cyt
GLC7	YER133W	Serine/threonine protein phosphatase	0	40	2	12	Nuc
CHS1	YNL192W	Chitin synthase	7	40	4	4	PM
THI3	YDL080C	Alpha-ketoisocaproate decarboxylase	0	39	4	8	Cyt

Standard Name	Systematic Name	Description summary	TMD	Score	Peptide	Sequence coverage (%)	Location
MDH3	YDL078C	Peroxisomal malate dehydrogenase	0	39	2	11	Peroxisome
ADH1	YOL086C	Alcohol dehydrogenase	0	39	2	7	Cyt
FPR3	YML074C	Nucleolar peptidyl-prolyl cis-trans isomerase	0	38	4	15	Nuc
QCR2	YPR191W	Ubiquinol cytochrome-c reductase complex	0	37	5	19	Mt
COX4	YGL187C	Subunit IV of cytochrome c oxidase	0	36	2	17	Mt
ACC1	YNR016C	Acetyl-CoA carboxylase	0	33	16	24	ER
HFA1	YMR207C	Mitochondrial acetyl-coenzyme A carboxylase	0	33	10	6	Mt
YAT1	YAR035W	Outer mitochondrial carnitine acetyltransferase	0	32	8	14	Mt
GUA1	YMR217W	GMP synthase	0	32	5	12	Unknown
PFK26	YIL107C	6-phosphofructo-2-kinase	0	30	2	3	Cyt
LYS1	YIR034C	Saccharopine dehydrogenase	0	28	5	23	Cyt
MAE1	YKL029C	Mitochondrial malic enzyme	0	28	8	20	Mt
CPR2	YHR057C	Peptidyl-prolyl cis-trans isomerase	0	27	2	9	Unknown
PSA1	YDL055C	GDP-mannose pyrophosphorylase	0	27	2	6	Cyt
ARO9	YHR137W	Aromatic aminotransferase	0	26	3	8	Cyt
COX2	Q0250	cytochrome c oxidase	0	26	2	11	Mt
MET17	YLR303W	Methionine and cysteine synthase	0	26	2	8	Cyt
MSS4	YDR208W	Phosphatidylinositol-4-phosphate 5-kinase	0	25	6	11	PM
NDI1	YML120C	Ubiquinone oxidoreductase	1	25	3	9	Mt
DPM1	YPR183W	Dolichol phosphate mannose (Dol-P-Man) synthase	1	22	3	18	ER
Cellular organisation							

Standard Name	Systematic Name	Description summary	TMD	Score	Peptide	Sequence coverage (%)	Location
LSB3	YFR024C-A	Protein involved in actin patch assembly	0	93	7	18	Cyt
CDC10	YCR002C	Component of the septin ring of the mother-bud neck	0	70	3	16	Various
ACT1	YFL039C	Protein involved in cell polarization	0	63	3	12	Actin
TUB3	YML124C	Alpha-tubulin	0	40	2	7	Microtubule
SAC6	YDR129C	Fimbrin	0	37	4	10	Actin cortical patch
YNL194C	YNL194C	Protein required for sporulation and plasma membrane sphingolipid content	4	33	4	29	PM
HBT1	YDL223C	Polarized cell morphogenesis	0	28	5	8	Cyt
Ribosomal subunit associated							
RPL5	YPL131W	60S	0	207	6	34	Rib
RPL4B	YDR012W	60S	0	146	8	41	Rib
RPS3	YNL178W	40S	0	133	7	37	Rib
RPL3	YOR063W	60S	0	111	8	24	Rib
RPS4A	YJR145C	40S	0	104	5	29	Rib
RPL2A	YFR031C-A	60S	0	101	4	31	Rib
RPS0A	YGR214W	40S	0	101	5	32	Rib
RPS16A	YMR143W	40S	0	91	3	25	Rib
RPL27A	YHR010W	60S	0	90	3	28	Rib
RPL13B	YMR142C	60S	0	89	4	28	Rib
RPS2	YGL123W	40S	0	88	2	9	Rib
RPL10	YLR075W	60S	0	82	6	25	Rib
RPL17B	YJL177W	60S	0	78	3	21	Rib
RPS7A	YOR096W	40S	0	78	4	24	Rib
RPS20	YHL015W	40S	0	77	4	40	Rib
RPS5	YJR123W	40S	0	73	2	12	Rib
RPS7B	YNL096C	40S	0	69	2	12	Rib

Standard Name	Systematic Name	Description summary	TMD	Score	Peptide	Sequence coverage (%)	Location
RPS17A	YML024W	40S	0	64	4	11	Rib
RPL19A	YBR084C-A	60S	0	60	4	30	Rib
RPL7A	YGL076C	60S	0	59	4	21	Rib
RPL16B	YNL069C	60S	0	58	7	28	Rib
RPL15A	YLR029C	60S	0	51	2	13	Rib
RPS22A	YJL190C	40S	0	49	2	23	Rib
RPS15	YOL040C	40S	0	46	2	9	Rib
RPL1A	YPL220W	60S	0	43	2	16	Rib
RPS1A	YLR441C	40S	0	43	3	13	Rib
RPL25	YOL127W	60S	0	43	2	18	Rib
RPL9A	YGL147C	60S	0	42	2	16	Rib
RPS11A	YDR025W	40S	0	39	2	12	Rib
RPS29B	YDL061C	40S	0	38	2	37	Rib
RPL20A	YMR242C	60S	0	35	3	23	Rib
RPS8A	YBL072C	40S	0	32	3	21	Rib
RPS24A	YER074W	40S	0	28	2	15	Rib
RPS6A	YPL090C	40S	0	28	6	29	Rib
RPS9B	YBR189W	40S	0	27	3	18	Rib
RPL31A	YDL075W	60S	0	26	3	28	Rib
Unknown function							
OLA1	YBR025C	Protein of unknown function	0	137	8	29	Cyt
YRO2	YBR054W	Putative protein of unknown function	7	104	3	13	Mit
YJR1	YJL171C	GPI-anchored cell wall protein of unknown function	0	66	4	15	Wall, PM
TPA1	YER049W	Protein of unknown function	0	49	9	19	Nuc
	YLR413W	Putative protein of unknown function	4	42	4	6	Unknown
	YER080W	Protein of unknown function	0	38	6	12	Mit
TCB3	YML072C	Lipid-binding protein	1	36	11	11	Mit
FUN12	YAL035W	Protein of unknown function	0	33	6	9	Rib
YCP4	YCR004C	Protein of unknown	0	32	3	26	PM

		function					
SCS2	YER120W	Protein that regulates phospholipid metabolism	1	31	1	5	ER
	YGR266W	Localized to both the mitochondrial outer membrane and the plasma membrane	1	29	4	11	PM, Mt
DIA3	YDL024C	Protein of unknown function	0	24	2	6	Wall

Proteins are grouped according to functional similarities. TMD shows number of TMD, Peptide shows the number of identified peptides, Plasma membrane location is from SGD and the score is calculated by the Mascot algorithm.

Titre récents de la collection

2006

Département de biologie appliquée et des productions agricoles

N°71. Muratori, Frédéric, Reconnaissance des facteurs cuticulaires de l'hôte et conséquences sur l'exploitation des colonies par le parasitoïde de pucerons, *Aphidius rhopalosiphi* (Hymenoptera: Aphidiinae).

N°72. Condori Ali, Paulino Bruno, Analyse comparative et modélisation de la croissance et du développement de tubercules andins dans les Andes en Bolivie.

N°75. Doucet, Diane, Development of a model and similarities with a benyvirus.

N°76. Nkwembe Unsital, Guy-Bernard, La problématique de la pauvreté des ménages agricoles ruraux et urbains dans la périphérie de la ville de Kinshasa. Essai d'analyse du phénomène et de ses implications sur la sécurité alimentaire.

N°78. Ndayiragjie, Alexis, Relations entre métabolisme des polyamines et la résistance au stress salin chez le riz (*Oryza sativa* L.).

N°80. Secheli Ringot, Diana, Risk analysis of ochratoxin A and developpement of a decontamination procedure based on the biosorption of ochratoxin A onto yeast industry derivatives.

N°82. Abboudi, Tarik, The indispensable amino acid requirements for maintenance in Atlantic salmon fry.

N°83. Martins da Silva, Evaldo, Polyphenols from the Amazonian plant *Inga edulis*: process optimization for the production of purified extracts with high antioxidant capacity.

N°84. Fadlaoui, Aziz, Modélisation bioéconomique de la conservation des ressources génétiques animales.

N°85. Kambale Valimunzigha, Charles, Étude du comportement physiologique et agronomique de la tomate (*Solanum lycopersicum* L.) en réponse à un stress hydrique précoce.

N°86. Lepoint, Pascale, Speciation within the African Coffee Wilt Pathogen.

N°88. Mushagalusa Nachigera, Gustave, Competitive relationships in potato/maize intercropping: involvement of root system architecture

N°89. Nyamangyoku Ishibwela, Obedi, Ferrous iron toxicity: Mechanisms of resistance and impact on nutrient elements at the vegetative stage in cultivated rices (*Oryza sativa* L., *Oryza glaberrima* Steud and interspecific hybrids)

Département de chimie appliquée et des bio-industries

N°73. Pety de Thozée, Cédric, Implication of the ER quality control in the degradation of the yeast plasma membrane Pdr5^{L183P} ABC transporter.

N°79. Gurdak, Elzbieta, Supramolecular organization of collagen layers adsorbed on polymers.

N°87. Janssens, Xavier, Monitoring and predicting elusive species colonisation – Application to the otter in the Cévennes National Park (France).

Département des sciences du milieu et de l'aménagement du territoire

N°74. Kayitakire, François, Forest stand characterisation using very high resolutions satellite remote sensing

N°77. Van der Velde, Marijn, Agricultural and climatic impacts on the groundwater resources of a small island: measuring and modelling water and solute transport in soil and groundwater on Tongatapu.

N°81. Degen, Thomas, Dynamique initiale de la végétation herbacée et de la régénération ligneuse dans le cas de trouées, au sein d'une hêtraie (*Luzulo-Fagetum*).

2007

Département de biologie appliquée et des productions agricoles

N°97, De Dorlodot, Sophie, Root system architecture : a genetic analysis in rice.

N°99, Daoui, Khalid, Recherche de stratégies d'amélioration de l'efficience d'utilisation du phosphore chez la fève (*Vicia faba* L.) dans les conditions d'agriculture pluviale au Maroc.

N°101, Vanloqueren, Gaëtan, Penser et gérer l'innovation en agriculture à l'heure du génie génétique . Contribution d'une approche systémique d'innovations scientifiques dans deux filières agroalimentaires wallonnes pour l'évaluation, la gestion et les politiques d'innovation.

N°109, Pairon, Marie, Ecology and population genetics of an invasive forest tree species: *Prunus serotina* Ehrh.

N°111, Manyonga, Madika, Modelling the competition for light in maize (*Zea mays* L.)/bean (*Phaseolus vulgaris* L.) intercropping with three-dimensional approach.

N°115, Silva de Souza, Jesus Nazareno, Etude des propriétés antioxydantes *in vitro* d'extraits de feuilles de *Byrsonima crassifolia* et *Inga edulis* et caractérisation partielle des composés phénoliques.

N°116, Colinet, Hervé, Une approche écologique et biochimique de la résistance au froid chez un parasitoïde de puceron *Aphidius colemani* (Hymenoptera: Aphidiinae).

Département de chimie appliquée et des bio-industries

N°90. Eyers, Laurent, Characterization of bacterial populations of 2,4,6-trinitrotoluene (TNT) contaminated soils and isolation of a *Pseudomonas aeruginosa* strain with TNT denitration activities.

N°91. Dupré de Boulois, Hervé, Role of arbuscular mycorrhizal fungi on the accumulation of radiocaesium by plants.

N°92. Crouzet, Jérôme, Expression pattern, ectopic expression and gene silencing of two *Nicotiana* Pleiotropic Drug Resistance transporters.

N°93, Drugmand, Jean-Christophe, Characterization of Insect Cell Lines Is Required for Appropriate Industrial Processes.

N°94, De La Providencia, Ivan Enrique, Contribution of Anastomosis and Hyphal Healing Mechanism to the Extraradical Mycelium Architecture of Arbuscular Mycorrhizal Fungi.

N°95, Sebari, Karima, Optimisation de la gestion conjointe des ressources en eau de surface et des ressources en eau souterraines dans une région semi aride - la Vallée du Drâa.

N°100, Vandermeeren, Caroline, Quaternary Structure and Regulation of the *Nicotiana plumbaginifolia* Plasma Membrane Proton Pump ATPase.

N°102, Morales Belpaire Isabel, Fate of the active form of proteins in selected environmental matrices. Investigation with green fluorescent protein, β-glucosidase, and amyloid fibrils in wastewater sludges, biofilms and soils.

N°103, Trombik Tomasz, Characterization of two Pleiotropic Drug Resistance transporters from *Nicotiana plumbaginifolia.*

N°104, Callemien, Delphine, Use of new methodologies to study phenolic compounds through beer storage.

N°106, Van der Auwera, Géraldine, pAW63: A molecular wanderer in the *Bacillus cereus* gene pool.

N°107, Mateos Pedrero, Cecilia, Synthesis and characterization of Rh supported on Ti-modified oxides: catalytic activity in the partial oxidation of methane.

N°108, Voets, Liesbeth, Role of arbuscular mycorrhizal networks on plant interconnection and carbon transfer.

N°110, Jerkovic, Vesna, Découverte du resvératrol dans les houblons. Impact de la variété, de l'année de récolte et du conditionnement en vue de la préparation d'extraits polyphénoliques enrichis en stilbènes.

N°112, Dekeyser, Caroline, Elaboration and evaluation of nanostructured surfaces for the control of cell behavior.

N°113, Nonckreman, Cristèle, Design of materials with nanostructured surface to improve hemocompatibility.

N°114, Caillou, Samuel, Protein Adsorption: from Interfacial Interactions to Enzyme Activity.

N°96, Lefèvre, Isabelle, Investigation of three Mediterranean plant species suspected to accumulate and tolerate high cadmium and zinc levels: morphological, physiological and biochemical characterization under controlled conditions.

N°98, Desclée, Baudouin, Automated object-based change detection for forest monitoring by satellite remote sensing: applications in temperate and tropical regions.

N°105, André, Frédéric, Influence of the heterogeneity of canopy structure on the spatio-temporal variability of atmospheric deposition within a mixed oak-beech stand

2008

Département de biologie appliquée et des productions agricoles

N°120, Chirinos Gallardo, Rosana Sonia, Polyphenols from the Andean mashua (*Tropaeolum tuberosum*) tuber: Evaluation of genotypes, extraction, chemical characterization and antioxidant properties.

N°126, Romier, Béatrice, Modulation of intestinal inflammation by polyphenols.

N°130, Vaïanopoulos, Céline, Widespread occurrence of soil-borne mosaic viruses in Belgium. Preferential associations of *Polymyxa graminis* and mosaic viruses on cereals.

N°131, Tran, Thi Nang Thu, Nutritional value of sesame oil cake and lysine utilization efficiency in plant protein-based diets for rainbow trout.

N°134, Ngirente, Edouard, Les marchés agricoles intérieurs et les mutations agro-économiques en milieu rural rwandais. Application à la filière pomme de terre.

N°139, Gilbert, Valérie, Genetic and pathogenic diversity of *Pseudomonas syringae* isolates associated with diseases on Belgian fruit trees.

N°141, Delpierre, Matthieu, A Non-cooperative Approach to Rural Development Issues.

N°142, André, Christelle, Evaluation of Andean potato cultivars as a source of dietary antioxidants.

N°145, Bodin, Noëlie, Nutritional and interspecies effects on the estimation of threonine and lysine requirements in salmonid fry with a highlight on methodological impacts.

N°147, Pissard, Audrey, Structure and genetic diversity of two Andean tuber crops, oca (*Oxalis tuberosa* Mol.) and mashua (*Tropaeolum tuberosum* R.&P.): influence of the mode of conservation and of the agronomic and biological characteristics

Département de chimie appliquée et des bio-industries

N° 117, Zelazny, Enric, Regulation of maize aquaporin trafficking to the plasma membrane.

N°122, Bobik, Krzysztof, The two major tobacco plasma membrane H^+-ATPases, PMA2 and PMA4 are differentially phosphorylated on their penultimate threonine.

N° 123, Cabana, Hubert, Elimination des perturbateurs endocriniens nonylphénol, bisphénol A et triclosan à l'aide de laccase de Coriolopsis polyzona. C

N°133, Delannoy, Mélanie, Identification of peptidases in the *Nicotiana tabacum* leaf intercellular fluid.

N°132, De Palmenaer, Daniel, Genomic portrayal of IS*4* family –Modular insertion sequences, mobile insertion cassettes and overall family snapshot.

N°135, Manente, Myriam, Rta1, a yeast plasma membrane protein which confers resistance to fungicides.

N°129, Srasra, Mondher, Preparation and characterization of new basic catalyst by nitridation of Y zeolites.

N°137, Hachez, Charles, The expression pattern and activity of *Zea mays* plasma membrane aquaporins highlight their central role in the control of the cell membrane water permeability.

N°146, Soria, Miguel Angel, Etude des paramètres gouvernant les performances catalytiques d'AlPO, AlGaPO et GaPO purs et en présence de vanadium dans l'ammoxydation du propane

Département des sciences du milieu et de l'aménagement du territoire

N°118, Van Cauwenbergh, Nora, Expert and local knowledge in decision support for natural resource management.

N°119, Henriet, Céline, Silicon in banana (*Musa* spp.): a soil-plant system approach.C

N°121, Tidjani, Adamou Didier, Erosion éolienne dans le Damagaram Est (Sud-Est du Niger) : Paramétrisation, quantification et moyens de lutte.

N°124, Akponikpe, Pierre Bienvenu Irénikatché, Millet response to water and soil fertility management in the Sahelian Niger: experiments and modeling Erosion éolienne dans le Damagaram Est (Sud-Est du Niger) : Paramétrisation, quantification et moyens de lutte.

N°125, Vancutsem, Christelle, Revisiting satellite time series compositing for earth observation applications.

N°127, Opfergelt, Sophie, Silicon cycle in the soil-plant system: biogeochemical tracing using Si isotopes.

N°128, de Araujo Marinho Filho, Eduardo Celsio, Economics of Hunger: Several Methods, Levels and Scales.

N°136, Saqalli, Mehdi, Populations, Farming systems & Social transitions in Sahelian Niger: An Agent-based modeling approach.

N°138, Lucau-Danila, Cozmin Catalin, LAI retrieval from SAR remote sensing for crop monitoring at regional scale.

N°140, Iboukassene, Soraya, Dynamique de la végétation des forêts à *Quercus suber* anthropisées du Nord-Est de l'Algérie (Parc National d'El-Kala).

N°143, Fasbender, Dominique, Bayesian data fusion in environmental sciences : Theory and applications.

N°144, Hoang Thi Thai, Hoa, Soil characteristics, cropping patterns, and use of organic resources in the coastal sandy area of Thua Thien Hue province, Central Vietnam

2009

Département de biologie appliquée et des productions agricoles

N°149, de Lespinay, Alexis, Study of seed priming mechanisms of three plant species used in revegetation of industrial sites

N°153, Harahagazwe, Dieudonné, Heat tolerance assessment of the potato crop: evaluation of CIP clones in the lowlands of Burundi.

N°161, Mehrvar, Mohsen, Harahagazwe, Dieudonné, Diversity of soil-borne sugar beet viruses in Iran.

Département de chimie appliquée et des bio-industries

N°148, Pokrzywa, Wojcieh, Targeting of the yeast Sna3p and Sna4p to the endosomal pathway depends on their interaction with ubiquitin ligase Rsp5p.

N°150, Hoton, Florence, Insights into the Ecology and Genetic Diversity of Cereulide-producing Bacillus cereus strains.

N°151, Fornelos Martins, Nadine, GIL01 and relatives, a new generation of tectiviruses infecting the *Bacillus cereus* group.

N°154, Godet, Marie, Survey of filamentous fungi and development of molecular tools for their rapid and accurate identification, in advanced life support systems like the International Space Station.

N°155, Verbelen, Claire, Nanoscale probing of the mycobacterial cell wall.

N°156, Gaidashova, Svetlana, Effect of plant parasitic nematodes and arbuscular mycorrhizal fungi on banana (*Musa* spp.) in the East African highland cropping systems.

N°157, Gyuricza, Veronika, Influence of arbuscular mycorrhizal fungi on the uptake and accumulation of radiocesium by plants and on its redistribution between plants.

N°158, Stenuit, Benoît, Biological Degradation of 2,4,6-Trinitrotoluene (TNT): Bioprospecting for TNT-Denitrating Bacteria and Deciphering of Multiple TNT Denitration Pathways.

N°159, De Muyn, Benoit, Expression of a functional antibody in *Nicotiana tabacum* plants and culture cells: analysis of proteolytic products and identification of putative extracellular peptidases involved.

Département des sciences du milieu et de l'aménagement du territoire

N°152, Marghadi, Saïd, Intégration des méthodes d’aide à la décision dans l’aménagement multifonctionnel des forêts au Maroc.

N°160, Mattern, Samuel, Mapping and source identification of groundwater pollution by nitrate. Theory and application to the Brusselian sand groundwater body.